Maxime François

Stability of dehydration glycols MEG and TEG

Master's thesis in Chemical Engineering
Supervisor: Hanna Knuutila, Karen Karolina Høisæter
June 2020

NTNU
**Norwegian University of
Science and Technology**

Maxime François

Stability of dehydration glycols MEG and TEG

Master's thesis in Chemical Engineering
Supervisor: Hanna Knuutila, Karen Karolina Høisæter
June 2020

Norwegian University of Science and Technology
Faculty of Natural Sciences
Department of Chemical Engineering

NTNU
Norwegian University of
Science and Technology

Abstract

The offshore process of natural gas dehydration is of crucial importance in meeting the required specifications and avoiding the formation of hydrates when transporting rich gas by pipeline. Monoethylene glycol or triethylene glycol, molecules with a high affinity for water, are generally used as desiccants. After dehydration, the absorbent is regenerated by heating it to a high temperature. Unfortunately, it would seem that successive regenerations gradually alter the desiccant capacities of the two glycols.

This master thesis therefore focuses on the degradation of MEG and TEG glycols used as absorbents for natural gas dehydration. Through a series of experiments and analyses, we have tried to better understand the functioning of this degradation.

For different temperatures, MEG and TEG were heated in the presence of oxygen for three weeks. Samples were regularly taken, inerted and stored in cold. These samples were then analysed by ion chromatograph, pH-metric titration, and spectroscopy. These analyses enabled us, among other things, to identify certain degradation products of the two glycols, to understand the influence of time and temperature on the composition of the degradation products, to highlight the differences in the behaviour of MEG and TEG or to quantify the acids present among the degradation products.

Surplus to the experimental work, the first steps towards simulation of the degradation was taken but comparing predictions of different physical and thermodynamic property models in Aspen Plus. To this end, the calculated values of certain physical and thermodynamic properties were compared with experimental values found in the scientific literature. It was found that the appropriate model is highly dependent on the choice of the used desiccant.

Preface

This work was carried out in the Department of Chemical Engineering of the Norwegian University of Science and Technology during the first semester of 2020.

First of all, I would like to thank my two supervisors, Hanna Knuutila and Karen Karolina Høisæter, for their help, their advice, their kindness to me, their listening and their patience. I sincerely hope to have the opportunity to work with them again soon.

A special thanks to Gøril Flatberg, who has always been there to answer my questions and try to solve with me the problems I have faced, and God knows I have often knocked on her door.

I would also like to thank Vanja Buvik, Ricardo Wanderley, Lukas Braakhuis, and more generally all the PhD students, for their help, advice and the good humour they brought to the team every day, despite the strange period we have been going through.

Finally, I would like to take this opportunity to thank my partner, Teymur Gogiyev, for his support, his encouragement, and to make each day that passes a true moment of happiness.

I declare that this is an independent work carried out at the Norwegian University of Science and Technology within the framework of my Erasmus exchange.

Table of contents

List of Figures

List of Tables

List of Abbreviations

CH$_4$	Methane
CO$_2$	Carbon dioxide
CPA	Cubin Plus Association
D	Day
DG	Degradation product(s)
EoS	Equation of State
H$^+$	Proton
HO$^-$	Hydroxide
H$_2$0	Water
H$_2$S	Hydrogen sulfide
IC	Ion Chromatography
IEA	International Energy Agency
LACM	Liquid Activity Coefficient Model
MEG	MonoEthylene Glycol
NaOH	Sodium hydroxide (soda)
NMR	Nuclear Magnetic Resonance
NRTL	Non-Liquid Two Random
TEG	TriEthylene Glycol
VLE	Vapor-Liquid Equilibrium

List of Symbols

A	Absorbance
A_λ	Absorbance for a fixed wavelength λ
c	Molar concentration [mol.L^{-1}]
f_i^L	Fugacity of compound i in the liquid phase
f_i^V	Fugacity of compound i in the vapor phase
$f_i^{L,0}$	Fugacity of pure compound i in the liquid phase
l	Length [cm]
P	Pressure [Pa]
P_{sim}	Simulated pressure [Pa]
P_{exp}	Experimental pressure [Pa]
pH	Potential hydrogen
pKa	Acid dissociation constant
R	Gas constant [J.mol^{-1}.K^{-1}]
T	Temperature [°C]
V_m	Molar volume [m^3.mol^{-1}]
x_i	Molar fraction of compound i in the liquid phase
γ_i	Activity coefficient of compound i
Δ%	Relative deviation
ε	Molar attenuation coefficient [L.mol^{-1}.cm^{-1}]
λ	Wavelength [nm]
λ_i	Ionic molar conductivity of compound i [S.m^{-1}.mol^{-1}]
φ_i^L	Fugacity coefficient of compound i in the liquid phase
σ	Conductivity [S.m^{-1}]

I. Introduction

As the production/consumption of natural gas continues to grow, and as the energy sector becomes increasingly strategic, it is important to understand how the processes used to produce it work. A better understanding opens the way to improving and optimizing these processes, making them more efficient and less polluting.

Let's take the example of offshore gas fields. Classically, natural gas is extracted by drilling the subsea reservoirs in which it has accumulated over time. The gas is then transported to an offshore platform for the first processing. This first treatment must enable the operator to meet certain specifications, such as the concentration of certain impurities (water or sour gases, for example), before sending the gas to the coast for the second treatment. Since each reservoir is different, the composition of the gas it contains will also be different, as will also, by necessity, the offshore treatment it will undergo.

This first treatment allows the natural gas to be dried and the mercury and sour gases it contains to be extracted. For the drying part, an absorption process involving compounds with a strong affinity for water is commonly used. The most commonly used family of desiccants remains glycols, mainly MEG and TEG. The glycol is brought into contact with the moist natural gas and becomes charged with water on contact with it. It is then heated to remove the absorbed water and can then be reused. Unfortunately, degradation of the glycols is observed over time, coupled with a decrease in the efficiency of the dehydration process.

1. Objectives

The COVID-19 pandemic forced to change the focus of thesis by closing access to campus and laboratories for two months. Adjustments were, therefore, needed, and the thesis include both experimental and simulation work. The changes influenced both the objectives and structure of the thesis.

The main objective of this work is the study of the degradation of MEG and TEG glycols. In particular, the experimental parameters influencing the degradation, the composition of the degradation products, and the consequences of this degradation on the efficiency of the dehydration process will be examined. Specifically, in this thesis will focus on the influence of temperature on the degradation, the presence or absence of organic acids among the degradation products and the choice of the best thermodynamic model available in Aspen Plus to later model the dehydration process and simulate the influence of the degradation on its efficiency.

2. Thesis structure

This thesis is divided into 7 chapters.

Chapter I, which the reader is currently reading, gives a brief description of the motivation and objectives of this work.

Chapter II provides an overview of the importance of natural gas in the world today and a description of the use of MEG and TEG glycols during the production process.

Chapter III summarizes the existing scientific literature on glycol degradation.

Chapter IV presents the various experiments and analyses that have been carried out as well as the methodology put in place.

Chapter V sets out the results obtained from the analyses carried out and the conclusions that can be drawn from them.

Chapter VI provides a comparison of models that could potentially be used on Aspen Plus to simulate the operation of a dehydration unit. The data obtained from these models were then compared with experimental values found in the scientific literature.

Finally, Chapter VII will serve as a conclusion to this work and will try to answer the questions and objectives raised previously.

II.   Background

The purpose of this chapter is to contextualize this work and highlight its importance, given the current place of natural gas in our society. It includes a brief analysis of the importance of natural gas as an energy source, a description of the processes used in its production, and an explanation of the importance of glycols in these processes.

1. Overview

Natural gas is a gaseous mixture of hydrocarbons consisting mainly of methane but also including some other alkanes, and sometimes small amounts of carbon dioxide, hydrogen sulphide and other compounds. Naturally present in certain porous rocks, natural gas is extracted by drilling, both onshore and offshore. Natural gas can be classified according to its geological origin. Gas commonly referred to as natural gas is conventional non-associated gas, i.e. it is not associated with an oil field. There is also shale gas for example, which, unlike conventional natural gas, is trapped in an impermeable rock. This latter must therefore be fractured to extract the gas. The production of shale gas has exploded in recent years in the United States, despite its catastrophic environmental impact.

Although exploited as early as the 4th century BC by the Chinese for salt production, natural gas will only reach its hour of glory with the advent of post-WWII globalization. In fact, it was not until the oil shocks of 73 and 79 that there was a significant increase in the world production/consumption of natural gas. According to the International Energy Agency (IEA), in 2017 natural gas was the second most important source of electricity (it was only fourth in 1990 behind coal, nuclear and hydroelectricity) and the first source of heat energy (although it has gradually been equalled by coal in recent years). Natural gas ranked second overall (Figure 1) [17].
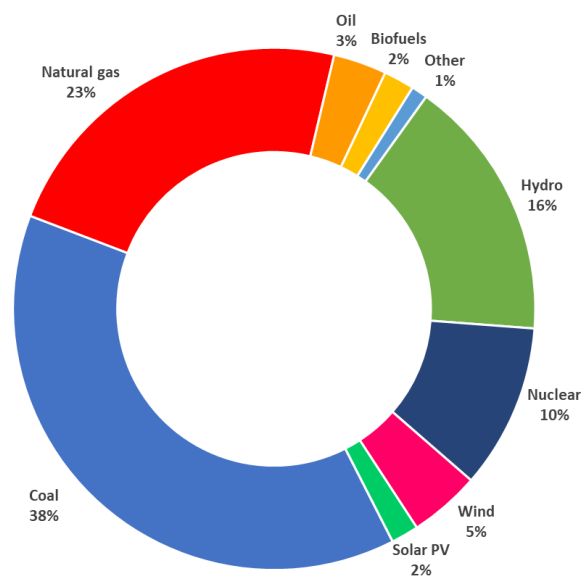
Figure 1 : Global energy mix for electricity and heat production in 2017 (IEA) [16]

Natural gas is the fastest growing fossil energy source in terms of its presence in the global energy mix. This can be explained by the fact that it is the "cleanest" of fossil fuels, an asset in the fight against climate change. However, this observation must be put into perspective: although it emits less carbon dioxide over its entire life cycle than coal or oil (for the production of the same amount of energy), its use causes the emission of methane, another greenhouse gas, which partially cancels out this advantage.

The main consumers of natural gas are the United States (21.2%), the Russian Federation (11.8%) and Iran (5.9%). The main sectors using natural gas are industry (37.8%), residential (29.3%), tertiary (12.7%), mainly for heat production, and the chemicals industry (12.4%) [10].

Natural gas production has increased from 78.6 EJ (10^{18} J) in 1990 to 147 EJ in 2017, an increase of almost 100% in just 30 years. The main producing countries in 2018 were the United States (21.5%), the Russian Federation (17.3%), Iran (6.2%) and, to a lesser extent, Canada, China, Qatar, Australia and Norway. Thus, some of the largest natural gas producing countries are included. Nevertheless, although the vast majority of natural gas production is for domestic use, important trade routes have developed to supply the various markets around the world (Figure 2). In 2018, Norway was the world's third largest exporter of natural gas, far behind the Russian Federation but almost at the same level as Qatar. Its main customers remain the countries of the European Union, with Germany and France in the lead.
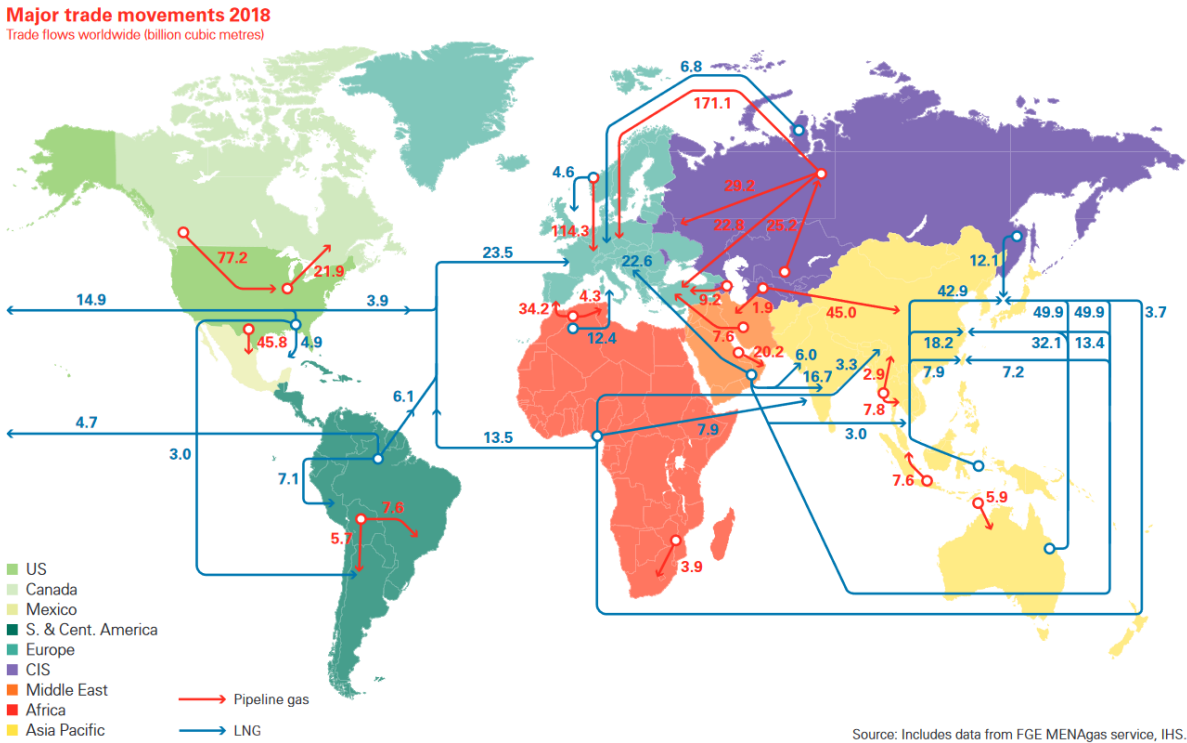
Figure 2 : Natural gas trade flows in 2018 [10]

2. Natural gas production process

For this work, we focus on the case of non-associated natural gas exploited offshore, as is the case for most fields in Norway.

The natural gas production process can be divided into four main stages [2]. The gas is first extracted by drilling and then transported to the offshore platform. It is then processed for the first time, separated from the water it contains and acid gases such as carbon dioxide or hydrogen sulfide. The rich gas is then sent by pipeline to an onshore facility where it is processed a second time. It is freed of these heavier compounds, which can then be recovered. Finally, the resulting dry gas is sent for distribution.

The operation and layout of the offshore part of the process depends, among other things, on the composition of the gas in the reservoir and the operating conditions. In particular, it is necessary to ensure good gas circulation between the reservoir and the offshore platform. However, some of the gas will condense as it rises, for two reasons. Firstly, the temperature in the pipe will gradually decrease when it comes into contact with seawater. Secondly, the pressure in the pipe will also decrease due to the friction of the fluid against the wall. So it is a multi-phase flow that most often arrives at the offshore platform for processing. This is an additional difficulty in ensuring proper flow assurance. By flow assurance, we generally mean that all measures have been taken to avoid a decrease or even a stop in the flow of fluid throughout the process, and therefore between the reservoir and the offshore platform. The main problems encountered are the formation of scale, wax or hydrates [2].

Scale is a deposit of precipitated salts on the walls of a pipeline. Wax results from the precipitation of paraffins. As mentioned above, as the gas rises from the well to the platform, the temperature and internal pressure gradually decrease. This results in a decrease in the solubility of the salts present, as well as the paraffins, and thus their precipitation. These deposits are problematic because, on the one hand, they gradually reduce the pipe's diameter of use and thus the flow rate of fluid that can be transported through it. On the other hand, they can also call into question the safety of the process. Both of these phenomena are usually combated by the addition of certain chemical additives. The hydrate problem is a different matter, and that's what we're going to look at now.

3. Hydrates formation

Hydrates (or more correctly clathrate hydrates) are compounds of organic origin consisting of a thin cage of ice containing a gaseous compound; methane in the case of methane hydrates for example. The latter are naturally present on the seafloor as well as in permafrost.

As mentioned earlier, hydrates are also the cause of many incidents in gas pipelines and transmission lines, particularly underwater. This is because methane hydrates are stable at high pressure and low temperature, conditions found in these pipelines. However, it is important to remember that if the water in the reservoir is in gaseous form mixed with natural gas, it will gradually condense as it rises to the surface. The liquid water will therefore be able to react with the methane gas (and to a lesser extent with the other alkanes present) to form hydrates. Hydrates have a structure close to that of ice. They are therefore plugs that can potentially form if no attention is paid to this problem, with the consequences that one can imagine on the efficiency of the process as well as its safety. Figure 3 shows an example of a hydrate plug obstructing a pipe.

Figure 3 : Hydrate plug

There are different ways to avoid hydrate formation. For example, the temperature can be kept high enough throughout the process to avoid conditions conducive to hydrate formation. There are two ways to achieve this: heating to compensate for heat loss, or insulation to prevent heat loss. For this purpose, there are certain types of pipes with built-in heating.

It is also possible to reduce the rate of hydrate formation using specific inhibitors or to prevent the hydrates formed from agglomerating and thus creating plugs with other inhibitors.

However, the most common solution is still to reduce the hydrate formation temperature by injecting chemicals into the header. The industry mainly uses monoethylene glycol (MEG) and triethylene glycol (TEG). The latter have a strong affinity for water; reacting with it, they inhibit hydrate formation. It can be seen in Figure 4 that the higher the mass proportion of MEG in the stream, the lower the hydrate formation temperature. It is easy to reach 5°C without hydrate formation with a mass proportion of 30% MEG. All that remains to be done is to separate the water/glycol mixture from the gas on arrival at the offshore platform.
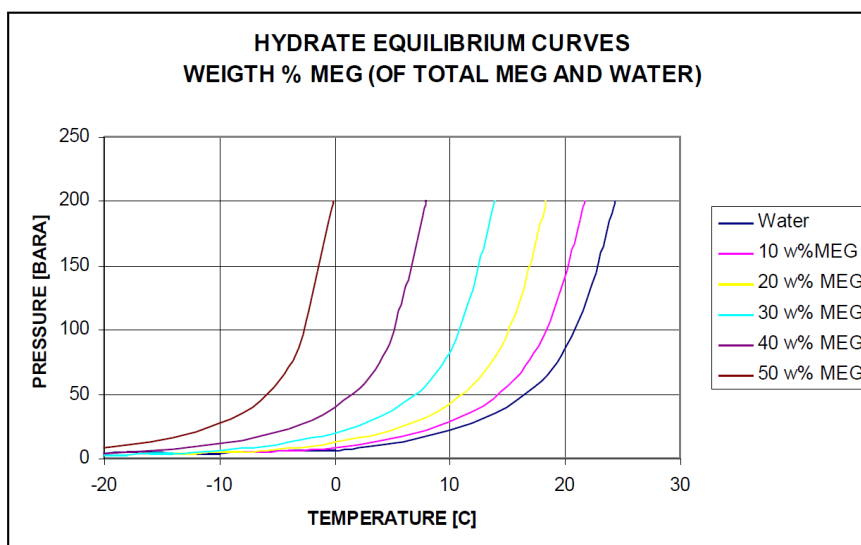
Figure 4 : Hydrate inhibition by using MEG [2]

4. Dehydration process and glycol degradation

As discussed above, MEG and TEG glycols are used to inhibit hydrate formation from the reservoir to the offshore platform. But as we said above, once the gas is separated from the bulk of the water/glycol mixture, it still remains saturated with water. This is because the glycol used could only react with the water in liquid form, not the water that remained in gaseous form. It is therefore necessary to dry it in order to reach the required specifications. This dehydration step usually takes place after treatment to remove acid gases.

Figure 5 below shows the position of the dehydration unit (red dotted square) as well as the arrival of the natural gas-water-glycol mixture on the platform (bottom left). The glycol used to inhibit the hydrate formation then follows the green path to the regeneration unit, before being returned to the wellhead.
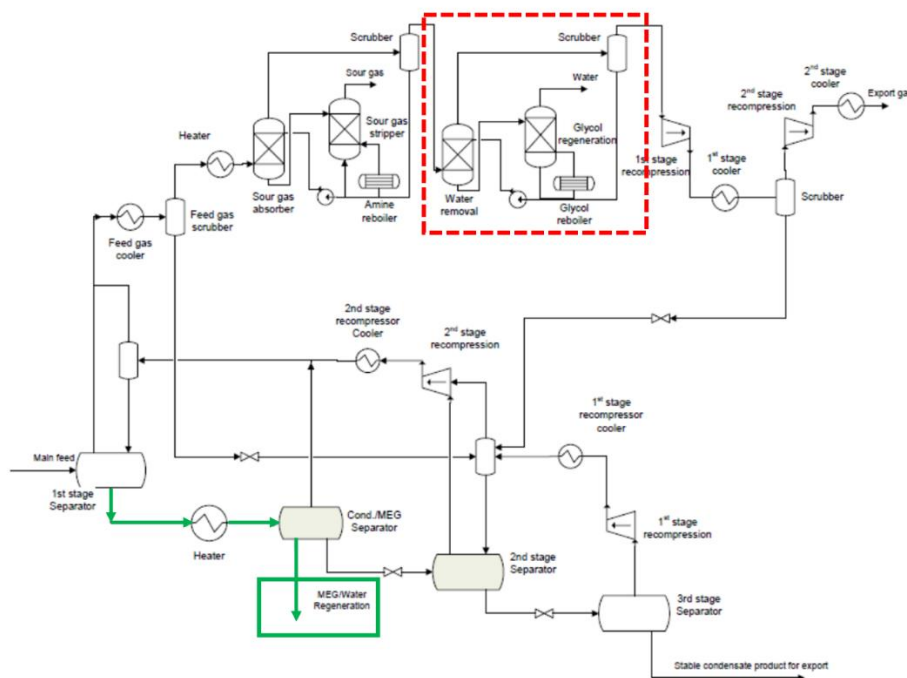
Figure 5 : Offshore process [3]. The dehydration part is located in the red square.

There are different technologies available to dry the natural gas. The expansion and separation process is based on the fact that when the water-saturated gas is cooled and expanded, the water gas will condense, allowing it to be separated from the gas. The process must then be repeated several times to reach the required specifications. It is also possible to use an adsorption process, on molecular sieve or silica gel. But the most common process and the one we are interested in for this work is absorption. It is generally implemented using glycol (MEG or TEG).

This process can be divided into two main steps: absorption and regeneration (Figure 6) [23][25]. First, glycol and natural gas are brought into contact in an absorber. The glycol comes at the top and goes down in counter flow of gas. During the descent, it slowly absorbs the water contained in the gaseous phase. We obtain a dry gas flow and rich glycol flow. The rich glycol is then sent to the regenerator. It is heated to a high temperature, which causes the most volatile compounds, including water, to evaporate. The glycol obtained at the bottom of the column is finally mixed with fresh glycol to be returned to the absorber. The temperatures reached by the glycol range from 25 to 50°C in the contactor, and up to 200°C in the regenerator (Figure 7).
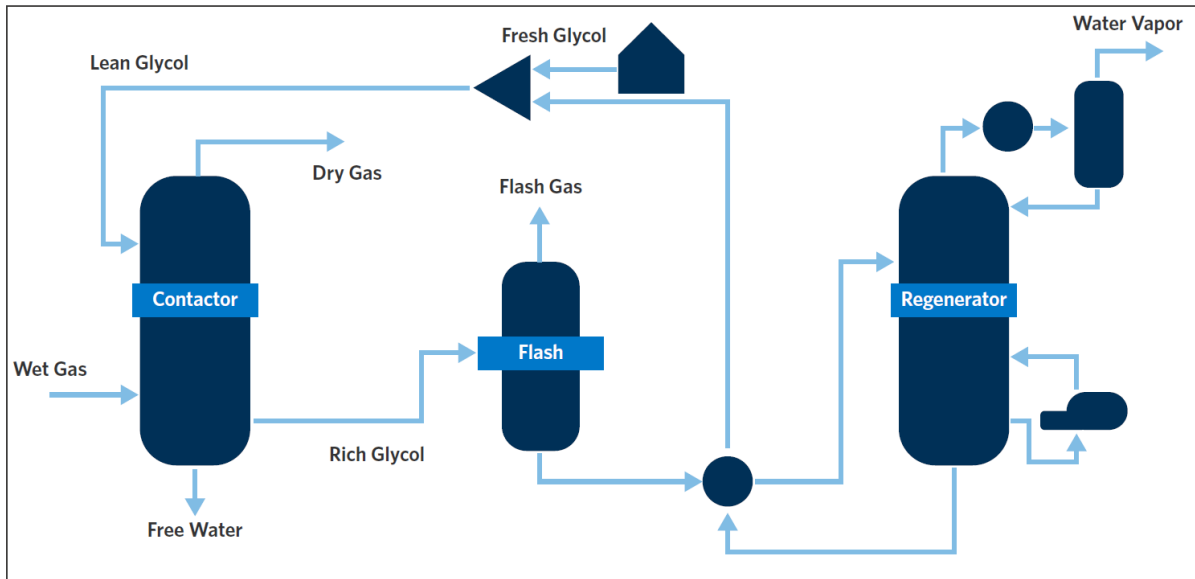
Figure 6 : Classical dehydration process [7]
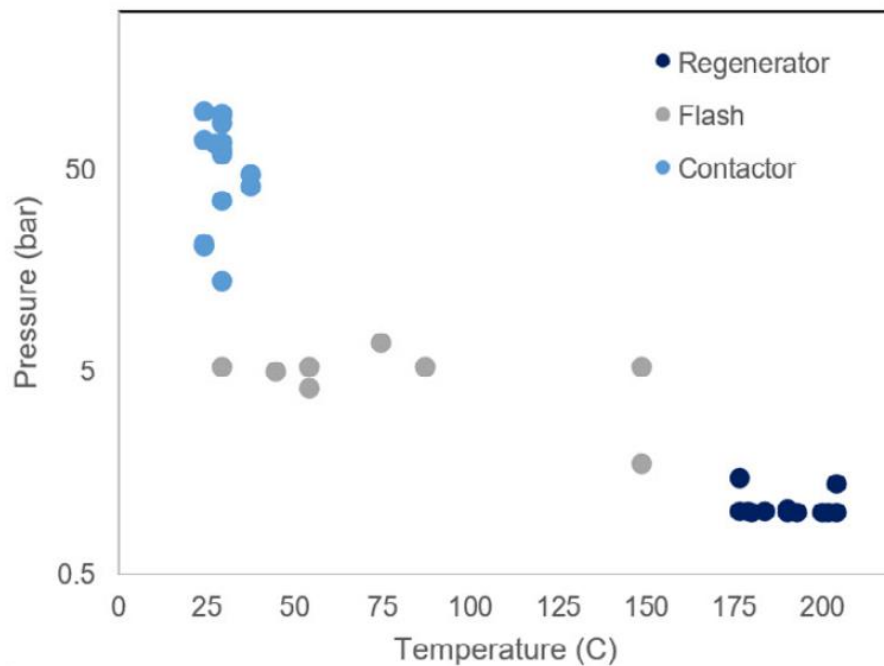
Figure 7 : Temperatures usually encountered during the various stages of the dehydration process [7]

However, this is where the problem lies. Every time glycol passes through the loop, it is heated to a high temperature and gradually degrades, reducing its effectiveness as a hydrate formation inhibitor/desiccant. In addition, in contact with many other chemical species, this degradation can potentially be enhanced. Therefore, it is essential to understand how the degradation of glycols works, how each experimental condition influences the speed of degradation, and the consequences of degradation on the inhibitory/dehydration efficiency.

5. Glycols, powerful desiccants

Ethane-1,2-diol, better known as monoethylene glycol (MEG) or even ethylene glycol, is the simplest chemical compound of the glycol family. Triethylene glycol (TEG), or more formally 2,2'-[Ethane-1,2-diylbis(oxy)]di(ethan-1-ol), also belongs to the glycol family. These two molecules have a strong affinity for water because of their two hydroxyl groups. In the natural gas industry, MEG is used primarily as a hydrate formation inhibitor. The TEG will be preferred for the offshore dehydration process [2].

III. Literature review about glycols degradation

The degradation of glycols used for natural gas production is a significant issue. It is, therefore, necessary to better understand this phenomenon and the degradation mechanisms in order to improve the efficiency of the natural gas dehydration process. The first thing to do is to see what the scientific literature can teach us on the subject. Surprisingly enough, while natural gas is the fastest growing source of energy in the world's energy mix today, the literature on the degradation about MEG and TEG glycols is more than limited. This lack of literature is even more glaring for TEG. The purpose of this chapter is to summarize the information available.

1. MEG degradation

Almost all the literature agrees that temperature is the key factor in glycol degradation: higher temperature increases the final concentration of degradation products. The presence of oxygen and more specifically its partial pressure is the second key factor; a greater quantity of oxygen in contact with the glycol will increase the rate of degradation. The same applies to mineral salts [5] or some metals like copper [11]. Their presence amplifies the effects of degradation. Apparently, the presence of certain metals can selectively increase the presence of certain degradation products [28][29]. Finally, when degradation takes place in the absence of oxygen, the influence of temperature tends to decrease (26).

1.1. Degradation products

Most of the articles published on MEG degradation agree that the main degradation products of MEG are organic acids. But that's where the scientific consensus ends. Indeed, the published data diverge more or less on the composition of the degradation products, as illustrated in Table 1 for the organic acids. The organic acids presented as degradation products are not always the same, and their relative quantity among the degradation products can vary a lot. Nevertheless, a certain trend is emerging; five organic acids are regularly cited as common degradation products of MEG: formic acid, acetic acid, glycolic acid, oxalic acid and finally glyoxylic acid. Figure 8 below shows a proposed mechanism for the formation of these acids from MEG.

The differences observed can be explained in several ways. On the one hand, it is obvious that not looking for a compound in an analysis will reduce the chances of detecting or identifying it. In fact, the literature studies demonstrate the presence of certain compounds among the degradation products but do not confirm the absence of other compounds among these degradation products. On the other hand, the experimental conditions implemented in each of the studies are very different. These include the temperature range, the proportion of water in the glycol solutions subject to degradation, the presence or absence of oxygen, and the duration of each experiment. Since the experimental conditions vary, it is not surprising to find different/different amounts of different compounds among the degradation products.
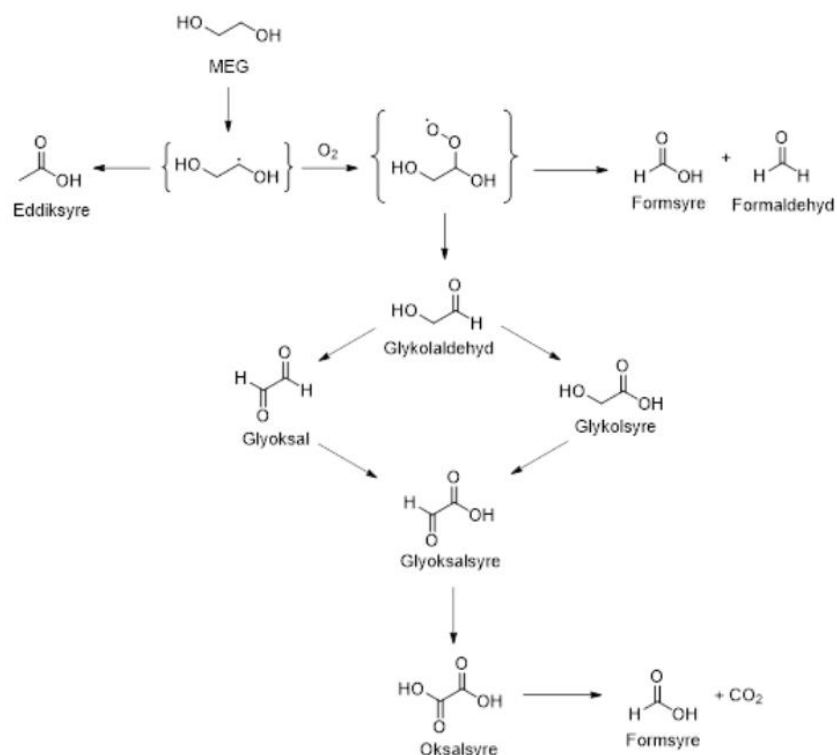
Figure 8 : Proposed reaction chain by my supervisor Karen Karolina Høisæter [1]

Table 1 : Relative amount of each of the following organic acids among the organic acids identified as degradation products according to différentes studies [28][29][21][26][6]

	Acetic acid	Formic acid	Glycolic acid	Oxalic acid	Glyoxylic acid
Rossiter et al. (1983-85)		+++	+++	+++	
Madera et al. (2003)	+++	++	++	+	+
Psarrou et al. (2011)	+	+++	+++		
AlHarooni et al. (2015)	+++	++	++		

Finally, it is, also, possible that the use of different analytical methods is the reason for these results, although all the degradation products concerned have a very similar structure. Table 1 below summarizes the conclusions of the main studies concerning the presence or absence of each of the above-mentioned organic acids (and their relative amounts when the necessary data are available). This table is intended only to give an idea of the diversity of results in the literature. Numerical results should not be compared since the experimental conditions are different for each study.

1.2. Degradation consequences

As degradation progresses, a change in the visual appearance of the glycol is immediately noticeable. This one, of colorless pulling on the yellow before any degradation, it turns gradually to a more pronounced yellow, then towards the orange, the brown to finish close to the black. The opacity of the solution declines at the same time. Foaming is sometimes observed on the surface of the glycol solution, but this seems to be more related to the presence of certain chemical species in the process than to the degradation itself.

Concerning the pH, the degradation of glycols (neutral species in the sense of Bronsted) into organic acids irremediably causes a drop in pH. However, the pH-concentration correlation of the degradation products is not clearly established. For example, let's take a glycolic solution with a pH of 7 originally. After subjecting this solution to experimental conditions favouring degradation, the concentration of degradation products is measured. The result is 20 ppm at pH 5; if the same solution is exposed to even more favourable conditions, it could, for example, have had a degradation product concentration of 2000 ppm without the pH being influenced. The mechanisms governing this phenomenon are still not well understood.

Finally, glycols are perfectly neutral compounds electronically speaking. However, during the degradation phenomenon, ionic species will appear, which irremediably causes an increase in the conductivity of the glycolic solution.

2. TEG degradation
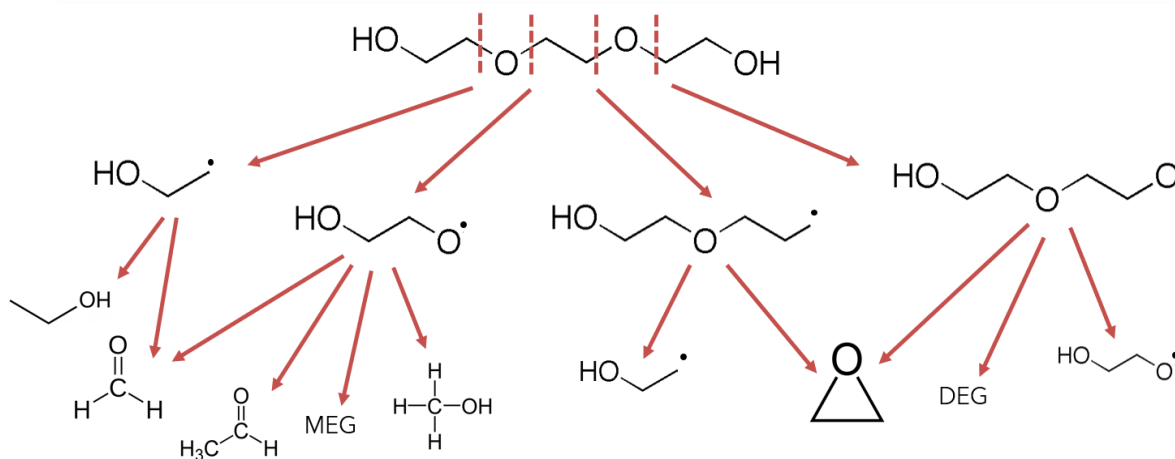
Figure 9 : Reactions and products from cracking of TEG [27]

As much concerning the MEG, the scientific literature exists although tenuous, as much concerning the TEG, the scientific literature is non-existent. It was possible to only find one article presenting possible degradation products [27]. But no experimental studies have been published concerning the thermal or oxidative degradation of the TEG. According to the authors, the TEG molecule would be sensitive to thermal cracking. Being greater than MEG, the diversity of degradation

products is also greater than that of MEG. According to the authors, the main cracking products are small alkanes, small alcohols, the MEG and DEG (di-ethylene glycol) glycols themselves, and other small organic molecules (Figure 9).

Of course, TEG can also be oxidized; the products are then largely similar to those resulting from cracking (and since MEG is among these "primary" products, it is easy to imagine that organic acids are among the "secondary" degradation products). Finally, to explain the presence of some atypical degradation products (gulose, adamentane...), the authors put forward the hypothesis of ionic reactions.

IV. Experiments description and Methodology

We are now getting down to the heart of the matter: the experimental part of this work. This chapter sets out the experiments and analyses carried out and the problems encountered.

As explained above, the existing scientific literature addressing the degradation of MEG and TEG glycols is quite limited. This was both a disadvantage for this work, for the impossibility of predicting in advance the result of this or that experiment, and thus potentially controlling its accuracy, but also a source of great motivation, as much remains to be discovered.

The objective of this first experimental part is to study the degradation parameters of MEG and TEG glycols. How do they degrade? How to characterize this degradation? How is does temperature in presence of oxygen influencing the degradation?

This experimental work can be divided into two parts: the experiment itself, which provided us with many samples for given experimental conditions, and then the analysis of these samples by different methods.

1. Degradation experiments

As we have seen in the literature, temperature has a great influence on the final concentration of degradation products after a given heating time. This means that temperature has a significant influence on the rate of degradation of MEG and TEG. A series of experiments was therefore set up to highlight this influence.

The experimental set-up consists of four glass jacketed reactors with a capacity of 250 mL. Jackets allow the reactors and their contents to be heated by circulating hot fluid. A heating bath with a pump allows the hot fluid to circulate continuously through the jackets. For this work, TEG was used as the heating fluid. The reactors are based on magnetic stirrer plates, allowing the use of stirrers during the experiments (Figure 10).

The reactors used are quadri-col: the main neck is topped by a condenser column to prevent the loss of MEG/TEG and degradation compounds. Nevertheless, each of them gives directly to the atmosphere. Two of the secondary necks are closed but can be opened, mainly for temperature measurement or sampling. In the last secondary neck, a sintered bubbler is introduced into the reactor, directly connected to the university gas network. In these experiments, oxygen is sent to ensure good oxygenation of the glycol solutions, the initial idea being to maximize the concentration of degradation products.. Due to this influx of oxygen, there is an overpressure in the reactor and the glycol solution is rather good isolated from the atmosphere.

For the last experiment (Oks 4, 140°C), this set-up was slightly modified. The outlet gas from the condensers were connected to wash bottles filled with soda at a concentration of 0.1 mol.L^{-1}, the idea being then to capture the volatile degradation compounds for analysis. After the wash bottles the gas was released to the atmosphere. The experiments were formed in fume cabinet to prevent contact with the volatile compounds.

Figure 10 : Experimental set-up with the guards

The protocol of the experiment was as follows. There are 4 reactors: 2 will be filled with MEG (R1 and R2), the other two with TEG (R3 and R4). Oks 1 was not carried out with TEG thinking initially that TEG will be super stable at 80°C. It was not possible to try the experiment again afterwards. A weighed amount of glycol is introduced into each of the reactors (approximately 200 g). A magnetic stirrer is then added to stir the glycol within the reactor. The cold fluid circuit (5°C), for the condenser, and the hot fluid circuit, for the jackets, were then switched on. Although the temperature of the hot fluid is reached gradually to avoid thermal shock, the time required to reach the desired nominal temperature is neglected. It usually only took a few hours. Concerning the guards, it was necessary to fill them with fresh soda, while making sure to weigh the quantity introduced, with a view to a future material balance. The contents of the wash bottles were renewed one week after the start of the experiment. In total four series of experiments were performed as shown in Table 2.

Table 2 : Denomination of the 4 series of experiments, temperature associated with each one and other details

Oks 1	Oks 2	Oks 3	Oks 4
80°C	100°C	120°C	140°C
MEG	MEG/TEG	MEG/TEG	MEG/TEG
No guards	No guards	No guards	Guards

Each experiment lasts 21 days. Samples were taken on day 0 (D0), and then day 3, 7, 10, 14, 17 and 21. On each occasion, approximately 3 mL were taken (then weighed for accuracy) and placed in vials. Each vial is then inerted with nitrogen to prevent oxidation of the glycols by atmospheric oxygen. Finally, the samples are stored in a refrigerator at 4°C, in order to slow down as much as possible, the natural degradation of the glycols, and thus avoid distorting future analyses. At the end of the experiment, the glycol remaining in each reactor is completely collected, weighed, and also stored cold.

It turns out that the temperature of the R4 reactor, for unexplained reasons, was constantly below the nominal temperature (a difference of the order of 5 to 8°C). The occurrence of this phenomenon is certain for Oks 3 and Oks 4 but nothing can be asserted for Oks 2. We'll come back to that later.

2. Analytical methods

2.1. Ion chromatography

In many of the scientific articles encountered, the most commonly used analytical method was invariably ion exchange chromatography, more commonly known as ion chromatography. As a qualitative and quantitative method, it was naturally decided to use it.

2.1.1. Simplified description of the method

Chromatographic methods are physico-chemical methods based on the separation of the different elements of a mixture, whether liquid or gaseous. The sample containing one or more species is carried by a mobile phase, the eluent, in contact with a stationary phase. Each chemical species present in the sample will migrate on/through the stationary phase with a speed that depends on its characteristics and those of the two phases present (Van der Waals forces, hydrogen bonds, etc). The separation of the different compounds may result from their adsorption/desorption on the stationary phase, or from their different solubility in each of the phases (mobile and stationary). There are many different chromatographic methods, depending on the nature of the mobile phase used, the support or the type of interaction involved.

Ion chromatography allows, in particular, to identify the ionic species present in the solution to be analysed. It separates the molecules according to their respective charged groups; the ions present in solution interact with opposite charges fixed on the stationary phase, resulting in their retention. The principle then remains the same as for most chromatographic methods.

2.1.2. Equipment and protocol

The ion chromatography apparatus used for this work is the ICS-5000 from Dionex. It is equipped with the IonPac AG15/AS15 columns also from Dionex. Chromeleon software (v7.1) is used for data processing.

The first step in the separation process is to send the eluent alone into the system until the baseline visible on the processing software appears stable. This can take several hours. The sample to be analyzed is then introduced by the autosampler into an injection loop of known volume. The eluent then carries this sample to the column where the stationary phase is located.

At the outlet of the column, the electrolyte is fed into the suppressor-detector. The detector used for this work is a conductivity detector. In other circumstances, spectrophotometric detectors may be used. The conductivity of a solution is its ability to conduct electricity between two electrodes. Its conductivity will be proportional to its ionic species content. However, this detection technique is very sensitive. This is why it is important to use ultrapure water for sample dilution. Equation (1), known as Kohlrausch's Law, relates the conductivity σ of a solution to the concentration of each of the ionic species present in the same solution as well as to their respective ionic molar conductivity λ.

$$\sigma = \sum \lambda_i * [X_i] \qquad (1)$$

The detector will most often be coupled to a suppressor, which is the case for the system used. The suppressor makes it possible to reduce the background conductance of the eluent, and by consequence to improve the conductance of the ions. Finally, the conductivity as a function of time is displayed using the data processing software. A series of successive peaks is generally obtained, each associated with a chemical species, its area under the curve being proportional to the concentration of the species in question in the sample studied.

To be more precise, this process is subject to the execution of a method containing all the necessary parameters: elution time, volume of eluent injected, etc. Several trials were therefore necessary to find the best method, capable of analysing the organic acids that can reasonably be imagined to be the main degradation products of the glycols studied. Using solutions containing the following five acids (formic, acetic, glycolic, oxalic and glyoxylic), the analysis parameters were adjusted in order to obtain a good separation of the different peaks.

2.2.   pH-metric titration

It should be remembered that with regard to degradation products, our attention is focused in particular on organic acids. Indeed, the existing scientific literature on the subject is unanimous on the presence of these acids among the degradation products, especially for MEG. And acid means pH-metric titration.

2.2.1. Theory

Usually, to carry out the titration of an acidic species, the simplest remains to use a solution of sodium hydroxide, more commonly known as soda. As the acid-base water-ion hydroxide couple has a pKa of 14, it generally allows most acidic species to be assayed efficiently in aqueous solution. This is where the first problem arises: we are not originally in aqueous solution. The samples are made from pure glycol. However, the literature teaches us that measuring the pH of an organic solution with a

glass electrode can sometimes take more than an hour [18]. Moreover, the measured pH will not be equivalent to the "normal" pH because the latter only applies in the case of aqueous solutions. Fortunately, it is possible to think that a rather important dilution with water allows to overcome this first difficulty. Moreover, even if the measured pH does not have the same definition, it is the quantity of protons in solution that interests us, obtained by the change of curve and not thanks to pH values.

The configuration of the apparatus used for the assays requires an assay solution of at least 100 mL; since the samples taken were only 3 mL, it was necessary in any case to dilute the sample before assaying. Once this has been set up, we can assume that it is possible to measure the amount of total acid in each sample using this method. Unfortunately, one problem never comes alone, so two potential obstacles present themselves.

First, although ion chromatography has allowed us to identify some glycol degradation products, some remain unknown. However, it is not impossible that one of these compounds is also an organic acid, or at least a species that can react when soda is poured. This uncertainty makes it difficult to measure the concentration, even total, of organic acid.

Secondly, it is important to note that oxalic acid is a diacid. In other words, there is no simple soda-acid equivalence, since the titration of one mole of acid requires two moles of soda in this case. And since the relative amount of oxalic acid among the organic acids present is unknown to us, it becomes almost impossible to measure the total amount of organic acid.

For all these reasons, it is impossible to determine the cumulative amount of organic acids present among the degradation products. However, we can determine the amount of H protons available in the degradation products. Indeed, whether in the form of a monoacid or a diacid, an organic acid or a more conventional acid, a proton remains a proton. And the quantity of soda poured will allow us to obtain the quantity of protons available in the sample.

2.2.2. Preliminary experiments

The device used for dosing is the 800 Dosino by Metrohm, coupled with the 814 USB Sample Processor. The Timeo v3.2 software is used to follow the titration.

First of all, it was essential to understand how the organic acid mixture could react when dosed with soda. In fact, it is assumed that 4 acids were an integral part of this mixture: formic, acetic, glycolic, and oxalic acids. However, the titration of a solution containing several acids can be complex. Let us note already that the 4 acids concerned are weak acids. Usually, the titration of a solution containing a weak acid with a strong base (case of soda) gives a curve as shown in Figure 11.

However, if several weak acids are in solution, even though their pKa is quite similar, a single equivalent volume will appear on the dosing curve. Classically, a difference of at least 4 between two pKa is considered necessary to see the two equivalences appear. In our case, the pKa of the different acid-base couples involved are shown in Table 3. In the light of these values, it can be assumed that two equivalences will appear: one for the first acidity of oxalic acid and another for formic acid, acetic acid, glycolic acid and the second acidity of oxalic acid.

Weak Acid/Strong Base Titration Curve
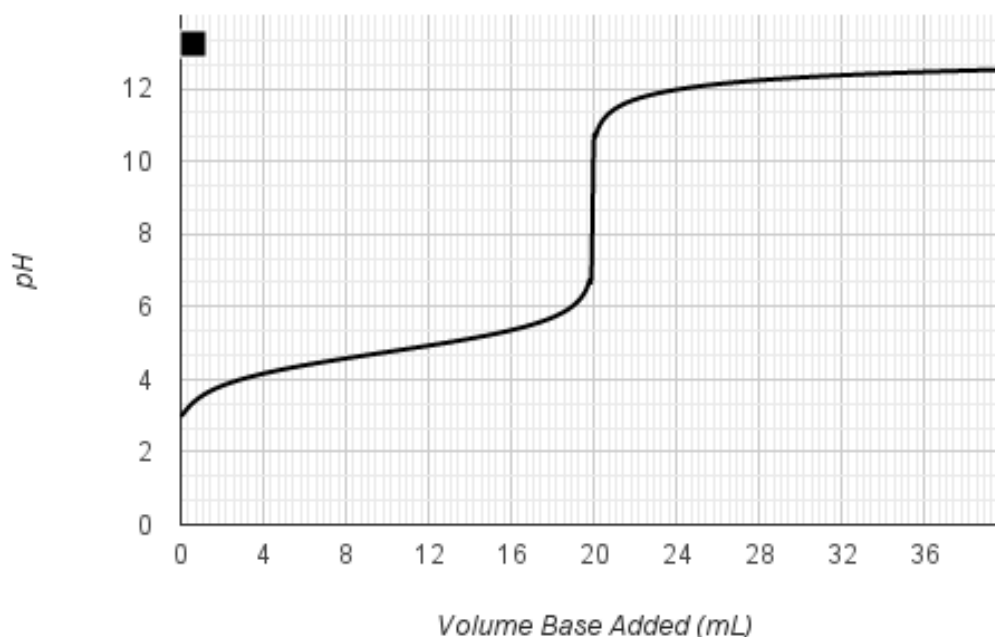
Figure 11 : Weak acid/strong base titration curve

Table 3 : pKa of organics acids studied [22][24]

Acid	pKa
Formic	3.75
Acetic	4.76
Glycolic	3.83
Oxalic	1.2/4.3

To verify this, solutions containing the four organic acids (equimolar) were prepared and then titrated with sodium hydroxide solution of concentration C = 0.1 mol.L^{-1}. The following curve is obtained (Figure 12). We finally observe that even if a slight inflection appears, the first equivalence that was supposed to be visible is not. On the other hand, the second is perfectly visible. We will consider for the rest of this work that the only visible equivalence (if there is only one in the case of degraded glycol samples) represents the titration of all the organic acids present.
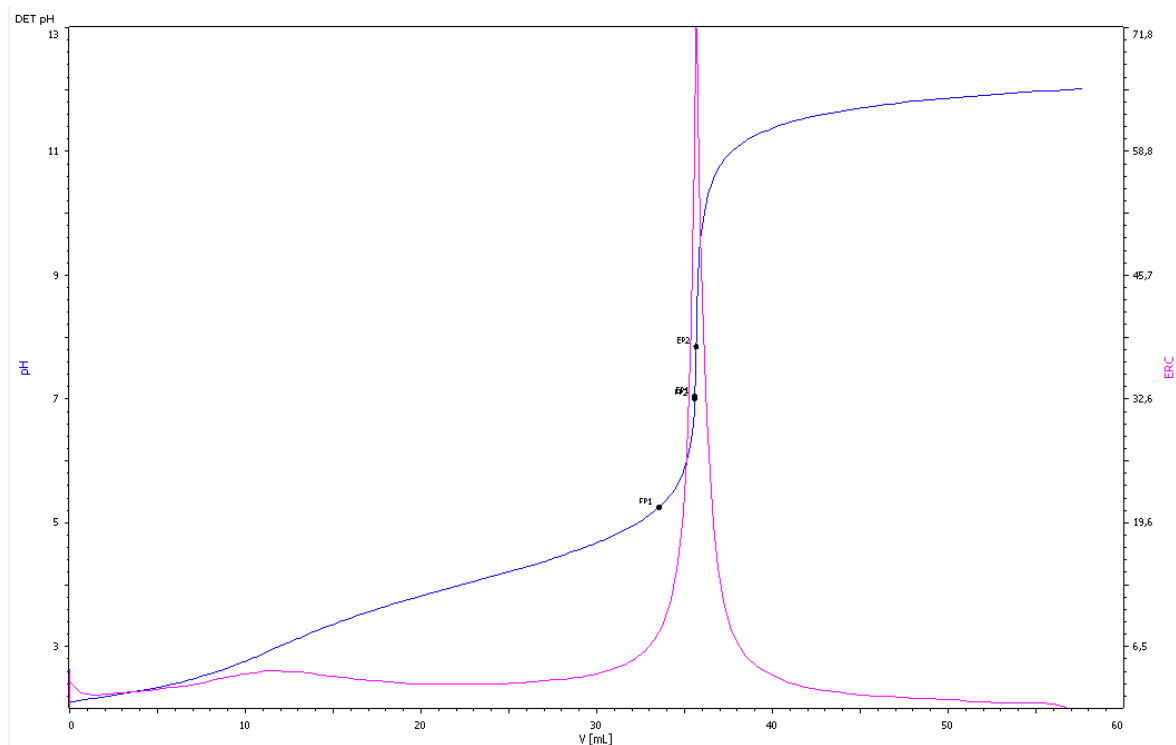
Figure 12 : Titration curve for the mix of four acids

2.2.3. Equipment and protocol

As stated previously, a 100 mL sample is required for the electrode to plunge properly. Since we have a limited amount of degraded glycol, and since this method of analysis is destructive, diluting a small amount of sample seemed to be the best solution.

Consequently, for each degraded sample at our disposal, a few drops were diluted in a volume of about 100 mL of distilled water and the sample masses used and the distilled water were weighed. The solution obtained was then titrated with sodium hydroxide solution of concentration C = 0.1 mol.L^{-1}. The data processing software then gave us access to the volume equivalence. From this, it is possible to determine the quantity of H$^+$ ions present in the sample using the following reaction equation (i.e. one mole of soda is poured in for each mole of acid present in solution):

$$H^+ + HO^- = H_2O$$
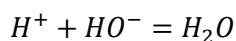
2.3. Spectrophotometric analysis

This work also looked at changes in the colour of samples taken during degradation. Indeed, as explained previously, the observations reported from natural gas facilities or the scientific literature agree on a progressive change in the colour of the glycol correlated with its degradation. It would therefore be possible to monitor the progress of the degradation phenomenon by tracking the colour of the glycol solution.

35

But first of all, a little memory refreshment is in order. Spectrophotometry is the name given to the scientific field concerned with the measurement of energy transported by electromagnetic radiation. Within this field, we find spectrometry, or spectroscopy, an analytical method that can be both qualitative and quantitative. This method consists of measuring the absorbance (the ability of a medium to absorb the light that passes through it) of a given chemical compound, usually in solution. The more concentrated the sample, the more light it absorbs. There are two equations to remember about spectroscopy. The first one physically defines the absorbance, commonly noted as A. Note that absorbance is a positive value, without a unit.

$$A = log\left(\frac{I_0}{I}\right)$$

When a light beam of intensity I_0 passes through a cell containing the solution to be analysed, part of the light is absorbed by the species present in solution. The intensity I of the transmitted light is therefore lower than I_0.
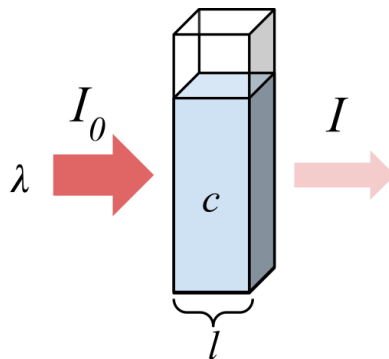
It is also possible to relate the absorbance and the concentration in solution of the solute analysed: this is the Beer-Lambert relationship. For a given wavelength, the absorbance of a solution is proportional to its concentration. Thus, for a solution containing a single absorbent substance:

$$A_\lambda = \varepsilon_\lambda * l * c$$

With ε the molar attenuation coefficient, l the tank length and c the solution concentration of the solute. Since absorbance is an additive quantity, the absorbance of a solution containing several chemical species capable of absorbing light will be equal to the sum of the absorbance of each of these species. In any case, not knowing the exhaustive list of degradation products, the Beer-Lambert relationship as such is of no use to us. But spectroscopy can allow us to follow the degradation process and perhaps understand some of these mechanisms.

The device used for this work is the Heλios γ by Thermo Electron Corporation. It was not possible in this state to export the data obtained. That is why photos of the spectrophotometer screen are used to illustrate the results. I apologize in advance for their poor quality.

3. Simulation tools

3.1.   A little reminder of thermodynamics

The physico-chemical, thermodynamic and phase equilibrium properties of pure components or mixtures depend, among other things, on the strength of intermolecular forces. However, the greater the amount of intermolecular forces, the more the behaviour of the fluid will be far from ideal. Roughly speaking, it can be said that systems consisting of pure fluids or mixtures of non-polar molecules are close to an ideal behaviour. Equations of state are therefore used to describe their behaviour. If, on the contrary, polar molecules dominate in the system under study, the behaviour of the system will be far from ideal, due to the formation of hydrogen bonds in particular. Models based on liquid activity coefficients (LACM) will therefore be used.

The calculation of the phase equilibrium is the basis for any simulation of thermodynamic properties. And for the calculation of phase equilibrium, it is imperative to use fugacity. In the case of a liquid-vapor equilibrium, the following equation can be written:

$$f_i^L = f_i^V$$

With f_i^L the fugacity of compound i in the liquid phase

f_i^V the fugacity of compound i in the vapor phase

Vapour phase fugacity is systematically calculated using a state equation, whereas for liquid phase fugacity, a equation of state or activity coefficient model can be used. And of course, this depends on the polar or non-polar nature of the chemical species making up the system.

In the case of an equation of state, the following formula shall be used:

$$f_i^L = \varphi_i^L * x_i * P$$

With φ_i^L the fugacity coefficient of compound i in the liquid phase

x_i the molar fraction of compound i in the liquid phase

P the system pressure

If an activity coefficient model is used, the equations below will be used:

$$f_i^L = \gamma_i * x_i * f_i^{L,0}$$

$$f_i^{L,0} \approx P_i^{sat}$$

With γ_i the activity coefficient of compound i

$f_i^{L,0}$ the fugacity of pure compound i in the liquid phase

3.2.   Tested models

As we have seen, the main criterion for selecting the appropriate model remains the presence or absence of polar molecules among the compounds present in the system. Water and the glycols MEG and TEG happen to be polar molecules. The NRTL (non-random two-liquid) model is classically used to describe non-ideal systems. But other models are available on Aspen Plus. Moreover, the polarity of the molecules present is not always decisive in the choice of model. Two other models are worthy of attention, as they exist, among others, to describe the natural gas dehydration process.

3.2.1.   Glycol package

The Glycol package is a model originally available on Aspen HYSYS, but it is also available on Aspen Plus. This model was chosen for this comparative study because it is a model created to describe the interactions between TEG and water, to simulate satisfactorily the natural gas dehydration process using TEG as an absorbent. This model is based in particular on the Twu-Sim-Tassone equation of state:

$$P = \frac{RT}{V_m - b} - \frac{a}{(V_m - 0,5b)(V_m + 3b)}$$

3.2.2.   CPA

The second model chosen for comparison is the CPA (Cubic-Plus-Association) package. This is a model classically used to simulate processes involving hydrocarbons. However, Aspen also encourages the use of this model for the simulation of the dehydration process, in order to, fill the

gaps in the Glycol model (use of MEG as a sorbent for example). It is based on the modified Soave-Redlich-Kwong State Equation (SRK), with a second part including terms describing association and polarity effects.

$$P = \frac{RT}{V_m - b} - \frac{a(T)}{V_m(V_m + b)} - \frac{1}{2}\left(\frac{RT}{V_m}\right)\left(1 + \frac{1}{V_m}\frac{\partial lng}{\partial(\frac{1}{V_m})}\right)\sum_i x_i \sum_{A_i}(1 - A_i)$$

3.2.3. ELECNRTL

The ELECNRTL model is a derivative of the NRTL model. It includes a wider range of interactions and allows in particular to simulate the presence of electrolytes, salt precipitation problems and the presence of acid gases in solutions. The main equation of the model remains that of the NRTL model:

$$ln\gamma_i = \frac{\sum_j x_j \tau_{ji} G_{ji}}{\sum_k x_k G_{ki}} + \sum_j \frac{x_j G_{ij}}{\sum_k x_k G_{kj}}\left(\tau_{ij} - \frac{\sum_m x_m \tau_{mj} G_{mj}}{\sum_k x_k G_{kj}}\right)$$

$$G_{ij} = f(\alpha_{ij}, \tau_{ij}), \ \tau_{ij} = f(a_{ij}, b_{ij}, e_{ij}, f_{ij}) \ and \ \alpha_{ij} = f(c_{ij}, d_{ij})$$

3.3.   Methodology

Let us now talk about the simulations carried out in order to compare the different models with each other. On Aspen Plus, a flash was used for liquid-vapor equilibrium calculations. The flowsheet used is shown below (Figure 13). The main objective of these simulations was to calculate the maximum solubility of certain solutes (liquid or gas) in given solvents. The flash reactor is fed by two streams, one for the solvent, the other one for the solute (whose solubility is to be determined). Two other streams allow the exit of the gas and liquid phases of the flash. For each simulation, the temperature within the flash and the vapour fraction have been fixed. The vapour fraction has been fixed at 0.0001 to obtain a vapour stream rich in solute and a liquid stream rich in solvent at the output of the flash. The solvent flow rate remained constant. For each simulation, a sensitivity analysis was conducted by varying the solute flow rate; for each flow rate, a solute molar fraction-pressure couple was obtained. Between 100 and 200 points were obtained for each solvent/solute pair of interest.

Each of these sets of pairs was then plotted for comparison with experimental data available in the literature. In order to quantify the accuracy of the models, the deviation relative to the experimental value was calculated for each experimental point using the following formula:

$$\Delta\% = \frac{P_{sim} - P_{exp}}{P_{exp}} * 100$$

It should be noted that the molar fraction values available in the literature and those obtained through simulations are not necessarily the same. It was therefore necessary to perform a polynomial interpolation of the available calculated data. Using the LINEST function, the coefficients of a 6th-order polynomial regression of the calculated data were obtained. Using these coefficients, the total pressure values corresponding to the molar fractions of solute available in the literature were determined.
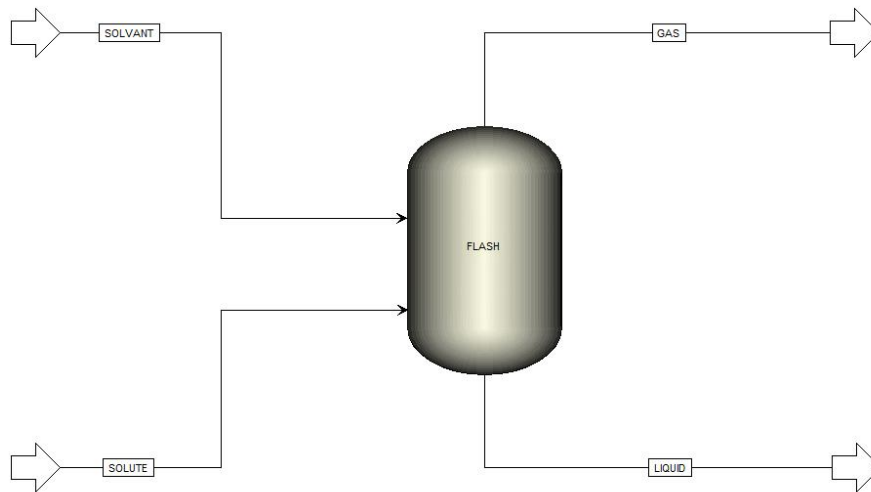
Figure 13 : Flowsheet used for calculations

V.   Results and discussion

It should be noticed here that all the analyses were carried out on D21 samples. Due to lack of time, we were unable to analyse less degraded samples. D21 samples were chosen as a priority for analysis because we assumed, they had the highest expected concentration of degradation products. Similarly, the MEG samples will always be those from the R2 reactor, and the TEG samples from the R3 reactor (with some exceptions).

1. Initial observations

Although only a rigorous analysis of the samples by proven methods can allow us to establish with certainty the quantity and composition of the degradation products, it is possible to speculate on certain hypotheses simply by observing the experiment.

1.1.   Evolution of the colour

First of all, it is obvious that the colour of the glycolic solution changes during the experiment. On the one hand, during the same experiment, the solution becomes darker and darker, going from yellow to orange and then to a very pronounced amber colour. On the other hand, for same sampling day, the glycolic solution also gets darker and darker with increasing temperature (Figure 14). However, as we have been discussed earlier, a darker colour is often the manifestation of a greater degradation of the glycol. It is therefore reasonable to suggest that the degradation becomes more significant over time at the same temperature, and more significant as the temperature rises for fixed sampling day. Observations that are consistent with the literature.

It should be noted that this colour variation is much more important for the TEG. In other words, for the same temperature and progress of the experiment, the TEG will have a darker colour than the MEG. It can therefore be hypothesized that the TEG degrades faster than the MEG, or at least that the impact of temperature in presence of oxygen on degradation is greater in the case of the TEG than the MEG.

It is difficult to conclude anything about the composition of glycol degradation products. Formic, acetic, glycolic and oxalic acids are colourless. However, glyoxylic acid happens to have a beautiful orange-yellow colour. It can therefore be hypothesized that the concentration of glyoxylic acid increases in the degraded samples during the experiments. Also, acetaldehyde and crotonaldehyde has been proposed to be responsible for the colour [1], but it was not possible to confirm this during the master thesis.

Figure 14 : We can see on this image the evolution of the colour of degraded TEG samples (R3). The background row corresponds to Oks 2 (100°C), the middle row to Oks 3 (120°C) and the front row to Oks 4 (140°C).

1.2.   Proportion of volatile compounds

At the end of each experiment, the mass of glycol contained in each reactor is weighed. Since the same mass has been weighed before the experiment and the samples withdrawn during the experiments are weighted, it is possible to compare the change in mass due to degradation. In the first experiment at 100°C (Oks 2) it is observed that the amount of glycol is more or less the same after degradation for both MEG and TEG. However, for a temperature of 120°C (Oks 3), the mass of TEG after the experiment is much lower than the mass initially introduced, a phenomenon that is not observed for MEG. This difference is even more obvious with a temperature of 140°C (Oks 4). It can be assumed that the proportion of volatile degradation products increases with time and temperature. Since it would appear that the oxidative degradation of TEG is faster than MEG, the amount of TEG in the reactor decreases much faster than that of MEG.

1.3.   Odour of the samples

Finally, it is easy to notice that the degraded samples give off a vinegar smell, which may be associated with the presence of acetic acid among the degradation products; this would be perfectly consistent with the scientific literature. It should be noted that the strength of this vinegar odour increases with time, with the final samples having the most pronounced odour. It is necessary to specify that at no time did I voluntarily smell the samples. It is just something that happened during the dilutions of the samples for different analysis.

2. Ion chromatography results

These initial observations thus enabled us to establish that the TEG was more easily degradable in the presence oxygen, and that the proportion of volatiles among the degradation products increases for high temperatures. However, this is not sufficient to understand the influence of temperature on glycol degradation. Fortunately, after conducting these experiments, we had a large set of samples available for analysis. And we start now with IC results. All chromatograms of interest that are not presented in this chapter are available in Appendix A.

2.1.   First problems

The most important thing with ion chromatography is to get a chromatogram with well-separated peaks. And that's the rub. It was impossible to obtain a correct separation of the peaks, even though the extreme values of certain parameters were reached. For this reason, the contribution of ion chromatography will be purely qualitative and not quantitative.

In addition, the chromatograms of the first samples analysed show peaks, or at least "abnormal" bumps (particularly noticeable for MEG since MEG samples are less diluted for ion chromatography, as explained later). After verification, the same peaks and bumps can be found for pure undegraded glycol samples. This is rather difficult to explain; since glycols are not ionic species, their chromatogram should have been more or less flat. A sample of the pure glycols was analysed by NMR; it was found that the containers had not been contaminated, as one might have thought.
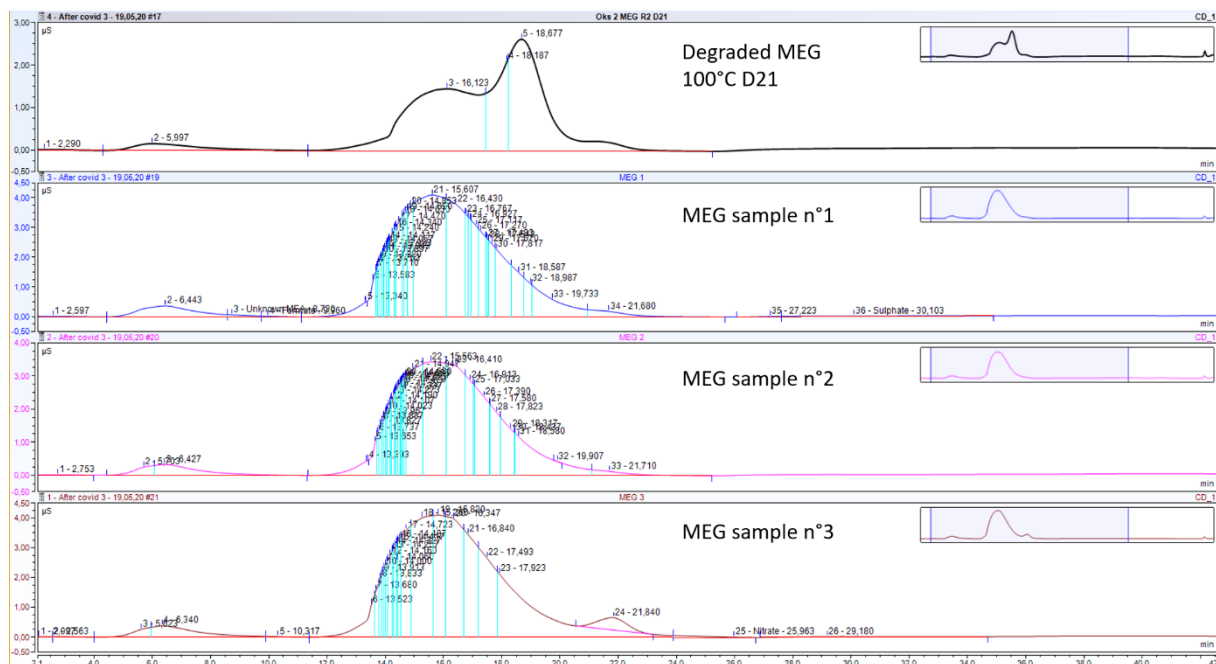
Figure 15 : Degraded MEG/undegraded MEG comparison

After further analysis, it was found that the MEG from different bottles, and even from different batches, always had the same profile. This is therefore not a problem of contamination but of MEG interference with the column. No explanation could be found. Figure 15 shows the chromatogram of a degraded MEG sample as well as those of three MEG samples from three different bottles. The large bump in the middle is clearly visible and is overlapping with the peak of a degradation product.

2.2. Identification of degradation products

Despite the problems encountered, it is still quite possible to identify certain degradation products, at least those visible on chromatograms. Indeed, since the area of each peak (and thus its height) depends on the concentration of the compound in the sample, an artificial increase in this same concentration will be immediately visible on the chromatogram. A series of vials has therefore been prepared containing degraded glycol, some of the acid whose presence we wish to confirm, and ultrapure water to dilute the whole.

The diluted samples without added acids were analysed first. Then comes the turn of the samples containing an excess of acid. If the area or height of a peak increases significantly between these two steps, we can reasonably assume that the peak in question corresponds to the acid in excess. The following acids were tested: formic, acetic, glycolic, oxalic, and glyoxylic. Initially, all the diluted samples had a concentration of about 100 ppm.

The first point we can make is that the concentration of organic acids in degraded MEG is much lower than in degraded TEG. The difference is at least a factor of 100, which is why it was necessary to prepare the vials for degraded MEG not from a diluted sample stock solution but from the sample itself. The concentration of the degraded sample for the analysis was therefore about 10,000 ppm.
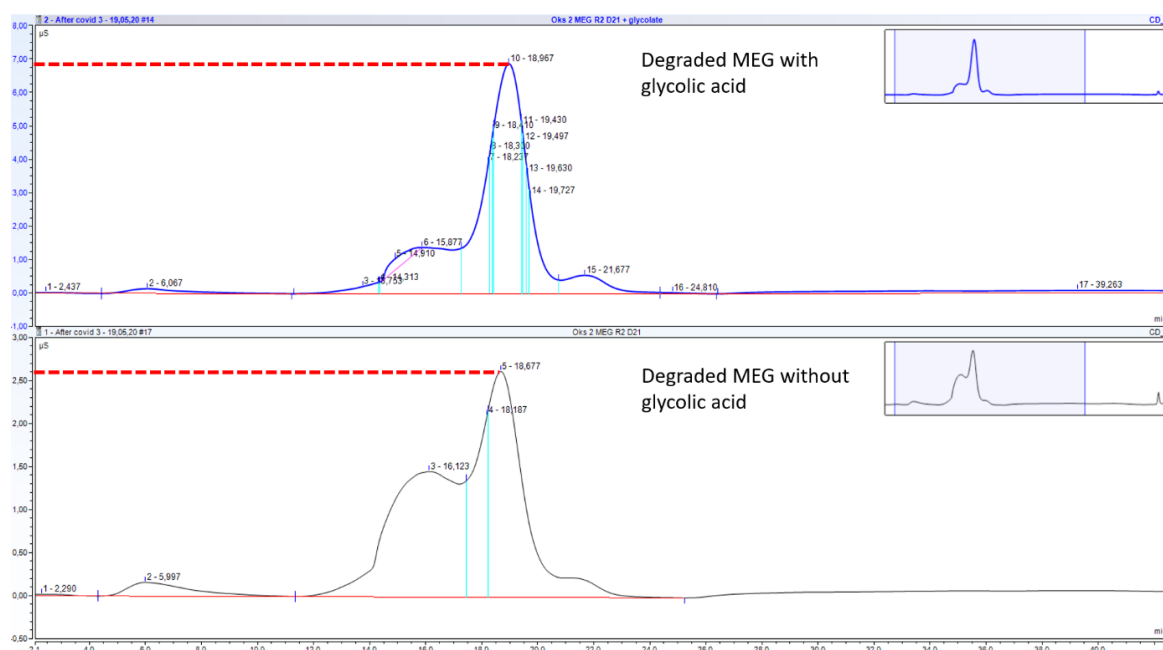
Figure 16 : Demonstration of the presence of glycolic acid among the degradation products of MEG

Figures 16 and 17 show two of the comparative analyses carried out. The first proves the presence of glycolic acid among the degradation products of MEG. The upper half (with excess acid) clearly shows the increase in peak height at about 19 minutes. The second figure shows the absence of glyoxylic acid among the TEG degradation products. The upper half (with excess acid) shows a flattened peak that is completely absent from the degraded glycol sample alone.
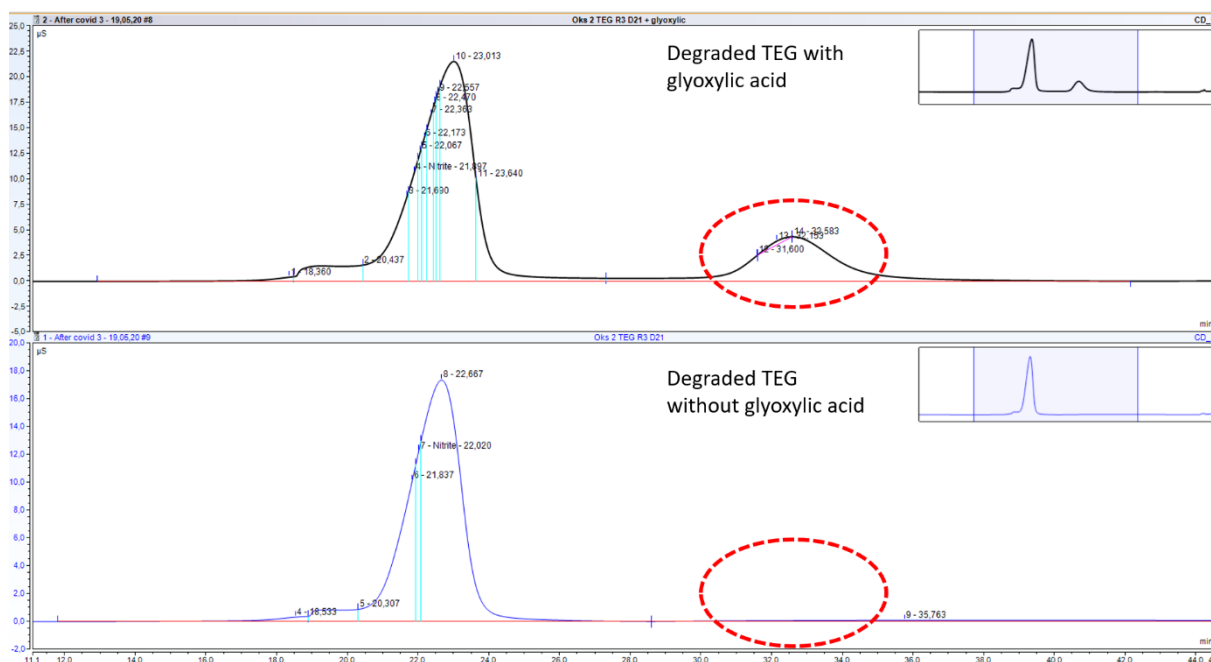
Figure 17 : Demonstration of the absence of glyoxylic acid among TEG degradation products

This trick allowed us to identify some degradation products for MEG and TEG. The results are reported in Table 4. It is immediately noticeable that in the absence of glyoxylic acid, we are unable to explain the colour of the degraded glycol. We are also limited by the fact, mentioned earlier, that the peaks corresponding to glycolic, acetic and formic acids are very close together. In each case (TEG and MEG), the presence (or absence) of two acids is uncertain; at least one of the two acids is present, and possibly both. But we cannot say with certainty whether or not both acids are present. Finally, it should be noted that an unidentified peak, present not far from that of oxalic acid, is found on chromatograms of all analysed degraded TEG samples. It was not possible to identify to which species this peak corresponded.

Table 4 : Summary presence (or not) of organic acids

	Formic acid	Acetic acid	Glycolic acid	Oxalic acid	Glyoxylic acid
MEG	/	/	Present	Present	Absent
TEG	Present	/	/	Present	Absent

2.3. Relative amount of organic acids

Ion chromatography can also give us an idea of the relative presence of each of the organic acids studied among the degradation products. At the beginning of this work, we had placed great hopes in ion chromatography, particularly to quantify the organic acids present in the degraded samples. Therefore, calibration curves for each of the acids studied was established. These curves were established by measuring the area of a peak obtained by analysing a solution of known concentration for each species. This procedure is repeated for solutions of different concentrations; a correlation between area and concentration can then be deduced. In this way, when a sample is analysed, all that remains to be done is to measure the area of the peak representative of the species of interest to obtain its concentration in the sample.

Such curves were established in the first part of this work. We therefore know the relationship between area under the curve and concentration for each of the acids studied. It turns out that the area/concentration ratio is more or less the same for each of the acids in aqueous blends of specific acid and non-degraded MEG/TEG, with at most a factor 2 difference. We can therefore imagine that if a peak, corresponding to an acid A, is 10 or 20 times larger than the peak of an acid B, the concentration of acid A in the sample analysed is certainly greater than that of acid B. Thus, it is possible to estimate the relative importance of each acid among the total sum of organic acids in the degraded samples. Table 5 below summarizes the conclusion of our observations.

Table 5 : Summary relative amount of each organic acid (+++ means "dominant", + means "few")

	Formic acid	Acetic acid	Glycolic acid	Oxalic acid	Glyoxylic acid
MEG	-	-	+++	+	/
TEG	+++	-	-	+	/

Glycolic acid appears as the main organic acid among the degradation products of MEG. However, it is formic acid that takes this place in the case of TEG. In both cases, oxalic acid is present, albeit in small quantities. Finally, in both cases, the last two acids (formic and acetic for MEG, acetic and glycolic for TEG), whose presence we remember, is not certain, have in any case an even lower concentration.

Finally, it should be noted that the calibration curves were initially obtained by diluting the acid concerned in a certain volume of ultrapure water. In order to ensure that the MEG or TEG had no effect on the ratio area/concentration, further analyses were carried out, this time with solutions containing the acid concerned but also one of the glycols. It turned out that the presence of glycol has no influence on this ratio, and so we can therefore use the first curves established without problems.

If we compare the results obtained so far for MEG with those of the scientific literature, we notice some differences. On the one hand, unlike Madera et al [21], no traces of glyoxylic acid were

found among the degradation products of MEG. On the other hand, we have demonstrated the presence of oxalic acid among the DGs. However, Psarrou [26] and AlHarooni [6] did not report it. But as we explained before, perhaps this is due to the fact that they did not try to demonstrate the presence of this acid. Finally, the relative distribution of the organic acids does not correspond to any case in the literature. In this work, the glycolic acid is the most present organic acid among the degradation products of MEG. However, in the literature, glycolic acid is at best in equal proportion to formic acid, at worst very little present. Again, this can be explained by differences in experimental protocol.

2.4.   Evolution of the relative quantify of organics acids

With ion chromatography, one can also compare the chromatograms of samples from the experiments at different temperatures. In this way, we would be able to observe the influence of temperature on the relative amount of each organic acid among the set of organic acids identified as degradation products of the glycols studied.
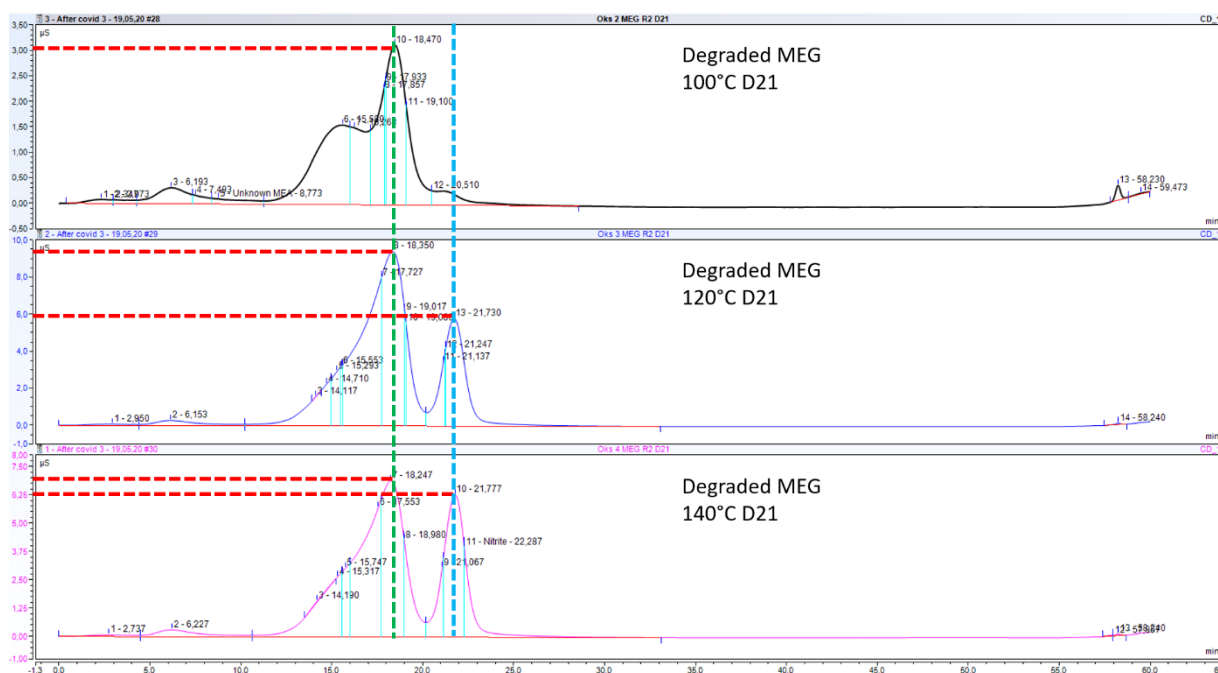
Figure 18 : Evolution of the chromatograms (100°C, 120°C then 140°C) MEG, R2. The peak in the middle corresponds to glycolic acid and the one on the right to formic acid.

Concerning TEG, there is no significant change (see Appendix A). However, the impact of temperature on the composition of the degradation products of MEG is much more interesting. We observe a strong increase in the quantity of formic acid as the temperature rises from 100°C to 120 then 140°C (Figure 18). At the same time, the quantity of glycolic acid increases between 100 and 120°C and then flows back. It would therefore appear that temperature has a significant impact on the distribution of degradation products, at least for MEG.

3. Titration results

Ion chromatography has allowed us to identify certain products resulting from the degradation of glycols. However, due to the almost generalized overlap of the constituent peaks of the various chromatograms obtained, it was impossible to establish the absolute quantity of each of the degradation products with precision. This is where pH-metric titration comes in.

First, it turned out that diluted 100-fold, there was no problem in measuring the samples of degraded TEG; the concentration of acidic species remained sufficiently high. However, for the MEG samples, once diluted, it was impossible to assay them properly. This dilution is necessary for the electrode to be in the solution. The soda solution used was therefore changed for another one, of concentration 0.001 mol.L^{-1}. Unfortunately, the concentration of acid species was so low that the starting pH of the diluted solution was around 6.5 making it impossible to titrate the solution. It was therefore decided not to assay the degraded MEG samples. It should be noted in passing that these facts confirm the observations made during the use of ion chromatography, namely that the organic acid concentration in degraded MEG was at least 100 times lower than the concentration in degraded TEG.

Additional support of low concentrations of degradation compounds in MEG comes from Nuclear Magnetic Resonance (NMR) analyses. NMR analyses were also planned, but due to the closure of the labs, only a few could be performed. In particular, the relative amount of MEG throughout the degradation. The analyses were carried out for Oks 4 (140°C) and were conducted by my co-supervisor Karen Karolina Høisæter. NMR allows us to quantify the compound being analysed. Indeed, the integrated intensity of a resonance signal is directly proportional to the number of nuclei represented by this signal. It was therefore decided to study the relative amount of glycol during degradation. The figure 19 clearly shows the progressive degradation of glycol and the relative loss it induces. But this loss remains moderate, just over 2% after three weeks. This may explain the low amount of acids detected during the ion chromatography and titration analyses.
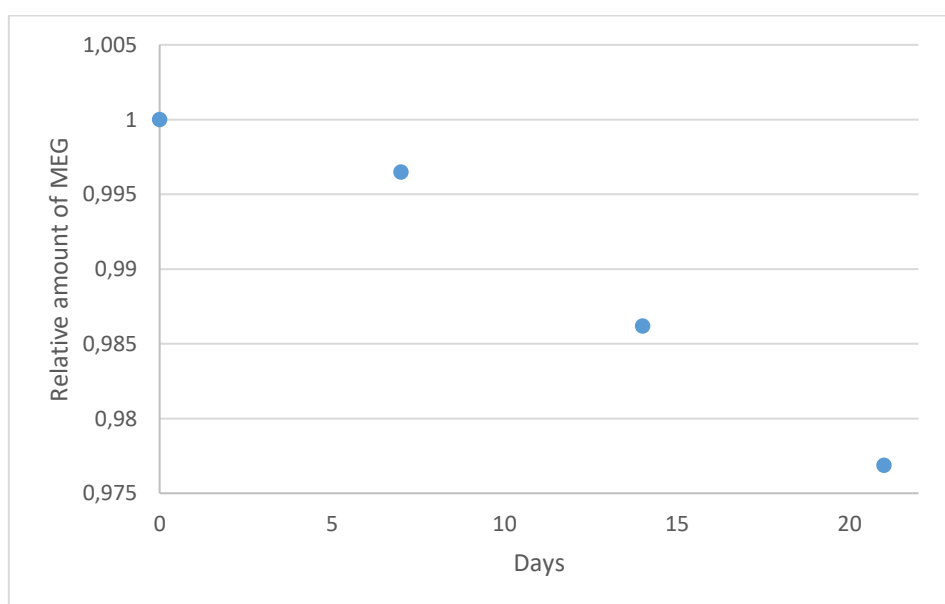
Figure 19 : Evolution of the relative amount of MEG in the reactor during degradation (Oks 4)

However, when it comes to TEG, titration method could be used. Figure 20 shows a typical pH curve obtained for the dosing of diluted solutions of TEG degraded. As aqueous NaOH is gradually added, the pH should increase as the dosage progresses. However, after the first equivalence, at pH around 9, the pH suddenly decreases even when NaOH is added. This happened for all diluted TEG degraded solutions. Initially it was assumed that this was related to the pH meter or electrode. But the titration of a hydrochloric acid solution (without TEG) using the same material and the same soda solution gave a perfectly normal dosing curve. It is therefore assumed that the sudden decrease is possible that an unknown compound in the degraded solution may react with NaOH, once the soda solution is in excess.
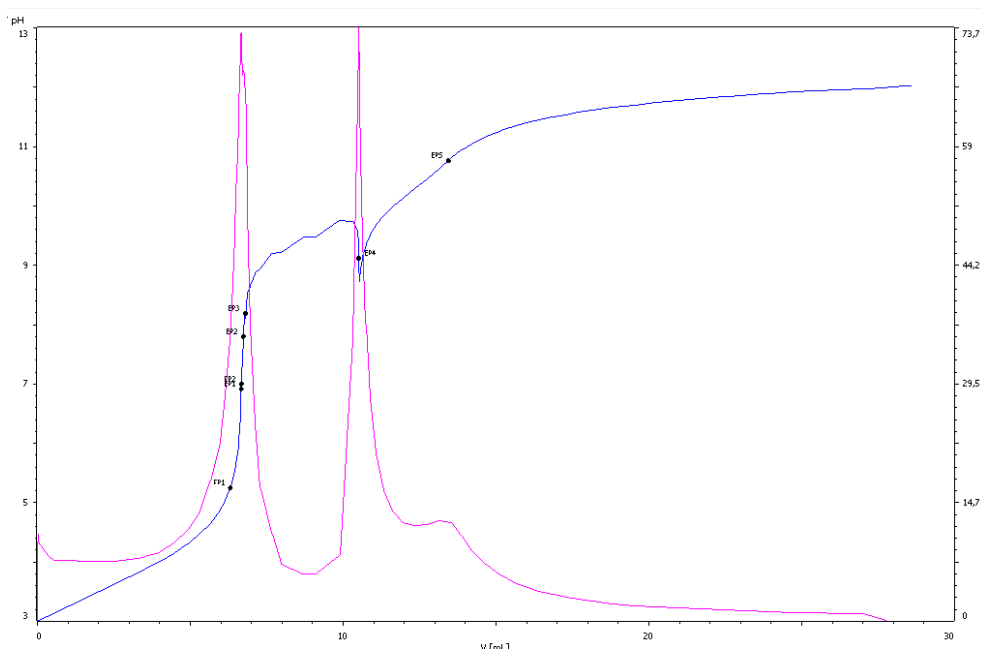
Figure 20 : Typical titration curve of degraded TEG samples

In any case, an equivalence can still be observed at pH around 7 to appear before the aberration occurs. It was therefore accepted that it was still possible to determine the quantity of protons contained in the samples taken. And even if we were to make an error of judgement, assuming this, the use of this volume at the equivalence would still allow us to see a trend in the concentration of protons.

The results obtained are shown in the tables 6 and 7 below. The tables show concentration of protons in the experiments performed at 100, 120 and 140°C from pure solvent (D0) until the end of the experiment (D21). It is immediately noticeable that the further the degradation progresses, the greater the concentration of acidic species (and thus organic acids). However, it can be seen that for the same sampling day, the acid concentration is higher for T=100°C than for 140°C.

49

	Day	"C"protons (mol/g)
Oks 2 (T=100°C)	0	< 0,0001
	3	0,0003
	7	0,0014
	10	0,0027
	14	0,0052
	17	0,0056
	21	0,0067
Oks 3 (T=120°C)	0	
	3	0,0003
	7	0,0012
	10	0,0018
	14	0,0027
	17	0,0039
	21	0,0051
Oks 4 (T=140°C)	0	
	3	0,0005
	7	0,0012
	10	0,0016
	14	0,0016
	17	0,0023
	21	0,0021

As mentioned earlier, the temperature of the R4 reactor was a few degrees lower during the experiments. The effect of temperature is clearly seen in the titration results. Indeed, the proton concentrations are higher in the samples from the R4 compared to R3 in the parallel experiments.

Table 7 : Proton concentration (mol.g-1) in experiments Oks 2, Oks 3 and Oks 4

	Oks 2		Oks 3		Oks 4	
	R4	R3	R4	R3	R4	R3
Day	T = ?	T = 100°C	T = 112/125 °C	T = 120°C	T = 132/135 °C	T = 140°C
3	0,0005	0,0003	0,0006	0,0003	0,0006	0,0005
7	0,0021	0,0014	0,0019	0,0012	0,0012	0,0012
10	0,0041	0,0027	0,0028	0,0018	0,0020	0,0016
14	0,0063	0,0052	0,0041	0,0027	0,0027	0,0016
17	0,0070	0,0056	0,0049	0,0039	0,0035	0,0023
21	0,0069	0,0067	0,0056	0,0051	0,0037	0,0021

4. Polymers as degradation products?

During the preparation of the diluted solutions for the pH-metric determinations, a surprising discovery was made. When introducing the few drops of samples into the distilled water, a yellow-orange substance appeared. This phenomenon only occurred for the TEG samples of the Oks 4 (140°C) series from days 14 to 21. Little of this substance is formed when diluted D14 sample was prepared, much more from a D21 sample. This substance is solid in appearance, granular in solution, but viscous when one tries to isolate it. A sample was taken, dissolved in organic phase and sent for NMR analysis. It is believed to be a polymeric compound. Figure 21 shows two photos of this substance.

In general polymer formation is favoured at high temperatures [1], which would explain why only the samples exposed for the longest time at the highest temperature allow its appearance in large enough quantities to be visible to the naked eye. However, as mentioned, the pH-metric assay allowed us to establish that the concentration of organic acids decreased, to our great surprise, when the temperature increased. It is generally reported that higher temperatures cause greater degradation. We can therefore assume that this polymer may be a secondary degradation product, formed from organic acids. The acids could also react to other secondary degradation compounds that were not identified in this work.

Figure 21 : Curious yellow and viscous substance observed during the dilution

5. Spectroscopy results

Concerning the first observations made, it should be remembered that the MEG hardly changed colour during the experiments, regardless of the temperature to which it was subjected (in fact, it is possible to perceive a very slight colour change in the last days of the Oks 4 experiment). The following analyses are therefore exclusively dedicated to the TEG.

5.1. Preliminary observations

The first idea was to scan a wide range of wavelengths in order to get an overview of the absorbance profile of the samples, and more precisely of the wavelength corresponding to the absorption peak. Since the color of the degraded samples changes from a slightly greenish yellow to a reddish brown (when color evolution occurs), we can assume that the absorption peak will not be located at the same place for two different advancements (in days). For a greenish-yellow sample, the absorption peak will be located around 350 nm (wavelengths correspond to indigo, complementary colour). And for an orange-brown sample, it should be located around 450-500 nm (wavelength corresponding to turquoise). But all this remains theoretical.

In fact, all samples give the same absorbance profile, at least as far as the position of the absorption "peak" is concerned. It's even a little more complicated than that. Because below about 300 nm, it is a succession of peaks and troughs of different values. Then appears a straight half of what appears to be the absorption peak. I apologize in advance for the poor quality of Figure 22. Not being able to extract the data or make a screenshot, I had to improvise. A scanner was made to obtain an enlargement of the ante peak part. Nothing conclusive could be drawn from it. It's just a succession of peaks and troughs without much meaning. On the other hand, concerning the "peak", it seems that we only have a part of it, so it is impossible to observe any shift. The only noticeable difference on the profiles between the different samples is the absorbance value for this "peak". It is all the more important as the solution is orange, and thus as the degradation is advanced. Note finally that the position of this pseudo peak is always the same, 288 nm.
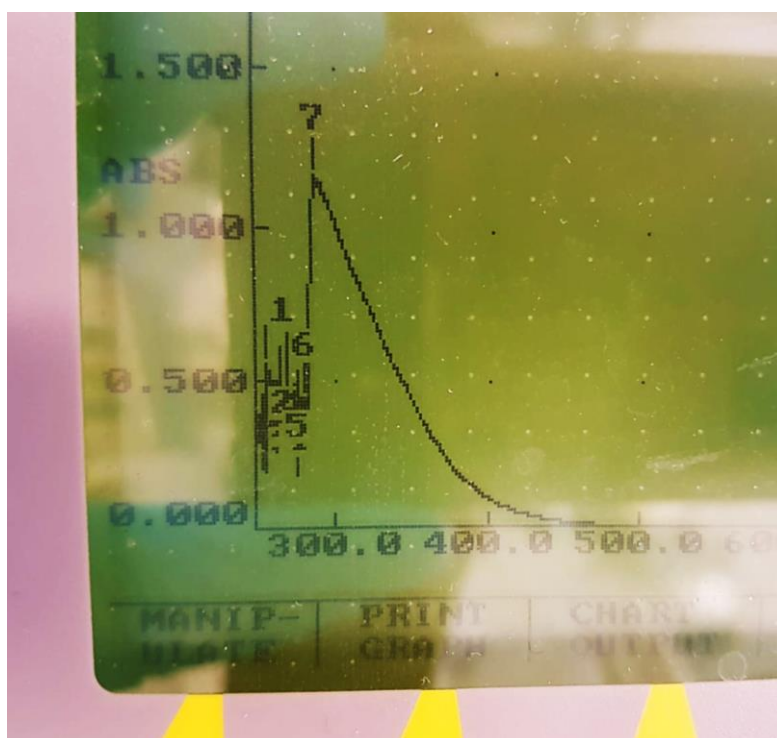
Figure 22 : Typical absorbance profile for degraded TEG

It was therefore decided to study the absorbance of each sample (diluted) for a fixed wavelength. To obtain conclusive results, the wavelength chosen (300 nm) is within the absorption peak but slightly distant from the pseudo peak. Diluted solutions were therefore prepared by accurately weighing the mass of sample used and the mass of water required for dilution. Then the

absorbance of each of these solutions was measured. Dilution was necessary because the absorbance of the sample would have been too high.

It should be noted that it was then necessary to correct these absorbances because not all of them were measured for the same sample concentration. A correction factor therefore made it possible to obtain the absorbance of each solution for the same concentration. This is not a problem because the composition of each solution does not change. According to Beer-Lambert's law, the absorbance depends only on the concentration of the sample.

5.2. Results

When the absorbance curves are plotted as a function of the sampling day, Figure 23 is obtained. For the samples from Oks 2 (100°C), their absorbance is obviously extremely low in comparison, which is consistent with the colouring of the samples (not going beyond light yellow). For the samples from Oks 3 (120°C), we observe a slow take-off of the absorbance at the beginning and then it increases more significantly after the 10th day. Finally, we can observe a slowing down of this evolution, which we suppose to be a warning sign of a plateau. This could agree with the first observations, which saw a kind of stagnation of the evolution of the colour.
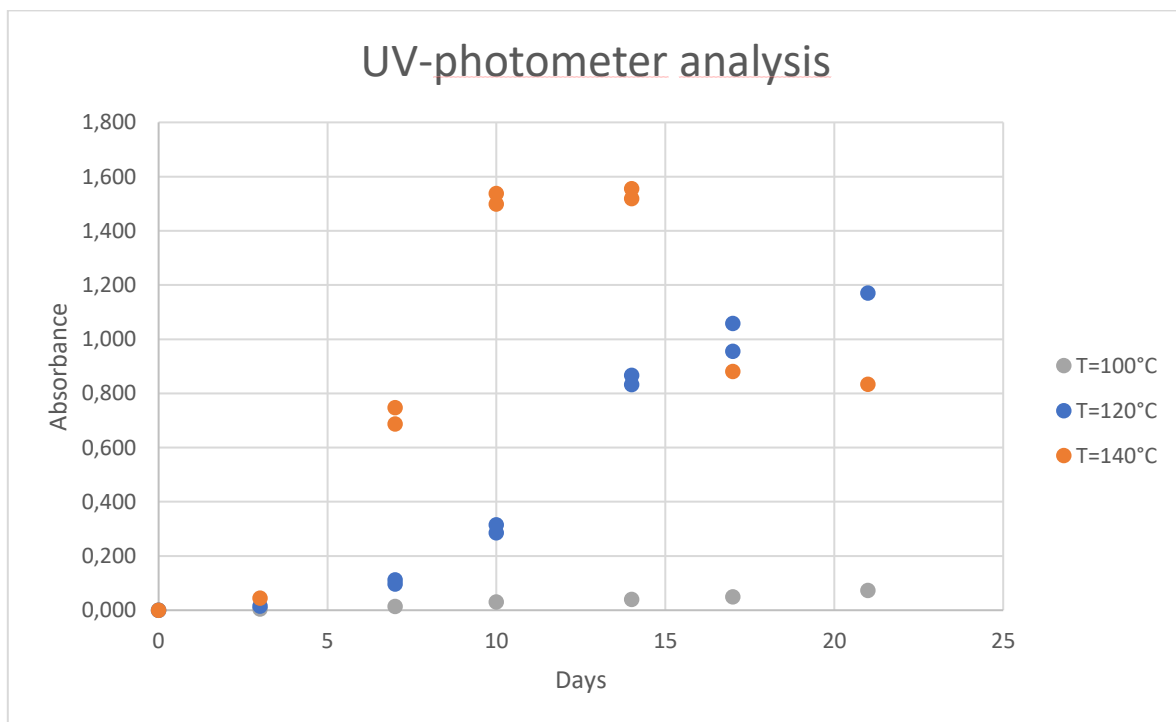
Figure 23 : Absorbance (λ=300 nm) of diluted TEG samples as a function of sampling days. Results for R3 are shown

At 140°C, absorbance first increases until 10-14 days, then starts to decrease. The initial increase is much faster for 140°C than for 100 and 120°C. But the subsequent decline is unique to Oks

4. This seems to be due (again) to the formation of the yellow, viscous compound when the degraded TEG samples are diluted in distilled water. Indeed, the formation of this compound is attested (at least to the naked eye) only for the dilution of Oks 4 D14, D17 and D21 samples. However, as the amount of precipitate formed seems to be increasing (more for D21 than for D14), it is likely that this phenomenon is correlated with the progressive decrease of the absorbance after day 10-14.

Acetone was used to isolate this compound for analysis. It was therefore attempted to circumvent this problem of polymer formation by using acetone as a solvent for spectroscopic analysis. For some unknown reason, it was not possible to obtain a stable value of pure acetone (for the blank) at this wavelength. In addition, it was important to precisely know the mass of solvent used for the dilution. Since acetone is very volatile, it was difficult to obtain an accurate value. This idea was subsequently abandoned.

VI.   Properties simulations in Aspen Plus

The experimental part of this work thus enabled us to identify certain products resulting from the degradation of MEG and TEG, to understand the influence of temperature on their degradation, and to compare the effects of the degradation on each of the glycols studied.

While this work was originally intended to be purely experimental, the COVID-19 pandemic caused the laboratories to close. Unable to continue experiments, it was decided to carry out simulation work on Aspen Plus. The initial objective was initially to understand the influence that the progressive degradation of the glycol could have on the efficiency of dehydration process. Indeed, feedbacks teaches us that the degradation of the desiccant is often correlated with a decrease in the efficiency of the dehydration process. But this correlation, this influence of the degradation on the efficiency of the dewatering process is poorly known.

However, it is first necessary to ensure that the thermodynamic model chosen correctly describes the physical properties of the pure components and mixtures. Due to lack of time, the simulation part of this work will therefore be exclusively devoted to the comparison of available models. In this purpose, some physical and thermodynamic properties were used as case studies. Experimental data available in the literature were compared with the results obtained using 3 different models, all of which may seem adequate.

It should be noted that in most cases only one temperature is compared. This is because, on the one hand, some experimental data were only found for one temperature. On the other hand, for lack of time. It is therefore obvious that the validity of a model for one temperature is not guaranteed for all of them.

1. Density

Before we begin to look at liquid-vapour equilibria, some comparisons have been made concerning the physical and thermodynamic properties of pure MEG and TEG glycol. Although less important for the simulation of the dehydration process, it is interesting to see how each model is able to describe these properties with more or less accuracy. It should be noted, however, that in this case it is not the equation of state itself that allows the calculation of these properties, but other equations integrated into the models. We start with the MEG density as a function of temperature.

The comparison is shown in Figure 24. It is immediately noticeable that the CPA model describes the density of MEG rather poorly, especially for low temperatures. The calculated values were compared with the experimental values of Afzal et al. [4]. In fact, even if the CPA model is indeed the least accurate, the difference with the experimental values remains adequate with a relative deviation of less than 4% for this temperature range. The ELECNRTL model that best describes the density of pure MEG, with a relative deviation of less than 0.1%. The Glycol model does well with a deviation of less than 1%. The deviations are shown in Appendix B.

Figure 24 : Density of MEG in the temperature range of 0 - 160°C. Blue figures represent experimental data [9][34][4][8] ; orange, grey and yellow lines represent models results

The same comparison was made for the TEG density. The results are more or less the same (Figure 25). The ELECNRTL model remains the best, with less than 0.5% relative deviation. The CPA model can reach a relative deviation of 6%.

Figure 25 : Density of TEG in the temperature range of 0 - 160°C. Blue figures represent experimental data [4] ; orange, grey and yellow lines represent models results

2. Viscosity

The same comparisons were made regarding the viscosity of the two glycols. Concerning the MEG, it is immediately observed that the curve of the Glycol model (Figure 26) shows a kind of hump around 60°C. The relative deviation then reaches 50% when the values from the simulation are compared with those of Bohne et al. [9]. Overall, the glycol model shows a relative deviation of more than 15% (except for low temperatures i.e. under 20°C). On the other hand, the two other models studied provide the same values. The CPA and ELECNRTL models are suitable for describing the evolution of the MEG viscosity, with a relative deviation of less than 2%. It is also normal that the CPA and ELECNRTL models show the same results since they use the same sub-model (Andrade) to calculate the viscosity.

Figure 26 : Viscosity of MEG in the temperature range of 0 - 160°C. Blue figures represent experimental data [31][9][34] ; orange, grey and yellow lines represent models results

Once again, the results are more or less the same for the TEG: the glycol model shows an hump between 80 and 110°C and the relative deviation exceeds in this case 200%. Even if the relative deviation is greater in the case of the TEG, the CPA and ELECNRTL models remain acceptable with a deviation that rarely exceeds 15% (Figure 27).
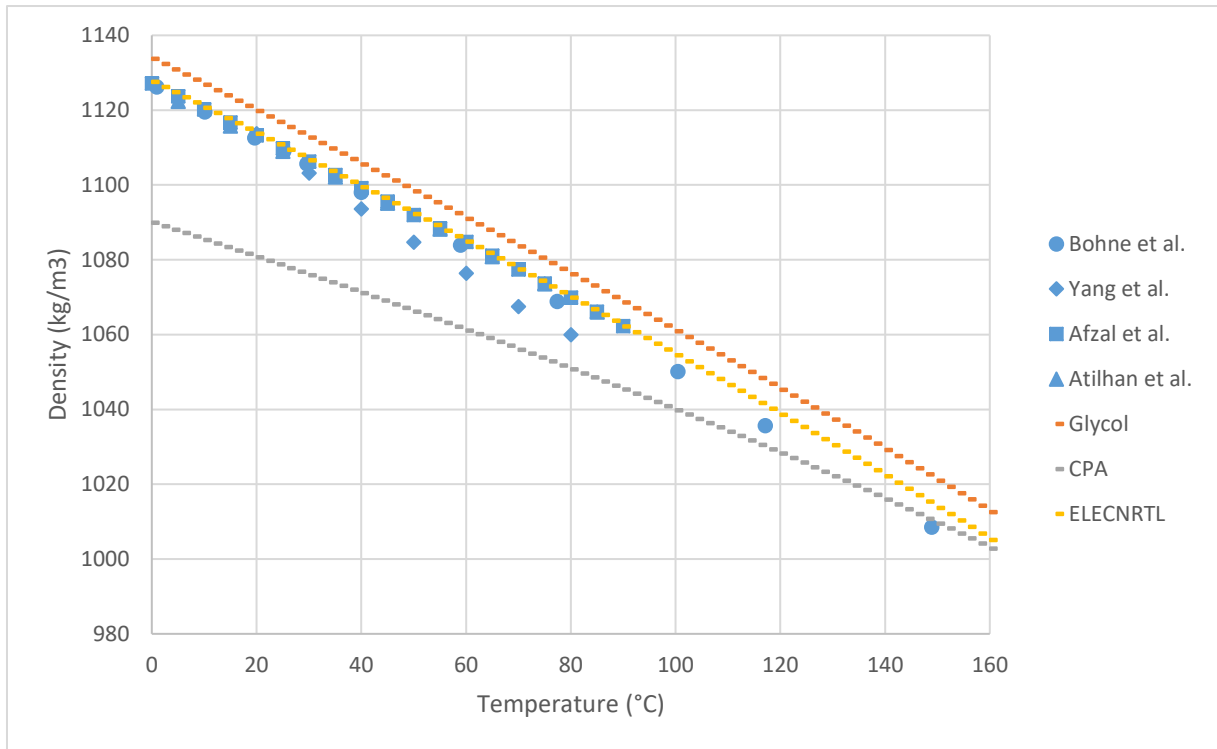
Figure 27 : Viscosity of TEG in the temperature range of 0 - 160°C. Blue figures represent experimental data [31] ; orange, grey and yellow lines represent models results

3. Thermal conductivity / Heat capacity

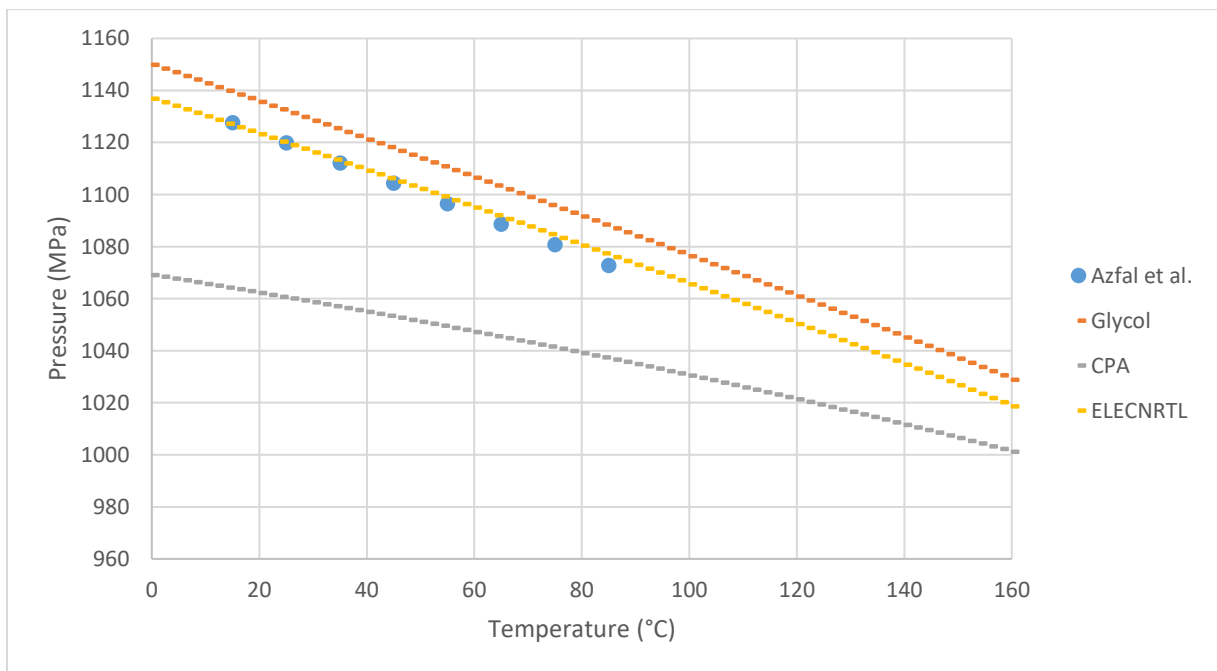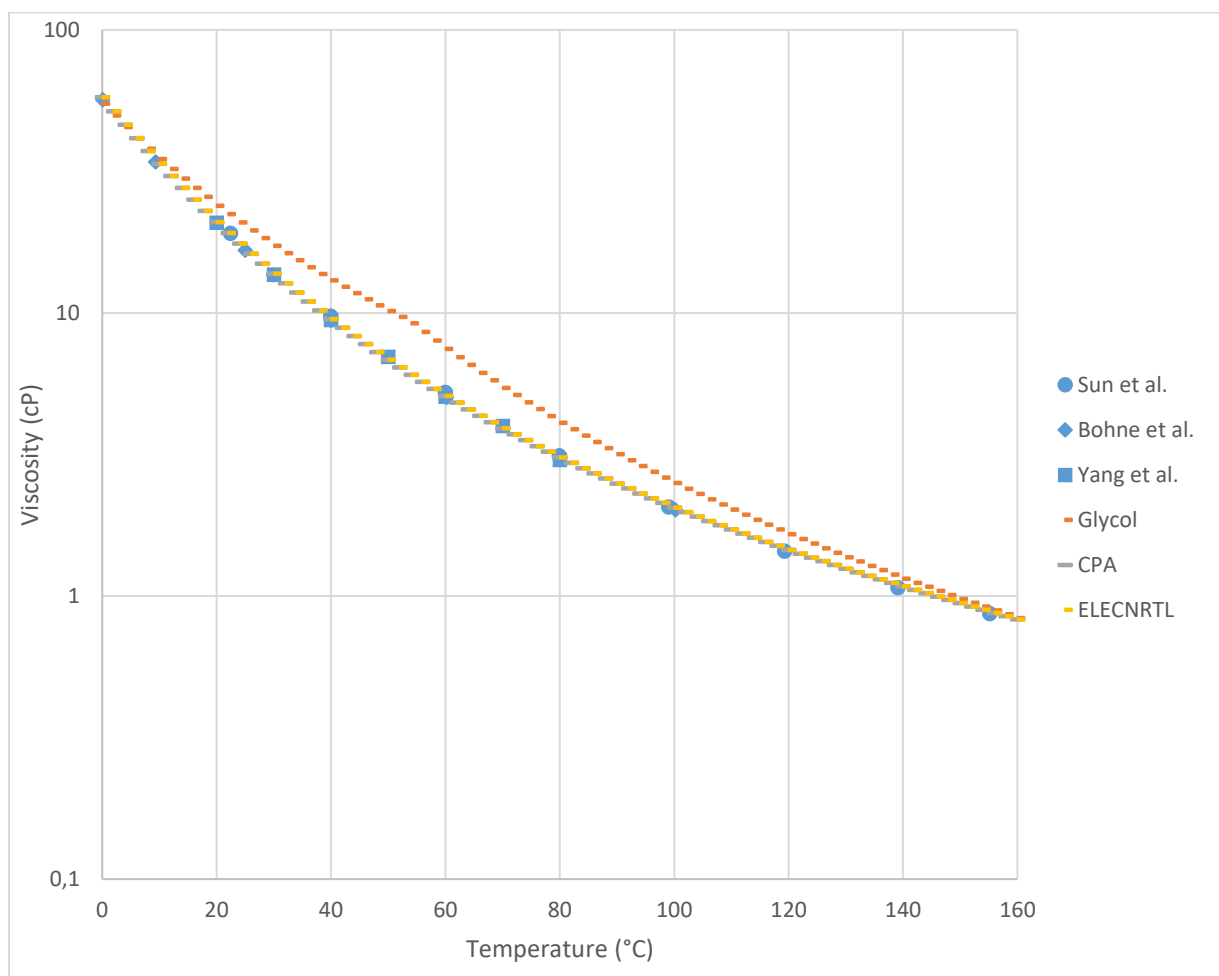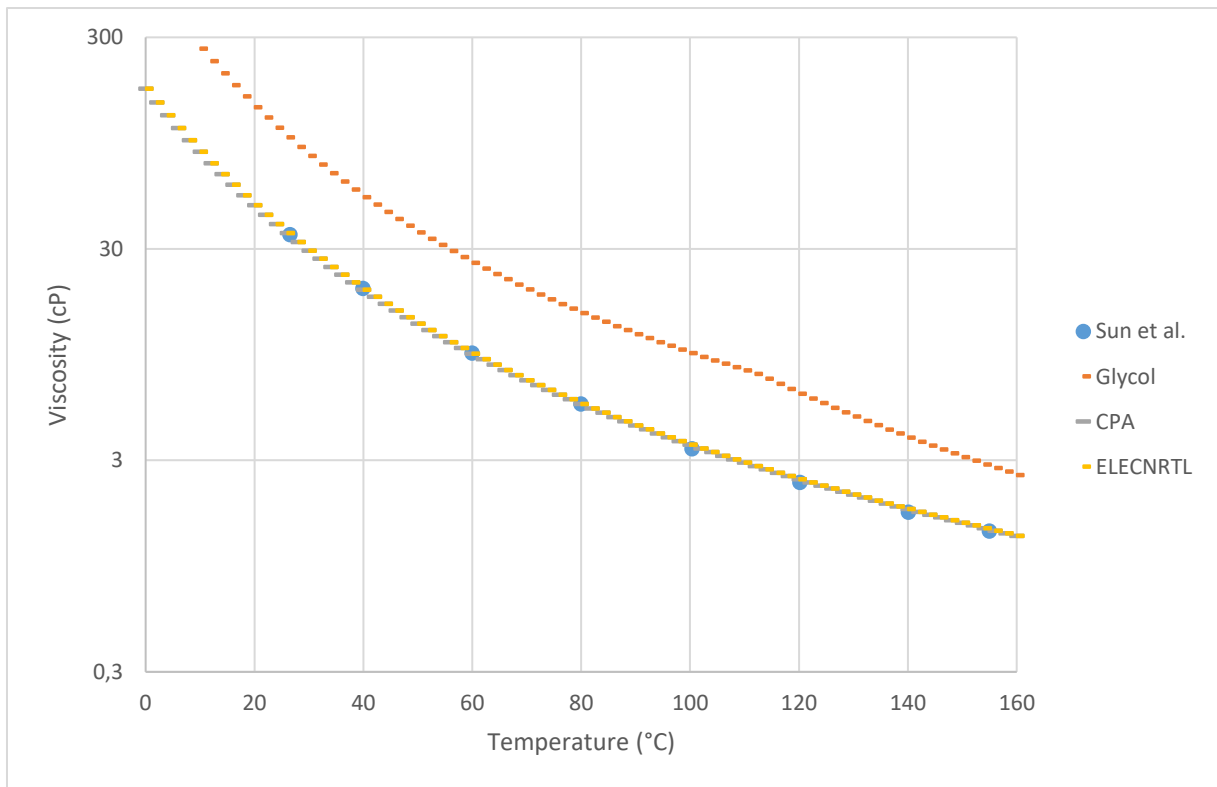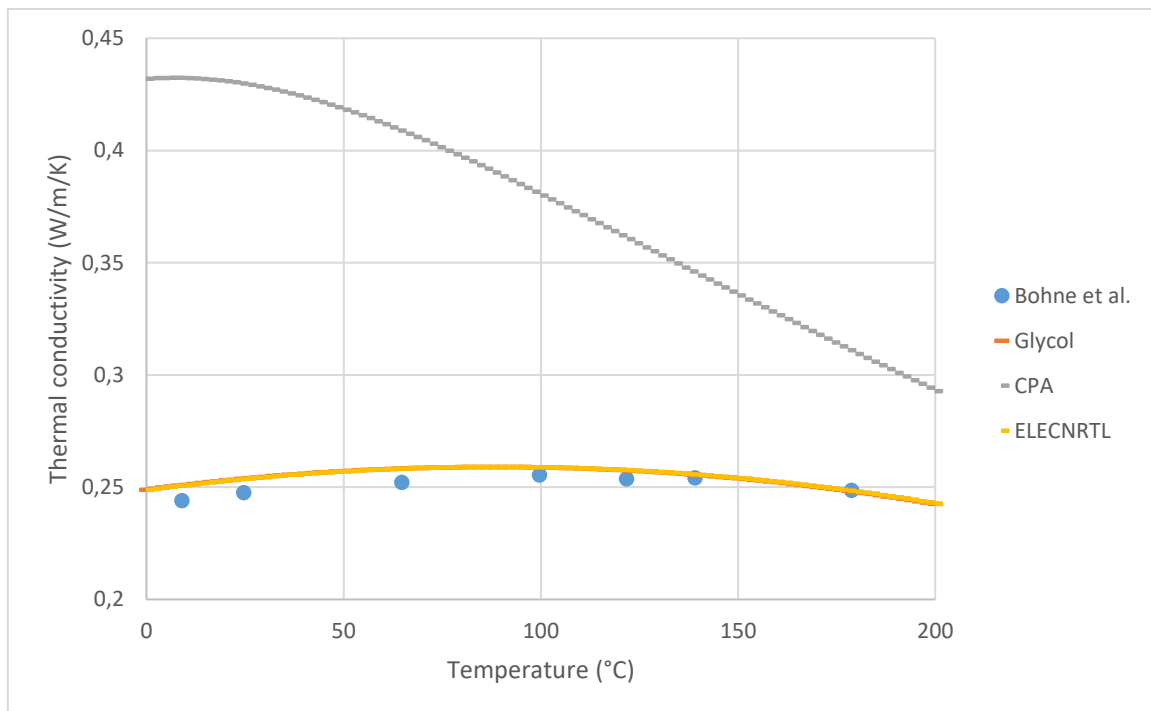*Figure 28 : Thermal conductivity of MEG in the temperature range of 0 - 200°C. Blue figures represent experimental data [9] ; orange, grey and yellow lines represent models results*

Concerning thermal conductivity, only one data set for MEG was found in the literature. Here, the CPA model is very bad, while the Glycol and ELECNRTL models on the contrary give results close to reality (Figure 28). Although this is not visible in Figure 28, the two models nevertheless give different results. This is because it uses two different sub-models to determine thermal conductivity. The Glycol package is based on the API model and calculates the volume using the main EoS. The ELECNRTL model uses the Sato-Riedel sub-model. For Glycol and ELECNRTL models, the relative deviation never exceeds 3%. On the other hand, it is always greater than 20% for the CPA model.

About heat capacity, the problem is that the experimental values are very different from each other (Figure 29). It is then impossible to choose with which series of experimental values to compare our calculated values. And to be honest, the calculated values do not help us as to which set of experimental values seems the most reliable. And that goes for both glycols. Nevertheless, it can be said that, to a certain extent, the 3 models describe the experimental values rather well.
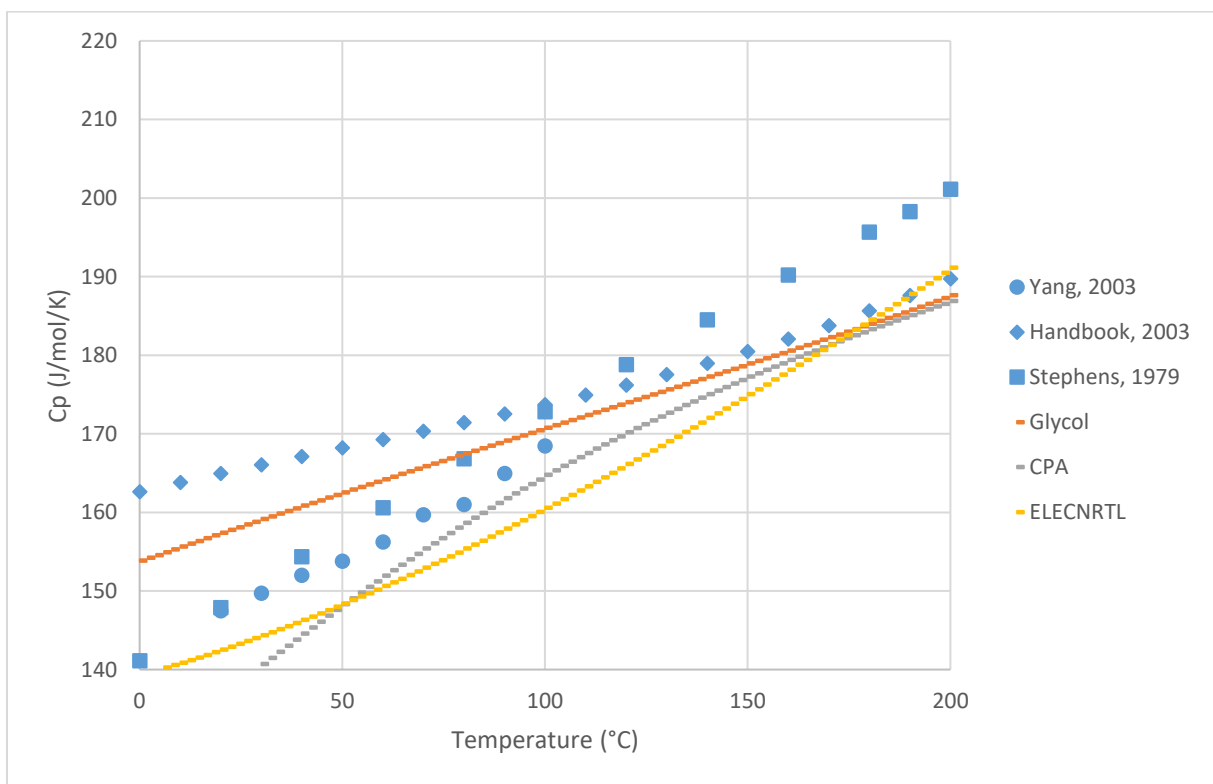
Figure 29 : Heat capacity of MEG in the temperature range of 0 - 200°C. Blue figures represent experimental data [34][3][30] ; orange, grey and yellow lines represent models results

4. Gases solubility

4.1. Carbon dioxide solubility in MEG

We now turn to the heart of the comparison: the liquid-vapor equilibrium. And we start with the solubility of CO2 in MEG, which is very important because carbon dioxide is one of the two most present acid gases among natural gas (along with H2S). In fact, the dehydration part of the process is

normally preceded by the step of extracting the acid gases from the natural gas. It is therefore in small quantities that these gases will be present at the inlet of the absorber.

As can be seen in Figure 30, for T=50°C, the Glycol and CPA models correctly describe the solubility of carbon dioxide in MEG. However, the ELECNRTL model shows the highest under-prediction. These observations are confirmed by the calculation of the deviation from the experimental values. On the other hand, although the CPA model seems to best describe the reality, it does so with a relative deviation that can reach more than 60%. In all cases, the relative deviation is greater beyond a carbon dioxide mole fraction of 0.1. For the last experimental value of Jou et al [20], with x_{CO2}= 0.1327, the deviation reaches 80% for the Glycol package and 73 percent for the CPA model, while it is around 50% for both for the lowest carbon dioxide fraction.

Figure 30 : Total pressure on a log scale as a function of carbon dioxide mole fraction in MEG for a temperature of 50°C. The blue figures represent the experimental data [15][20][35] and the lines the calculated ones.

4.2.   Methane solubility in MEG

It is, of course, important to simulate the solubility of methane in MEG well since methane is the main constituent of natural gas. However, as can be seen in Figure 31, only the CPA model seems to be able to correctly describe the solubility of methane. The glycol model did not converge at methane fractions above 0.00377 at 50°C. It can be seen that the pressure appears to increase suddenly on the graph and exceed 1000 MPa.

And in fact, the CPA model shows a relative deviation of less than 8% for all measurements at 50°C. The glycol and ELENRTL models do not seem to be able to correctly represent the solubility of methane in MEG at all.

Figure 31 : Total pressure on a log scale as a function of methane mole fraction in MEG for a temperature of 50°C. The blue figures represent the experimental data [15][35] and the lines the calculated ones.

4.3. Hydrogen sulfide dioxide solubility in MEG

Figure 32 : Total pressure on a log scale as a function of hydrogen sulfide mole fraction in MEG for a temperature of 50°C. The blue figures represent the experimental data [20] and the lines the calculated ones.

Finally, as a second acid gas commonly present in natural gas, it was therefore normal to compare the ability of each of the models to calculate the solubility of hydrogen sulphide in MEG. As can be seen (Figure 32), once again, the CPA model appears to be the best model to describe the solubility of hydrogen sulphide in MEG. If one looks at the relative differences in more detail, the CPA model still reaches 30-40%, which is not negligible. But it remains the best model. The Glycol model shows a deviation between 30 and 50%, deviation which is above 70% with ELECNRTL model for all the values compared.

4.4. Carbon dioxide solubility in TEG

Let's now move on to the solubility of these 3 gases in the TEG. The Glycol model finally manages to compete with the CPA model, while the ELECNRTL model still seems to be in the doldrums (Figure 33). When we look at the relative gap for each of the models, the Glycol model never exceeds 10%, while the CPA model increases rapidly as the carbon dioxide mole fraction increases, reaching nearly 60% for the highest carbon dioxide molar fraction studied (x_{CO_2}=0.4582). The relative deviation of the ELECNRTL model is well over 70-80%.
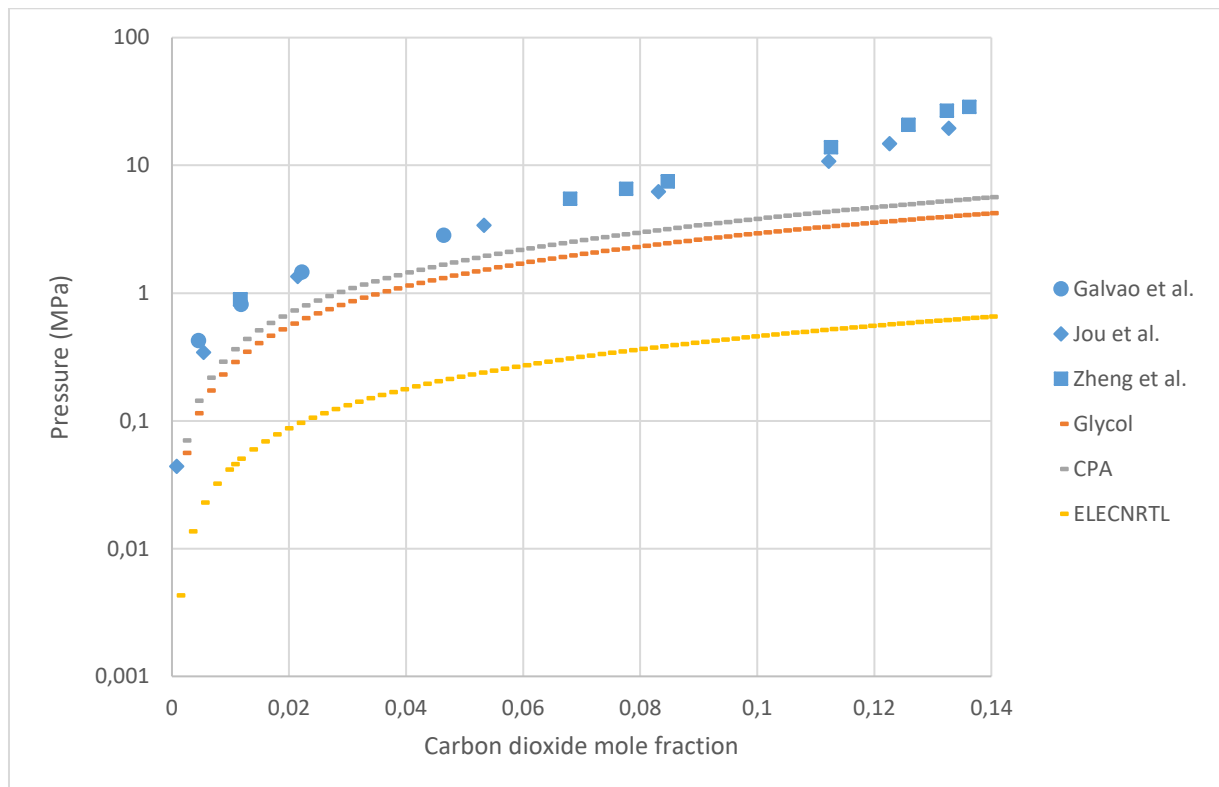

Figure 33 : Total pressure on a log scale as a function of carbon dioxide mole fraction in TEG for a temperature of 50°C. The blue figures represent the experimental data [19] and the lines the calculated ones.

4.5.   Methane solubility in TEG

The same applies to the solubility of methane in TEG. The curve corresponding to Glycol fitted perfectly with the experimental points (Figure 34). In fact, the relative deviation of this model never exceeds 8%. The deviation from reality of the ELECNRTL model reaches almost 100%. I must say that these results seem strange to me, since one of my colleagues who had worked on the same subject had obtained results showing that the ELECNRTL model was doing well [12]. It is therefore possible that an error may have been made. But this error was never identified.
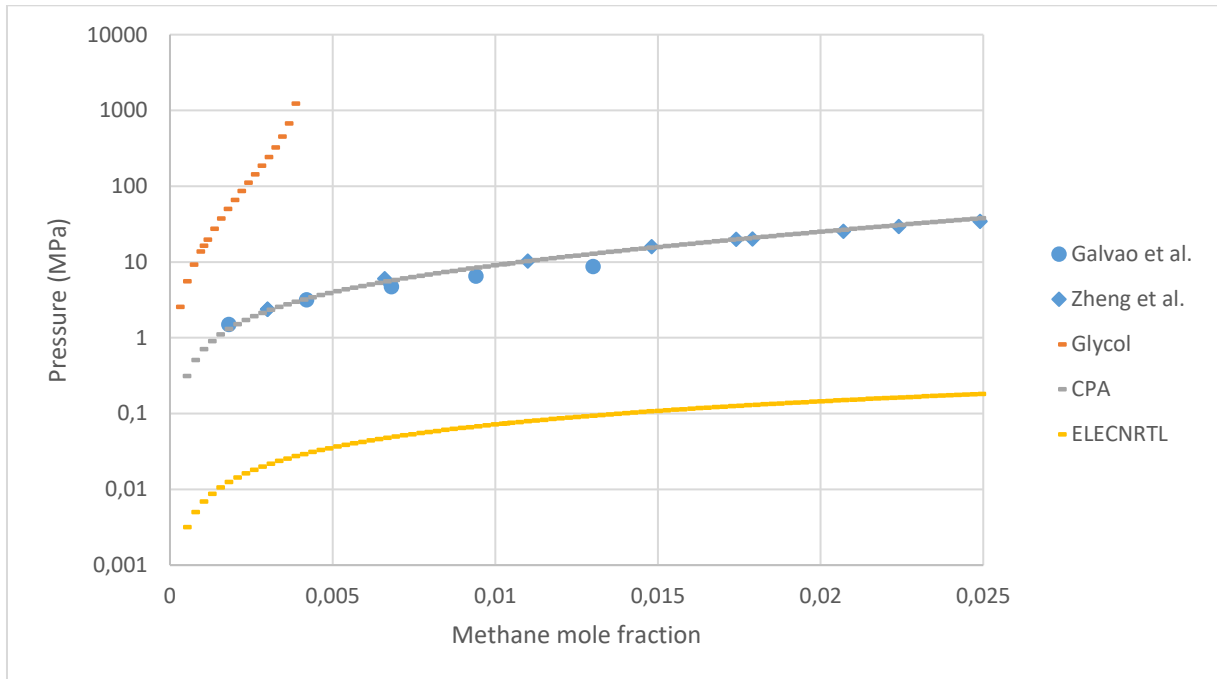

Figure 34 : Total pressure on a log scale as a function of hydrogen methane fraction in TEG for a temperature of 50°C. The blue figures represent the experimental data [19] and the lines the calculated ones.

4.6.   Sulfide hydrogen solubility in TEG

Let's finish with the solubility of hydrogen sulfide in TEG. It is quite rare, whereas most of the time models seem to underestimate the total pressure for a given mole fraction, the CPA model in this case overestimates it (Figure 35). The Glycol model is again very satisfactory, with less than 8% relative deviation. It should be noted, however, that for small quantities of H2S, the ELECNRTL model is perfectly suitable (deviation less than 3% for a molar fraction less than 0.1). This is good since in reality, the quantity of H2S present is very low (below 1%).
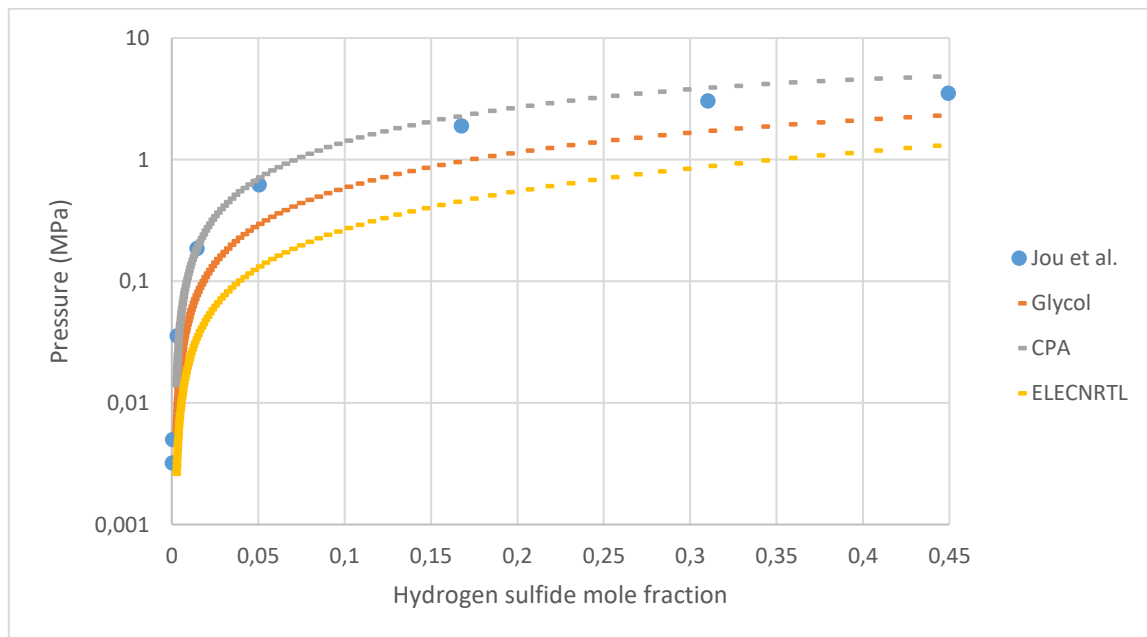
Figure 35 : Total pressure on a log scale as a function of hydrogen sulfide mole fraction in TEG for a temperature of 50°C. The blue figures represent the experimental data [19] and the lines the calculated ones.

4.7.   Methane solubility in water

The water-methane binary is another interesting binary, in that these two compounds are in constant contact throughout the process. Once again, the experimental values available in the literature were measured at a temperature well below the usual setting temperatures for the dewatering process. The experimental and calculated data are shown in Figure 36. The Glycol model describes the solubility of methane in water very well, with a relative deviation of less than 9%. The CPA model remains suitable with less than 30% deviation. The ELECNRTL model remains aberrant.

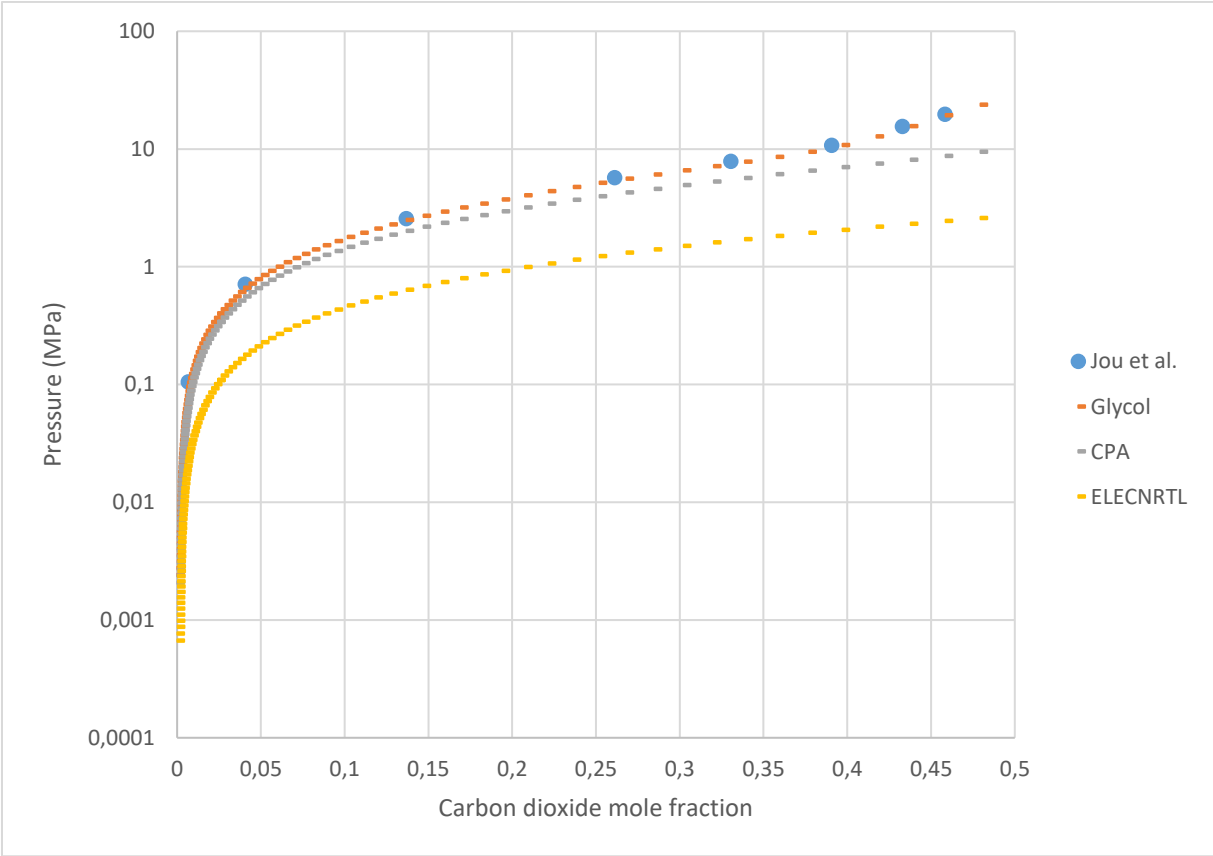*Figure 36 : Total pressure on a log scale as a function of methane mole fraction in water for a temperature of 40°C. The blue figures represent the experimental data [13][14] and the lines the calculated ones.*

5. Water solubility

The very principle of the dehydration process is to dry the natural gas in contact with glycol, which absorbs the water contained in the natural gas. Therefore, it is very important to check which model best describes the solubility of water in glycol.
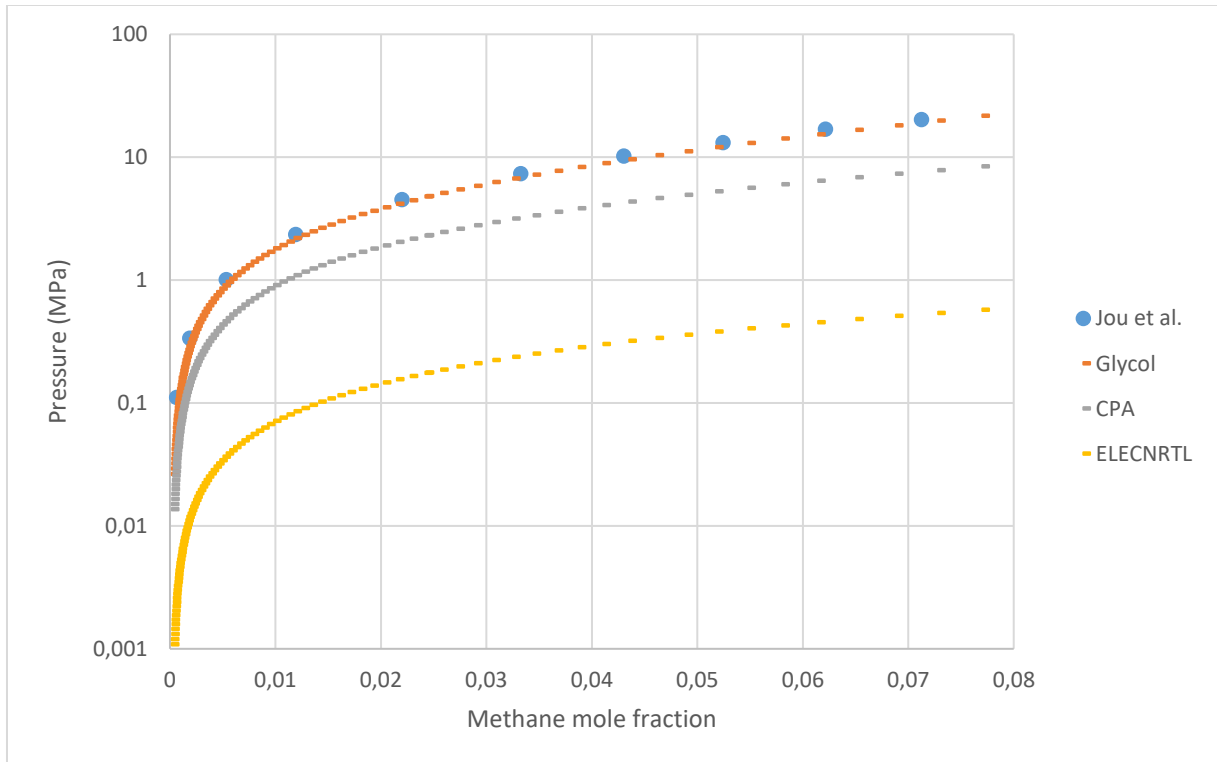
5.1. Water solubility in MEG

Figure 37 : Total pressure on a log scale as a function of liquid water mole fraction in MEG for a temperature of 60°C. The blue figures represent the experimental data [16][33] and the lines the calculated ones.

The study of the water-MEG binary is essential, since the very principle of the dehydration process is to absorb the water contained in the natural gas with MEG or TEG. The molar fractions of water were plotted against the corresponding total pressures. The experimental data available in the literature only cover low temperatures (50°C, 60°C and 80°C), temperatures more or less equivalent to those in force for the absorption part of the process but well below the usual temperatures of the regeneration part.

Even if this is not very visible, it can be seen in Figure 37 that the CPA and ELECNRTL models apparently describe the solubility of water in the TEG rather well, whereas the glycol model, which, it should be recalled, is basically intended to describe only the behaviour of the TEG despite its name,

shows a strong deviation. For a temperature of 60°C, the deviation relative to the experimental values has been calculated; it broadly confirms the initial observations made. As shown in Table 6, the deviations are not aberrant, regardless of the model used. More than 30% relative deviation is reached with the Glycol model, especially for low molar fractions in water. The CPA model is below 8% and ELECNRTL below 10%.

5.2.   Water solubility in TEG

Finally, as explained above, it is important to be able to correctly describe the behaviour of water and desiccant together. For this purpose, the same comparison concerning the solubility of water in the TEG was made. It is necessary to specify that the only data found relating to the water-TEG binary were measured at a temperature of 25°C, well below the usual temperatures of the dehydration process. Therefore, it cannot really be said that the comparative analysis carried out is the most relevant. It is just assumed that the results obtained are transposable to higher temperatures.
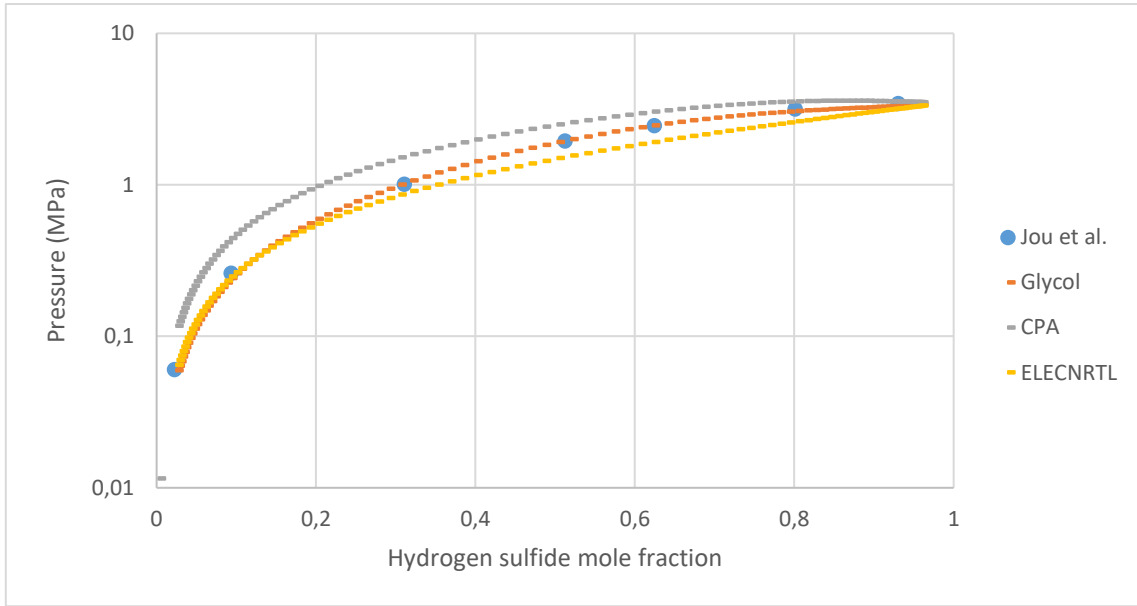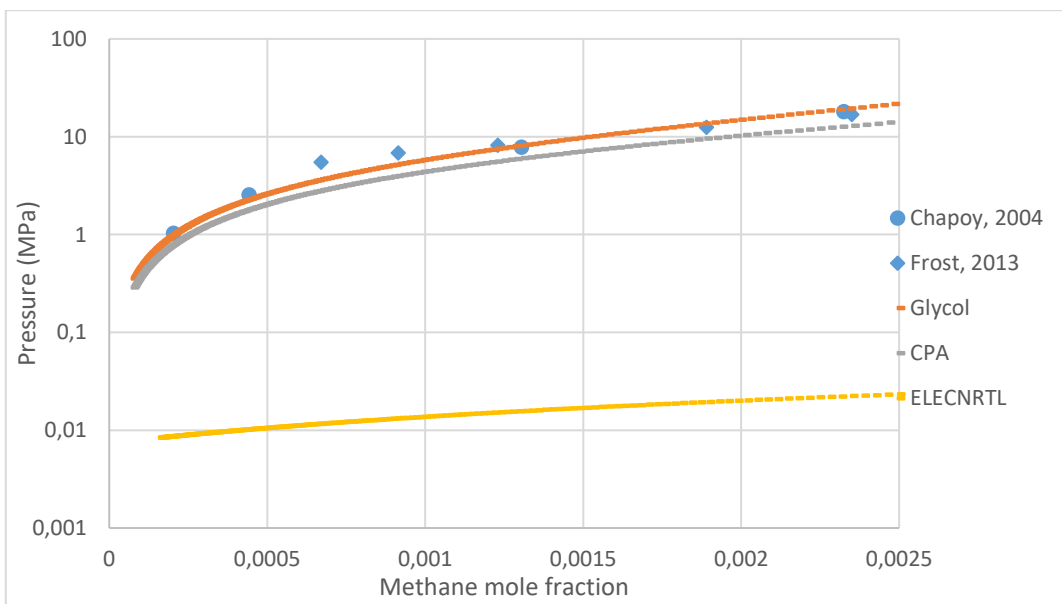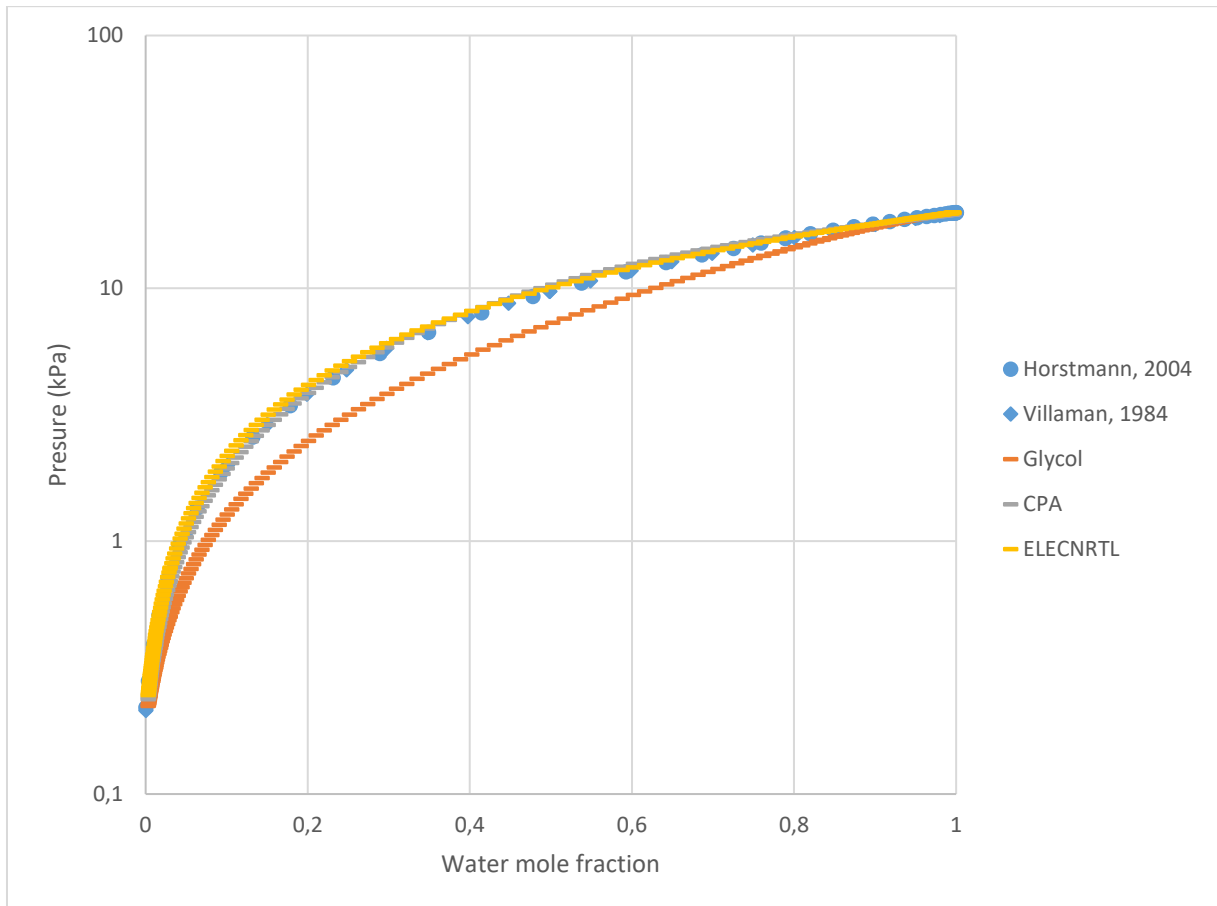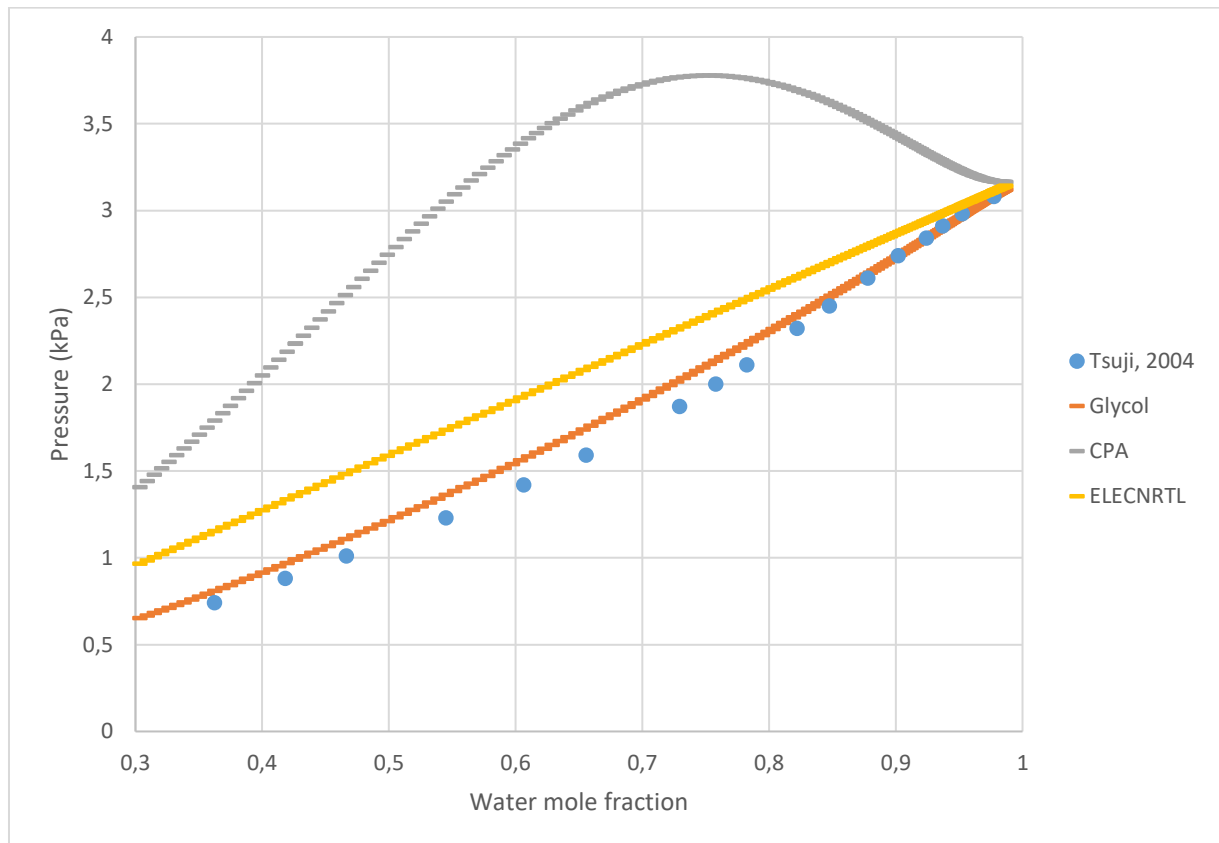

Figure 38 : Total pressure on a log scale as a function of liquid water mole fraction in TEG for a temperature of 25°C. The blue figures represent the experimental data [32] and the lines the calculated ones.

The ability to describe the water binary - TEG varies greatly from model to model. As shown in Appendix B, and as can easily be seen in Figure 38, the CPA model has an aberration. The relative deviation of the model reaches almost 150% at some locations. The ELECNRTL model is already better able to describe the binary, with a relative deviation reaching a maximum of 50-60%. But the best

66

model here is the Glycol model, which does not exceed 11% relative deviation. It is nevertheless surprising that this difference exists, given that the Glycol model exists in order to best describe the physical and thermodynamic properties of the TEG, as well as, among others, the water-TEG binary.

6. Concluding remarks

It was initially planned to use Aspen HYSYS for the simulation. The initial idea was that since both software are edited by the same company, a model available on both should normally behave in the same way. Moreover, it turns out that initially, the simulations concerning physical properties had been done with Aspen HYSYS and those concerning liquid-vapour equilibria with Aspen Plus. Fortunately, after discussions with the supervisor, the author of this work completely redid the simulations on Aspen Plus. It was a good idea. It turned out that the same model on the two software packages did not perform in the same way. Figures 39 et 40 show a comparison of the viscosity of MEG. It can clearly be seen that the Glycol model fits perfectly with the other two models on HYSYS, and on the contrary presents this protuberance on Aspen Plus. Moral of this story, use only one software.
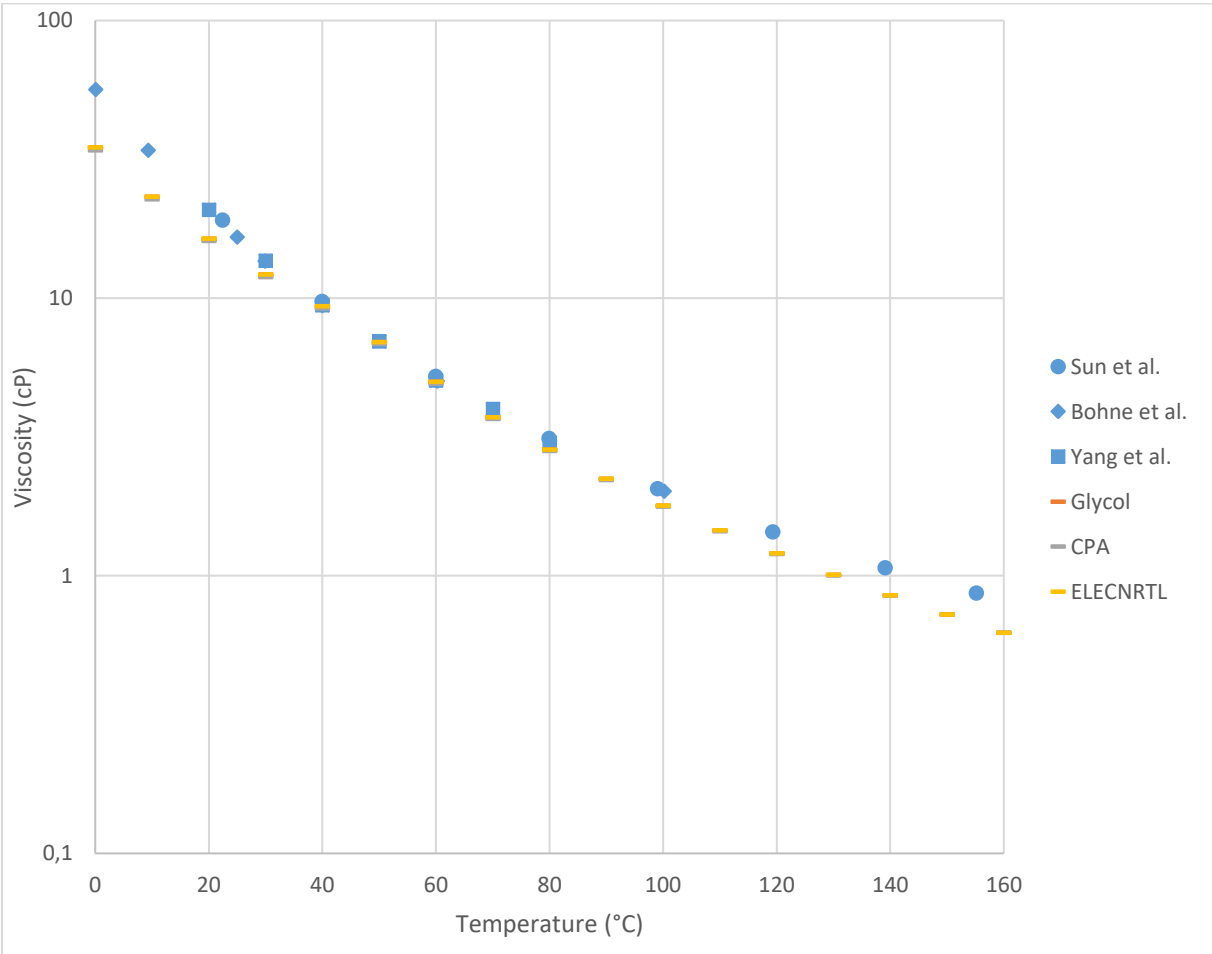
Figure 39 : Viscosity of MEG in the temperature range of 0 - 160°C. Blue figures represent experimental data ; orange, grey and yellow lines represent models results (Aspen HYSYS)

67
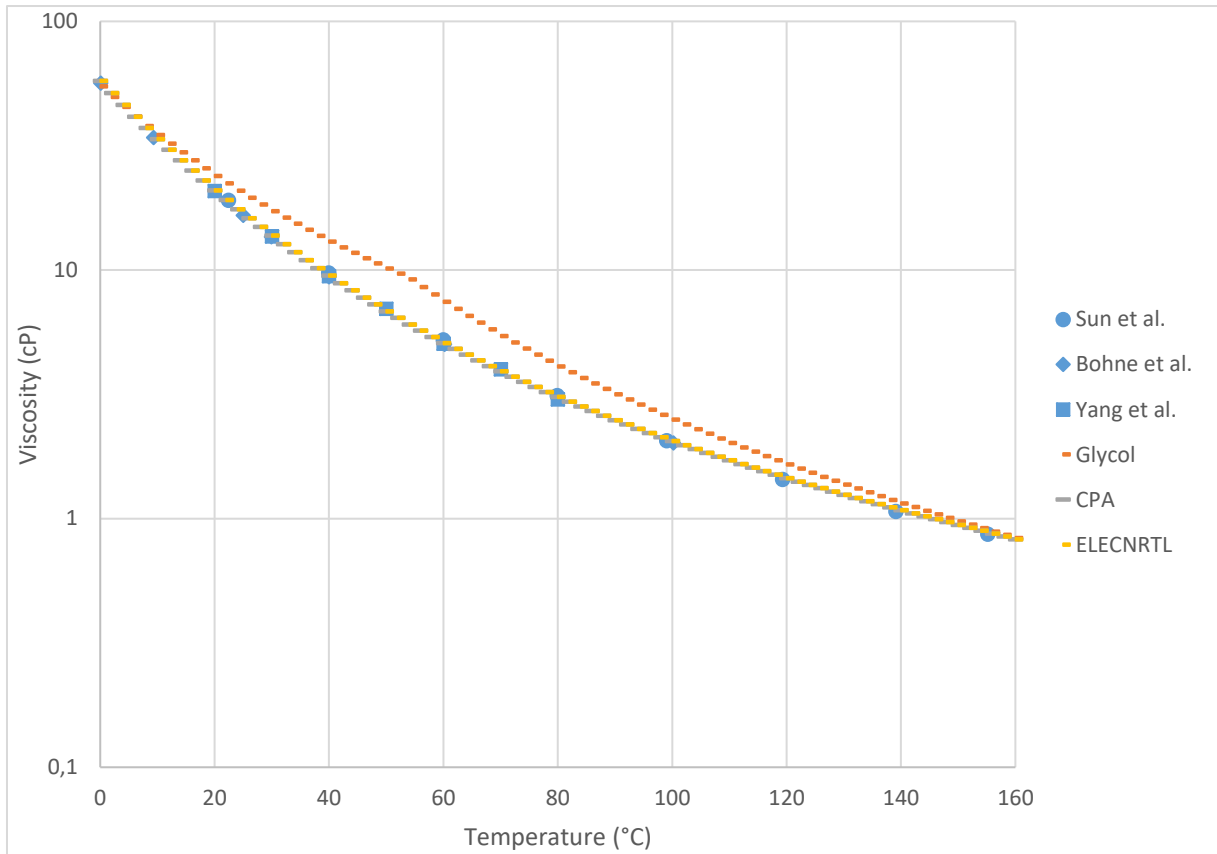
Figure 40 : Viscosity of MEG in the temperature range of 0 - 160°C. Blue figures represent experimental data ; orange, grey and yellow lines represent models results (Aspen Plus)

Above all, it is important to remember that not all comparative analyses carried out have the same "value". Indeed, in order to simulate the operation of the dehydration process, only the solubility data involving water, glycols and methane really matter. There are two main conclusions. Firstly, the ELECNRTL model seems to be the most accurate model for calculating classical physical properties such as density and viscosity for the two glycols studied. Concerning the liquid-vapour equilibria, the most suitable model depends which glycol is used as a desiccant. The CPA model seems to be the most suitable model to describe the equilibria involving MEG. For the TEG, it seems to be the Glycol model the most appropriate one (which seems logical, since this model was created to simulate the dehydration process using the TEG).

As explained earlier, It was initially planned to have purely experimental master thesis. Due to COVID-19 restrictions the work was changed to also include some modelling simulation work. Unfortunately, not all the this planned simulations could were completed due to limited time and since the laboratories opened again allowing more focus on experimental work.

VII. Conclusions and future work

1. Conclusions

Basically, the main objective of this work was to better understand the mechanisms governing the degradation of MEG and TEG. It should be remembered that the literature on this subject is rather limited. It was therefore very satisfying to obtain answers, even partial to our questions about glycol degradation. For this purpose, some MEG and TEG were heated for three weeks in the presence of oxygen and for different temperatures. Regularly collected samples have been then analysed by ion chromatography, pH-metric titration, and spectroscopy.

Firstly, we sought to understand what factors could influence degradation, and to what extent it did so. It is clear that the presence of oxygen during the degradation considerably weakened the thermal stability of the TEG. While it is normally stable above 150°C, the TEG degraded considerably during the experiments, changing colour very rapidly and becoming volatiles or polymers. Temperature was also found to have a significant effect on the distribution of organic acids among the degradation products, as well as on the presence of acid species in general among the degradation products. Contrary to expectations, higher temperature seems to reduce this amount of acidic compounds. This implies that other degradation products, which could be described as secondary, have appeared. And their appearance seems to be favoured by an increase in temperature. It is possible that these famous secondary products are in fact the volatiles which left the reactors during the degradation, or perhaps the compound that is suspected to be a polymer.

Secondly, we were able to identify some of the degradation products of the glycols studied. As the literature indicates, formic, acetic, glycolic and oxalic acids are among them, although in very different proportions. The presence of volatiles among the degradation products, particularly in the case of TEG, is evident from the proportion of glycol "disappeared" after degradation, and from the colour of the soda solution contained in the guards. Spectroscopic analyses also showed that the concentration of one or more coloured species among the degradation products became higher and higher over time and increased more and more rapidly with temperature. Finally, it would seem that the presence of polymers in the formation is favoured at high temperature and should be seriously considered.

Finally, the simulations we performed in Aspen Plus allowed us to identify the strengths and weaknesses of each of the models competing for the simulation of the dehydration process. Experimental values of physical and thermodynamic properties have been compared with the values calculated by the Glycol, CPA and ELECNRTL models. The CPA model seems much better when it comes to modelling the process using MEG, whereas the Glycol package should be used if TEG is preferred. It also tells us that no model is perfect, so it is always necessary to stay careful with the modelling results.

Although it is necessary to remain cautious, given that all these observations were made in the context of laboratory work, with operating conditions very different from the reality of the field, this project was exciting to carry out. It is true that given the importance of natural gas in the global energy mix, it is essential to understand and optimize the processes involved.

2. Future work

This work remains incomplete. So much remains to be done. The guards have to be analysed to determine the composition of the volatiles. Similarly, an NMR analysis of the yellowish and viscous compound could allow us to identify it, thus bringing to light a very interesting phenomenon. Finally, the comparison of thermodynamic models now calls of course for the realization of the simulation in order to calculate the influence of the degradation of the desiccant on the efficiency of the process.

Bibliography

[1]   Private communication with supervisors.

[2]   Compendium Natural Gas Technology course TEP4185. 2018. NTNU.

[3]   Yaws' Handbook of Thermodynamic and Physical Properties of Chemical compounds. (2003). In (pp. 1268-1323).

[4]   Afzal, W., Mohammadi, A. H., & Richon, D. (2009). Volumetric Properties of Mono-, Di-, Tri-, and Polyethylene Glycol Aqueous Solutions from (273.15 to 363.15) K: Experimental Measurements and Correlations. *Journal of Chemical and Engineering Data, 54*(4), 1254-1261. doi:10.1021/je800694a

[5]   Alef, K., Iglauer, S., & Barifcani, A. (2019). Degradation and hydrate phase equilibria measurement methods of monoethylene glycol. *Methodsx, 6*, 6-14. doi:10.1016/j.mex.2018.12.004

[6]   AlHarooni, K., Barifcani, A., Pack, D., Gubner, R., & Ghodkay, V. (2015). Inhibition effects of thermally degraded MEG on hydrate formation for gas systems. *Journal of Petroleum Science and Engineering, 135*, 608-617. doi:10.1016/j.petrol.2015.10.001

[7]   AspenTech. (2018). *Dehydration with Aspen HYSYS®: Validation of the CPA Property Package*. Retrieved from
https://www.google.com/url?sa=t&rct=j&q=&esrc=s&source=web&cd=&ved=2ahUKEwigleSpk4_qAhU
Bt4sKHUlKAXkQFjAAegQIBxAB&url=https%3A%2F%2Fwww.aspentech.com%2Fen%2F-
%2Fmedia%2Faspentech%2Fhome%2Fresources%2Fwhite-papers%2Fpdfs%2Fat-03609-wp-dehydration-
with-aspen-hysys.pdf&usg=AOvVaw0jUHzM-TcoMt2ZeOlXQ1Sr

[8]   Atilhan, M., & Aparicio, S. (2013). P rho T measurements and derived properties of liquid 1,2-alkanediols. *Journal of Chemical Thermodynamics, 57*, 137-144. doi:10.1016/j.jct.2012.08.014

[9]   Bohne, D., Fischer, S., & Obermeier, E. (1984). Thermal-Conductivity, Density, Viscosity, and Prandtl-Numbers of Ethylene Glycol-Water Mixtures. *Berichte Der Bunsen-Gesellschaft-Physical Chemistry Chemical Physics, 88*(8), 739-742. doi:DOI 10.1002/bbpc.19840880813

[10]   BP Statistical Review of World Energy. 2019. 68th edition.

[11]   Brown, P. W., Rossiter, W. J., & Galuk, K. G. (1986). A Mass-Spectrometric Investigation of the Thermal Oxidative Reactivity of Ethylene-Glycol. *Solar Energy Materials, 13*(3), 197-202. doi:Doi 10.1016/0165-1633(86)90018-3

[12]   Cervantes Gameros, B. Y. (2019). *Simulation of gas dehydration process with MEG using Aspen Plus.* NTNU

[13]   Chapoy, A., Mazloum, S., Burgass, R., Haghighi, H., & Tohidi, B. (2012). Clathrate hydrate equilibria in mixed monoethylene glycol and electrolyte aqueous solutions. *Journal of Chemical Thermodynamics, 48*, 7-12. doi:10.1016/j.jct.2011.12.031

[14]   Frost, M., Kontogeorgis, G. M., Stenby, E. H., Yussuf, M. A., Haugum, T., Christensen, K. O., . . . Lokken, T. V. (2013). Liquid-liquid equilibria for reservoir fluids plus monoethylene glycol and reservoir fluids plus monoethylene glycol plus water: Experimental measurements and modeling using the CPA EoS. *Fluid Phase Equilibria, 340*, 1-6. doi:10.1016/j.fluid.2012.11.028

[15]   Galvao, A. C., & Francesconi, A. Z. (2010). Solubility of methane and carbon dioxide in ethylene glycol at pressures up to 14 MPa and temperatures ranging from (303 to 423) K. *Journal of Chemical Thermodynamics, 42*(5), 684-688. doi:10.1016/j.jct.2009.12.009

[16]   Horstmann, S., Gardeler, H., Wilken, M., Fischer, K., & Gmehling, J. (2004). Isothermal vapor-liquid equilibrium and excess enthalpy data for the binary systems water+1,2-ethanediol and propene plus acetophenone. *Journal of Chemical and Engineering Data, 49*(6), 1508-1511. doi:10.1021/je0342522

[17]   IEA.   (2020).   Statistics.   Retrieved   from   https://www.iea.org/data-and-statistics?country=WORLD&fuel=Electricity%20and%20heat&indicator=Electricity%20generation%20by%20source

[18]   Izutsu, K. (2002). Potentiometry in Non-Aqueous Solutions. In (pp. 167-200).

[19]   Jou, F. Y., Deshmukh, R. D., Otto, F. D., & Mather, A. E. (1987). Vapor-Liquid-Equilibria for Acid Gases and Lower Alkanes in Triethylene Glycol. *Fluid Phase Equilibria, 36*, 121-140. doi:Doi 10.1016/0378-3812(87)85018-5

[20]   Jou, F. Y., Deshmukh, R. D., Otto, F. D., & Mather, A. E. (1990). Vapor-Liquid-Equilibria of H2s and Co2 and Ethylene-Glycol at Elevated Pressures. *Chemical Engineering Communications, 87*, 223-231. doi:Doi 10.1080/00986449008940694

[21]   Madera, M., Hoflinger, W., & Kadnar, R. (2003). Ion chromatographic identification and quantification of glycol degradation products. *Journal of Chromatography A, 997*(1-2), 279-284. doi:10.1016/S0021-9673(03)00060-8

[22]   Namazian, M., & Heidary, H. (2003). Ab initio calculations of pKa values of some organic acids in aqueous solution. *Journal of Molecular Structure-Theochem, 620*(2-3), 257-263. doi:Pii S0166-1280(02)00640-1 Doi 10.1016/S0166-1280(02)00640-1

[23]   Neagu, M., & Cursaru, D. L. (2017). Technical and economic evaluations of the triethylene glycol regeneration processes in natural gas dehydration plants. *Journal of Natural Gas Science and Engineering, 37*, 327-340. doi:10.1016/j.jngse.2016.11.052

[24]   Perrin, D. D., Dempsey, B., & Serjeant, E. P. (1981). *pKa prediction for organic acids and bases* (Vol. 1). London: Chapman and Hall.

[25]   Piemonte, V., Maschietti, M., & Gironi, F. (2012). A Triethylene Glycol-Water System: A Study of the TEG Regeneration Processes in Natural Gas Dehydration Plants. *Energy Sources Part a-Recovery Utilization and Environmental Effects, 34*(5-8), 456-464. doi:10.1080/15567031003627930

[26]   Psarrou, M. N., Josang, L. O., Sandengen, K., & Ostvold, T. (2011). Carbon Dioxide Solubility and Monoethylene Glycol (MEG) Degradation at MEG Reclaiming/Regeneration Conditions. *Journal of Chemical and Engineering Data, 56*(12), 4720-4724. doi:10.1021/je200709h

[27]   R., F. (1998). *Extending glycol life in natural gas dehydration systems*. Paper presented at the 1998 International Gas Research Conference, San Diego, California, USA.

[28]   Rossiter, W. J., Brown, P. W., & Godette, M. (1983). The Determination of Acidic Degradation Products in Aqueous Ethylene-Glycol and Propylene-Glycol Solutions Using Ion Chromatography. *Solar Energy Materials, 9*(3), 267-279. doi:Doi 10.1016/0165-1633(83)90049-7

[29]   Rossiter, W. J., Godette, M., Brown, P. W., & Galuk, K. G. (1985). An Investigation of the Degradation of Aqueous Ethylene-Glycol and Propylene-Glycol Solutions Using Ion Chromatography. *Solar Energy Materials, 11*(5-6), 455-467. doi:Doi 10.1016/0165-1633(85)90016-4

[30]   Stephens, M. A., & Tamplin, W. S. (1979). Saturated Liquid Specific-Heats of Ethylene-Glycol Homologs. *Journal of Chemical and Engineering Data, 24*(2), 81-82. doi:DOI 10.1021/je60081a027

[31]   Sun, T. F., & Teja, A. S. (2003). Density, viscosity, and thermal conductivity of aqueous ethylene, diethylene, and triethylene glycol mixtures between 290 K and 450 K. *Journal of Chemical and Engineering Data, 48*(1), 198-202. doi:10.1021/je025610o

[32]   Tsuji, T., Hiaki, T., & Hongo, M. (1998). Vapor-liquid equilibria of the three binary systems: Water plus tetraethylene glycol (TEG), ethanol plus TEG, and 2-propanol plus TEG. *Industrial & Engineering Chemistry Research, 37*(5), 1685-1691. doi:DOI 10.1021/ie9706469

[33]   Villamanan, M. A., Gonzalez, C., & Vanness, H. C. (1984). Excess Thermodynamic Properties for Water Ethylene-Glycol. *Journal of Chemical and Engineering Data, 29*(4), 427-429. doi:DOI 10.1021/je00038a018

[34]   Yang, C. S., Ma, P. S., Jing, F. M., & Tang, D. Q. (2003). Excess molar volumes, viscosities, and heat capacities for the mixtures of ethylene glycol plus water from 273.15 K to 353.15 K. *Journal of Chemical and Engineering Data, 48*(4), 836-840. doi:10.1021/je020140j

[35]   Zheng, D. Q., Ma, W. D., Wei, R., & Guo, T. M. (1999). Solubility study of methane, carbon dioxide and nitrogen in ethylene glycol at elevated temperatures and pressures. *Fluid Phase Equilibria, 155*(2), 277-286. doi:Doi 10.1016/S0378-3812(98)00469-5

Appendix A

This appendix compiles the chromatograms that were necessary to write this thesis.

Figure 41 : Degraded MEG (Oks 2 D21 R2); comparison with and without excess oxalic acid.

Figure 42 : Degraded MEG (Oks 2 D21 R2); comparison with and without excess glycolic acid.

Figure 43 : Degraded MEG (Oks 2 D21 R2); comparison with and without excess acetic acid.

Figure 44 : Degraded MEG (Oks 2 D21 R2); comparison with and without excess formic acid.

Figure 45 : Degraded TEG (Oks 2 D21 R3); comparison with and without excess glyoxylic acid.

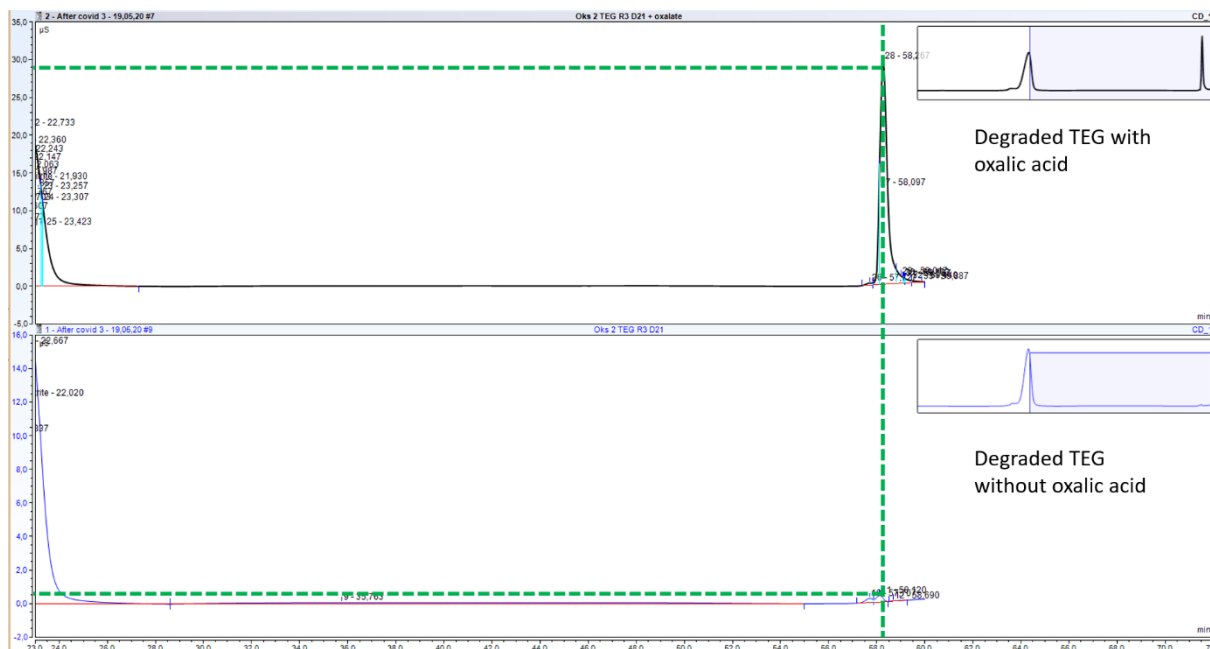*Figure 46 : Degraded TEG (Oks 2 D21 R3); comparison with and without excess oxalic acid.*

Figure 47 : Degraded TEG (Oks 2 D21 R3); comparison with and without excess acetic acid.

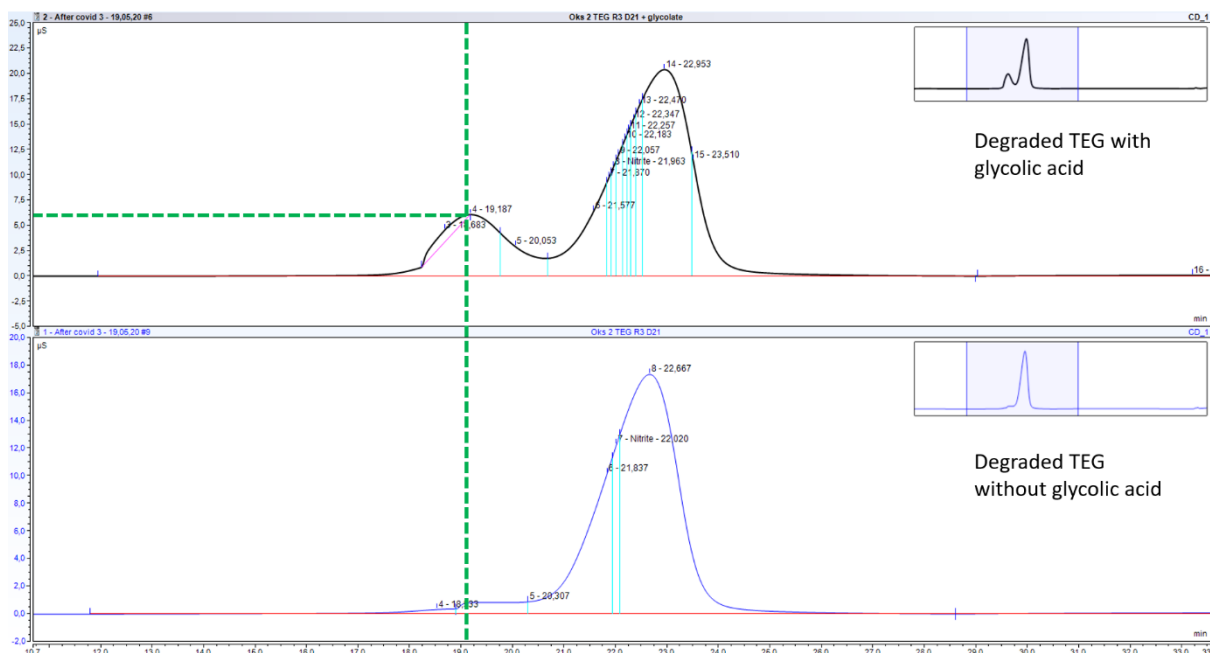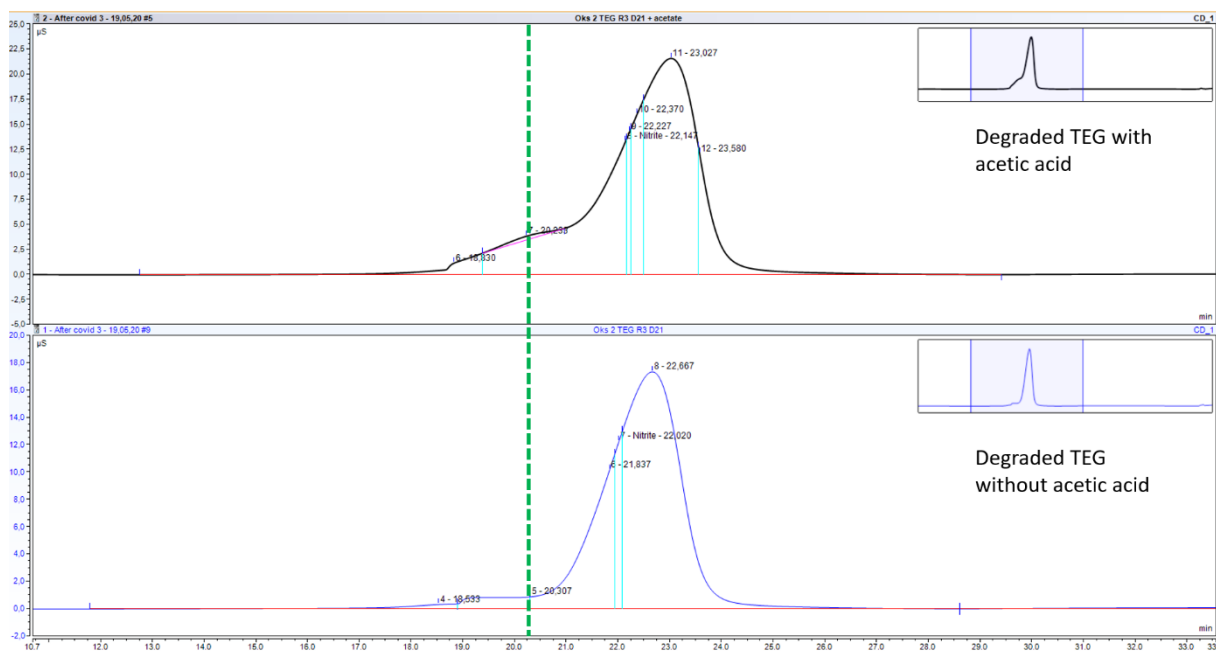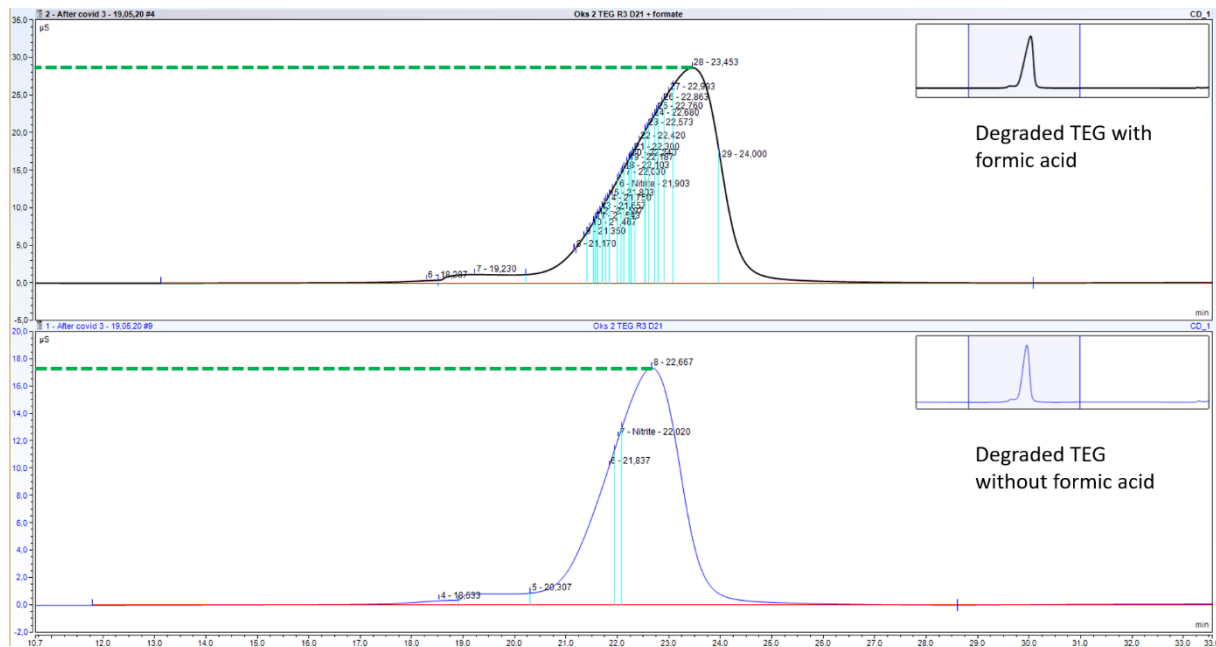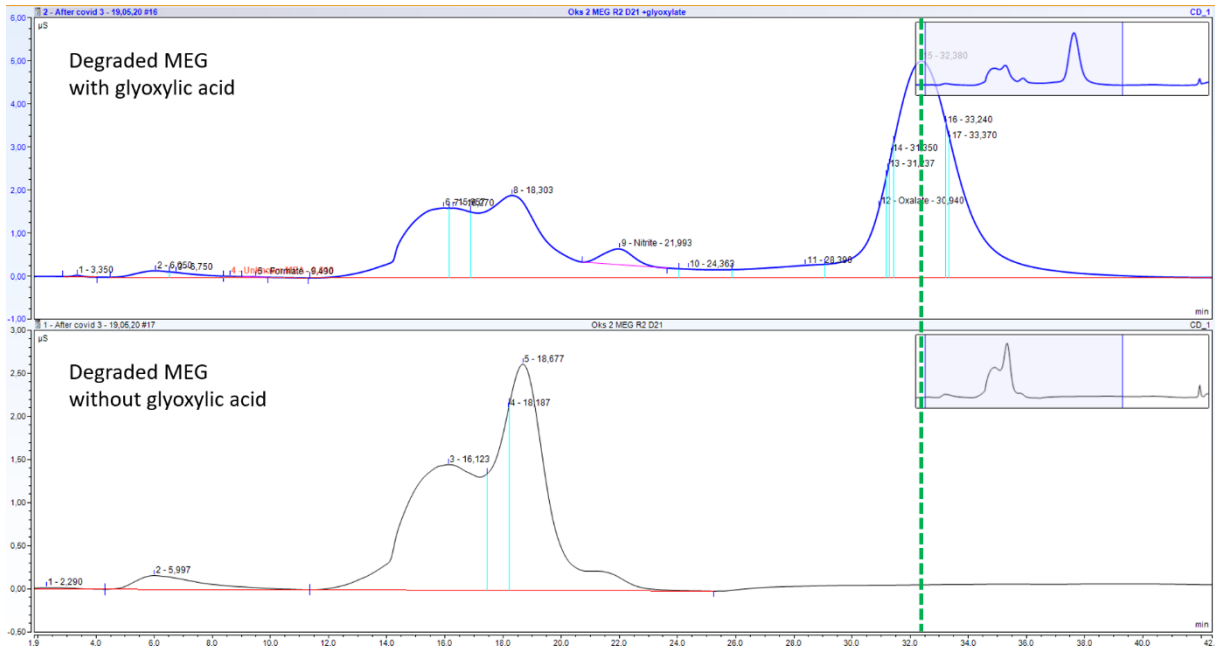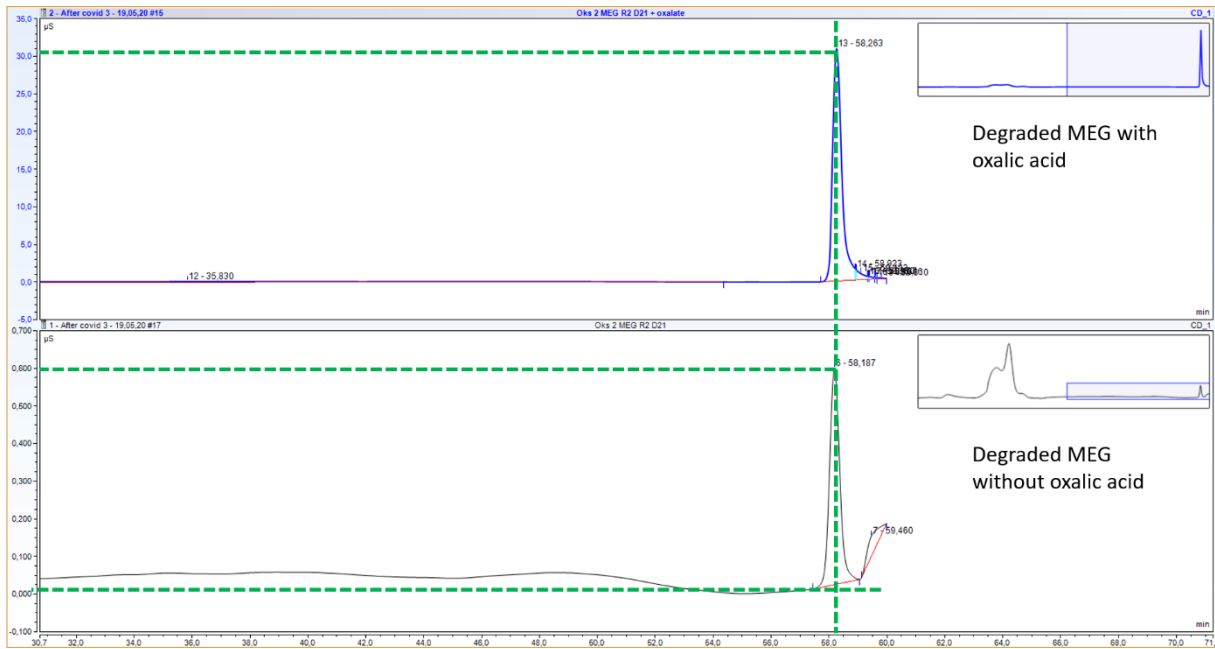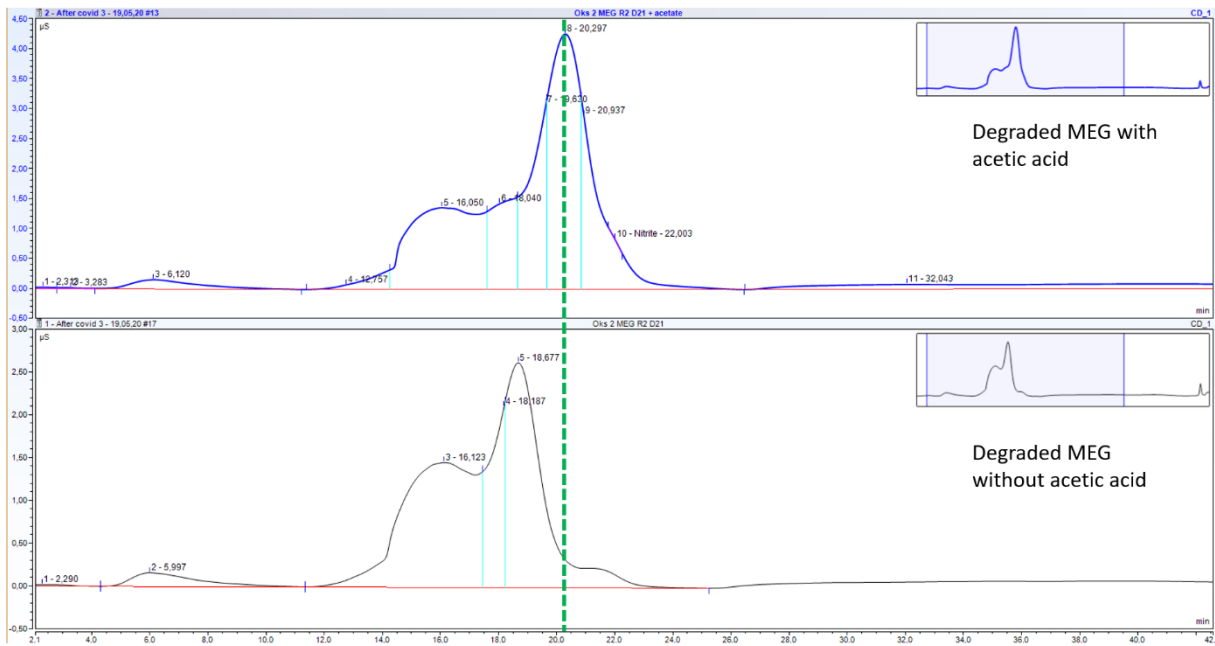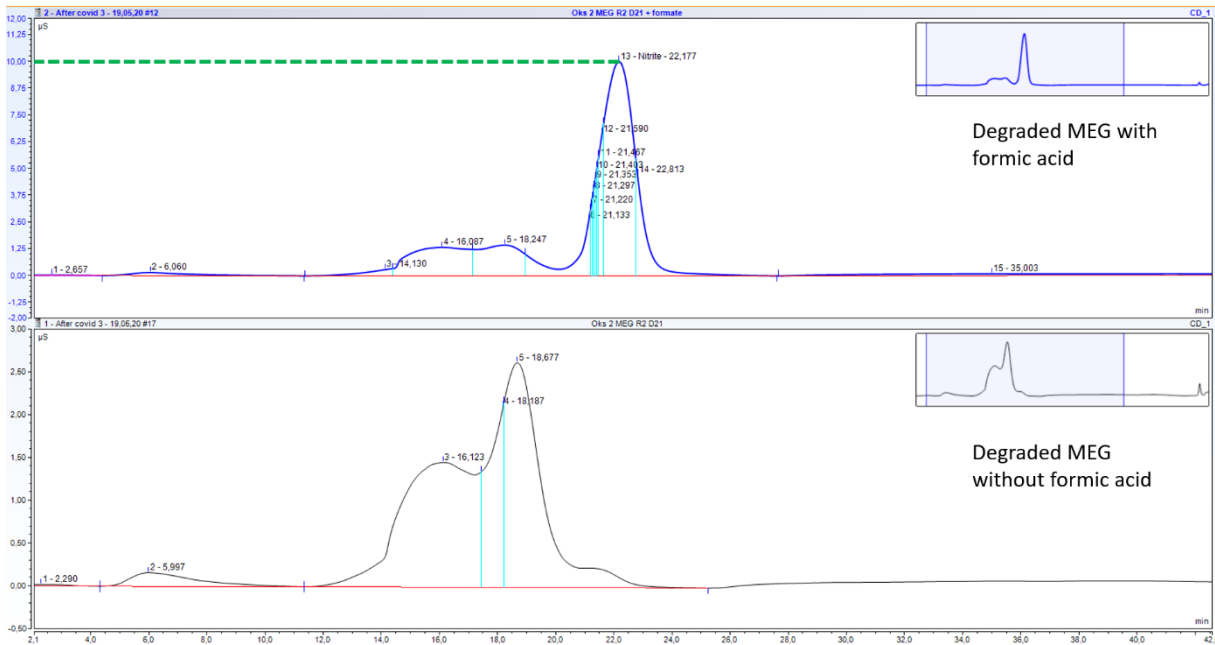*Figure 48 : Degraded TEG (Oks 2 D21 R3); comparison with and without excess formic acid.*

78
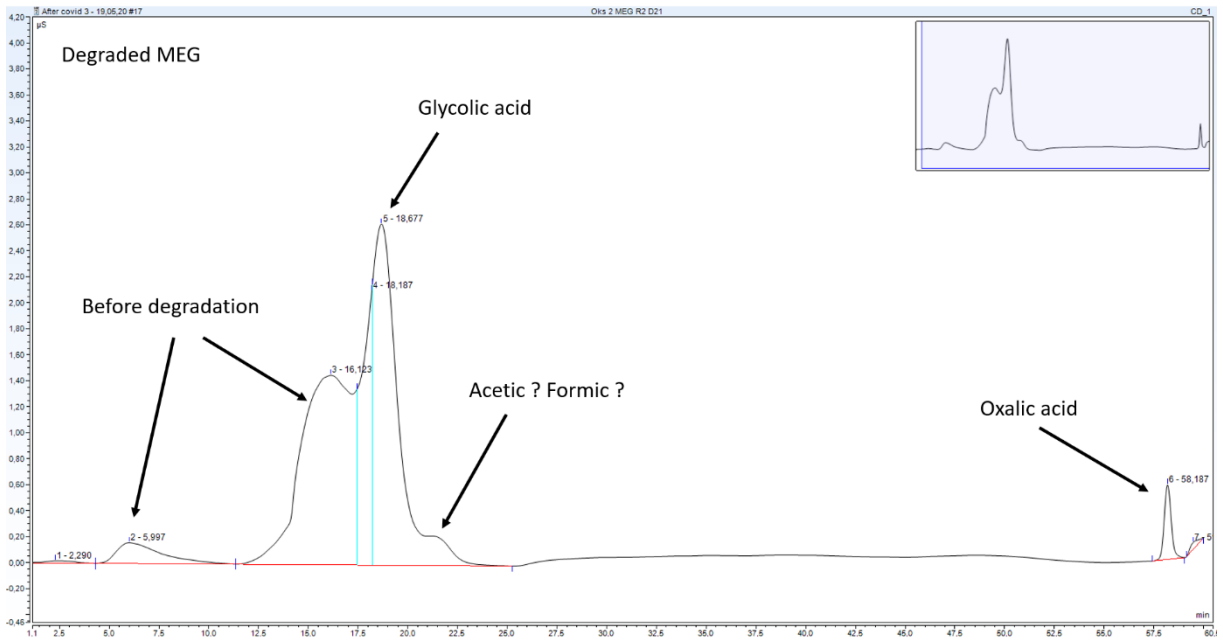
Figure 49 : Degraded MEG (Oks 2 D21 R2); peak identification
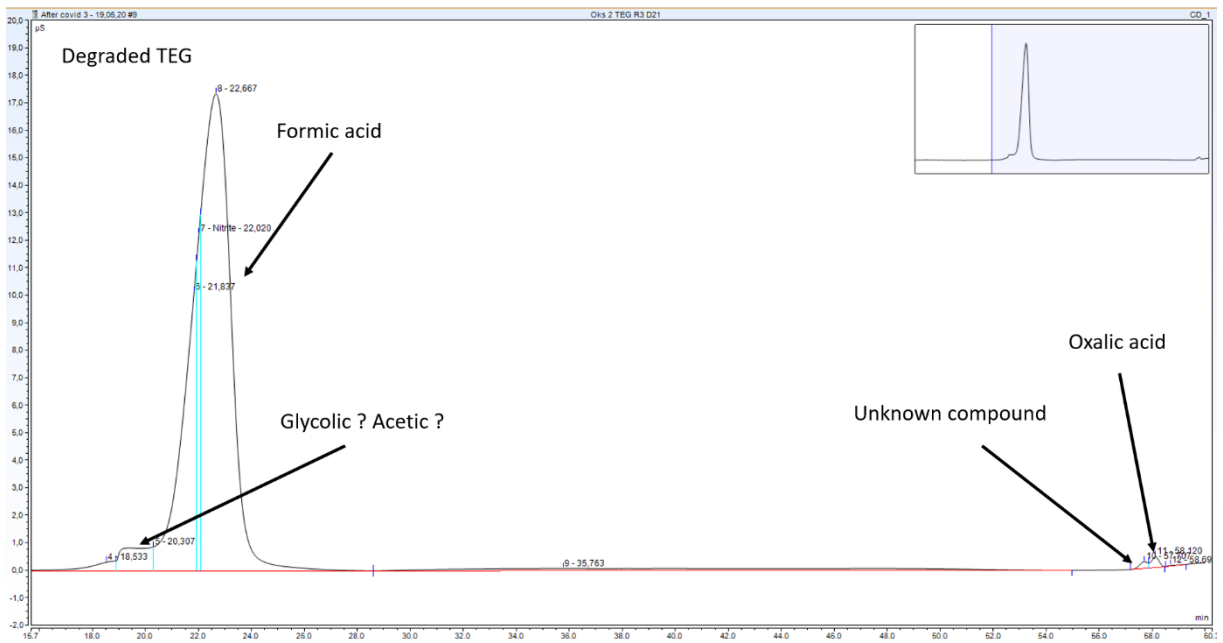
Figure 50 : Degraded TEG (Oks 2 D21 R3); peak identification
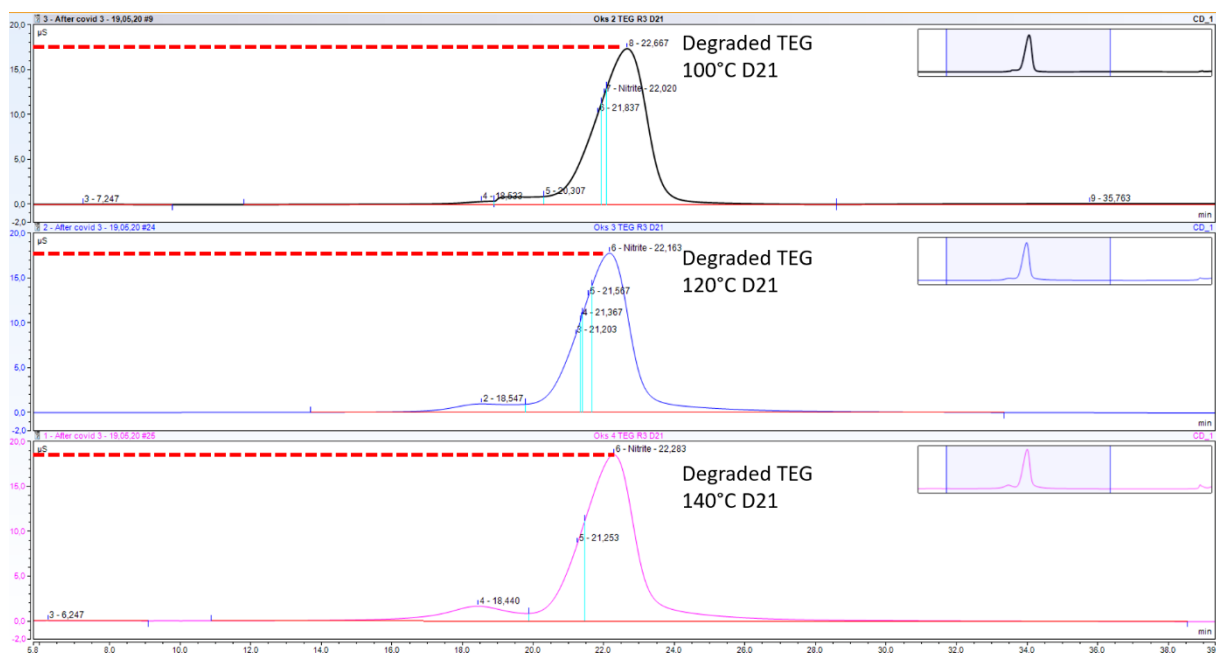
Figure 51 : Evolution of the chromatograms for MEG (R2). The big peak corresponds to formic acid and the little one on its left to glycolic acid

Appendix B

This appendix is devoted to Chapter VI and contains the tables of relative deviations for each of the comparisons carried out.

Table 8 : Absolute relative deviation between experimental data concerning MEG density from Afzal et al.[4] and calculated values

T (°C)	Δ%		
	Glycol	CPA	ELECNRTL
0,01	0,55	3,37	0,01
5	0,56	3,26	0,02
10	0,57	3,15	0,03
15	0,58	3,04	0,04
20	0,59	2,94	0,04
25	0,59	2,83	0,04
30	0,60	2,73	0,04
35	0,60	2,63	0,04
40	0,60	2,54	0,04
45	0,60	2,44	0,04
50	0,61	2,34	0,04
54,99	0,61	2,25	0,04
60	0,61	2,16	0,03
65	0,61	2,06	0,03
70	0,61	1,97	0,02
74,99	0,62	1,88	0,02
80	0,62	1,79	0,01
84,99	0,62	1,69	0,01
89,99	0,63	1,60	0,01

Table 9 : Absolute relative deviation between experimental data concerning TEG density from Afzal et al.[4] and calculated values

T (°C)	Δ%		
	Glycol	CPA	ELECNRTL
15	2,79	5,66	0,10
25	2,87	5,31	0,02
35	2,94	4,97	0,06
45	3,01	4,63	0,13
54,99	3,08	4,30	0,19
65	3,14	3,98	0,25
74,99	3,20	3,66	0,30
85	3,26	3,34	0,35

Table 10 : Absolute relative deviation between experimental data concerning MEG viscosity from Bohne et al. [9] and calculated values

T (°C)	Δ%	
	Glycol	CPA/ELECNRTL
0,1	3,5	1,2
9,3	5,3	2,4
25	21,7	0,9
29,9	28,0	1,2
40	39,1	1,4
60,2	47,9	1,0
80	34,8	1,1
100,2	21,0	2,4

Table 11 : Absolute relative deviation between experimental data concerning TEG viscosity from Sun et al. [31] and calculated values

T (°C)	Δ%	
	Glycol	CPA/ELECNRTL
26,5	173	2,4
39,9	180	0,8
59,95	172	0,6
79,9	139	6,2
100,35	203	8,1
120,15	209	13,2
140,1	50	12,8
154,95	52	8,4

Table 12 : Absolute relative deviation between experimental data concerning MEG thermal conductivity from Bohne et al. [9] and calculated values

T (°C)	Δ%		
	Glycol	CPA	ELECNRTL
8,94	2,82	77,2	2,82
24,62	2,51	73,6	2,51
64,76	2,45	62,0	2,45
99,64	1,33	48,8	1,33
121,66	1,53	42,2	1,53
139,03	0,57	35,8	0,57
178,74	0,13	24,9	0,13

Table 13 : Absolute relative deviation between experimental data concerning carbon dioxide solubility in MEG from Jou et al. [20] and calculated values

xCO2	Δ%		
	Glycol	CPA	ELECNRTL
0,1327	80	73	97
0,1226	75	67	96
0,1122	69	59	95
0,08309	61	50	94
0,0533	55	42	93
0,02144	55	43	93
0,005397	56	47	93

Table 14 : Absolute relative deviation between experimental data concerning methane solubility in MEG from Zheng et al. [35] and calculated values

xCH4	Δ%	
	CPA	ELECNRTL
0,003	1,2	99,1
0,003	0,3	99,1
0,0066	7,6	99,2
0,011	2,0	99,2
0,0148	5,5	99,3
0,0174	3,6	99,4
0,0179	0,2	99,3
0,0207	0,1	99,4
0,0224	0,7	99,4
0,0249	3,0	99,5
0,0268	2,3	99,5

Table 15 : Absolute relative deviation between experimental data concerning hydrogen sulfide solubility in MEG from Jou et al. [20] and calculated values

xH2S	Δ%		
	Glycol	CPA	ELECNRTL
0,4494	34	37	62
0,3104	43	28	71
0,1676	48	23	76
0,05057	51	17	78
0,01468	52	15	79
0,00316	46	34	76

Table 16 : Absolute relative deviation between experimental data concerning carbon dioxide solubility in TEG from Jou et al. [19] and calculated values

xCO2	Δ%		
	Glycol	CPA	ELECNRTL
0,00651	9	15	72
0,04063	2	19	74
0,1367	3	21	75
0,2611	5	27	78
0,3305	6	29	79
0,3906	2	36	81
0,4328	4	49	85
0,4582	4	56	88

Table 17 : Absolute relative deviation between experimental data concerning methane in TEG from Jou et al. [19] and calculated values

xCH4	Δ%		
	Glycol	CPA	ELECNRTL
0,000617	2	49	96
0,001859	2	50	96
0,005324	5	52	96
0,0119	6	53	96
0,02198	5	54	96
0,03326	6	56	97
0,04302	7	58	97
0,05243	7	59	97
0,06215	7	61	97
0,07124	5	62	97

Table 18 : Absolute relative deviation between experimental data concerning hydrogen sulfide solubility in TEG from Jou et al. [19] and calculated values

xH2S	Δ%		
	Glycol	CPA	ELECNRTL
0,0225	7	82	0
0,09328	5	74	3
0,3107	2	54	12
0,5122	1	31	21
0,6244	1	24	22
0,8009	3	12	17
0,9303	4	3	7

Table 19 : Absolute relative deviation between experimental data concerning methane solubility in water from Chapoy et al. [13] and calculated values à changer

	Δ%		
xCH4	Glycol	CPA	ELECNRTL
0,000204	1	20	99
0,000443	8	28	100
0,001305	4	23	100
0,002325	7	29	100

Table 20 : Absolute relative deviation between experimental data concerning water/MEG binary (60°C) from Villaman et al. [33] and calculated values

	Δ%		
XH2O	Glycol	CPA	ELECNRTL
0,0188	28,9	7,9	2,6
0,0487	33,3	4,4	8,5
0,1008	36,0	2,7	9,0
0,1497	36,1	1,1	8,7
0,1989	35,5	0,2	8,0
0,2479	34,5	1,1	6,8
0,2973	34,0	0,9	4,7
0,3477	31,2	3,7	5,7
0,3975	30,0	3,8	4,1
0,4478	27,9	4,7	3,7
0,4982	25,6	5,3	3,3
0,4987	25,5	5,5	3,4
0,5487	23,0	5,9	3,0
0,5989	20,6	5,7	2,4
0,6489	17,7	5,6	2,2
0,6988	14,6	5,0	1,8
0,7489	11,8	3,7	1,1
0,8003	8,5	2,7	0,9
0,8504	5,4	1,6	0,8
0,9001	2,8	0,4	0,5
0,9495	0,9	0,6	0,3
0,9797	0,4	0,4	0,8
1	0,1	1,0	0,2

Table 21 : Absolute relative deviation between experimental data concerning water/TEG (25°C) binary from Tsuji et al. [32] and calculated values

XH2O	Δ%		
	Glycol	CPA	ELECNRTL
0,9773	0,0	2,9	1,0
0,9524	0,4	8,5	1,8
0,937	0,4	12,9	2,5
0,924	0,0	17,4	3,6
0,9018	0,0	24,8	4,8
0,8778	0,9	34,6	7,1
0,8474	2,2	47,8	10,1
0,8221	3,3	59,2	12,8
0,7823	5,8	78,4	18,0
0,7579	6,7	89,1	20,7
0,7293	8,2	101,7	24,2
0,6554	9,8	126,7	31,2
0,6062	10,6	139,0	35,9
0,545	10,7	147,8	41,1
0,4663	9,9	149,6	47,0
0,418	9,7	147,5	51,2
0,3622	9,2	141,5	55,8